The University of Aston in Birmingham

Investigations into Practical Closed-loop Arc Control Systems

Graham Arnold Jullien

Ph.D Thesis. July 1969

SUMMARY

The work presented in this thesis is the result of an investigation into the closed loop velocity control of a d.c. arc, between parallel electrodes, subject to a transverse magnetic field. The velocity of the arc is in the order of 0.005 m/sec and has particular application to the processes of seam welding, profile cutting and zone refining.

Previous workers in this field have, over the past thirty years, amassed a great deal of literature on the high velocity behaviour of electric arcs in magnetic fields. This has been used, together with original experiments carried out by the author, to produce a mathematical model for a low velocity, low power arc.

A control system has been developed using an original arc velocity instrumentation technique; the controller uses a hybrid form of both a digital computer and analogue components. By constantly monitoring the gain of the system, the controller is able to adapt itself to long-term changes in electrode surface conditions and to changes in electrode materials.

Although it is not possible to control rapid variations in arc velocity, the feasibility of closed loop controlling the average velocity of electric arcs is demonstrated by output graphs of arc position versus time. These graphs indicate that average velocity can be controlled to within 10% of the input command indicating a suitability to the applications discussed above.

ACKNOWLEDGEMENTS

The author wishes to express his sincere thanks to Professor W.K. Roots for his sustained guidance and supervision throughout the research. Thanks are also expressed to Mr.J.L. Murgatroyd for taking over as supervisor towards the latter part of the research and for his and other colleagues' support and encouragement.

The help of Mr.J. Partlow and Mr.L. Reiter of the University technical staff has been invaluable.

CONTENTS

LIST OF SYMBOLS

c	General control system output (velocity m/second)
d	Electrode gap (metres)
e(t)	Time domain output or input of the discrete compensator
m	Dimensionless number
n	Dimensionless number Index Number of arc runs
p	Ambient gas pressure ($Kg./m^2$)
r	General control system input command (dimensionless)
s	Laplacian operator
t	Time (seconds)
v	Voltage (volts)
z	Z-transform operator
B	Transverse magnetic field (Tesla)
C	Capacitance (Farads)
C(s)	Analogue compensator transfer function
D	Denominator input to the analogue divider (volts) Circuit diagram notation for a diode
D_c	Digital compensator
$E^*(z)$	Z-transform of the sampled output or input signal associated with the digital compensator
G	Control system feedforward coefficient (dimensionless)
H	Control system feedback coefficient (dimensionless)
I	Current (Amperes)
K	Constant
L	Electrode width (metres)
N	Numerator input to analogue divider (volts)
O	Output of analogue divider (volts)
R	Resistance (ohms)
S_m	Value of mth digital sample (dimensionless)
S_n	Average value of n samples (dimensionless)
S_p	Average value of 32 samples (dimensionless)

T	Sample time (seconds) Circuit diagram notation for a transistor
U	Arc velocity associated with the arc model (m/second)
V	Carrier wave amplitude (volts)
V_o	Output velocity of arc model transfer function (m/sec.)
X, Y	Inputs to the analogue multiplier (volts)
α, β	Poles of a transfer function
ϵ	Value of signal at some point on the feedforward path of a control system (variable units)
ζ	Damping factor (dimensionless)
μ_o	Permeability of free space (S.I units)
ξ	Noise associated with the 'arc plant' gain (dimensionless)
ρ	Ambient gas density ($Kg./m^3$)
τ	Time constant (seconds)
Ψ	Electrode surface gain (dimensionless)
ω	Frequency (r/second)
Φ	Noise input to measurement apparatus (volts)
ξ $\xi^*(z)$	Z-transform of ξ after sampling

CHAPTER 1

Introduction

1.1 Research origins

The electric arc represents a most powerful and flexible tool for industrial and scientific uses. Its ability to generate large quantities of heat has made it an ideal element in the processes of welding, cutting and smelting. More recently, its uses have been extended to that of zone refining [1] and the transfer of heat to gases in the plasma torch [2].

The high-speed movement (greater than 1 m/sec.) of an electric arc in a transverse magnetic field has been under investigation for several years and was initially instigated to examine the possibilities of extinguishing arcs in circuit breakers (e.g. Guile and Mehta [3]); later research has been developed along more academic lines with interest centred on the mechanism of arc motion (see 1.3). Russian welding engineers have recently developed a process of welding tubes to tube plates utilising the high speed rotation of a welding arc in a magnetic field [4]; this technique differs from conventional welding practice by the fact that the welding arc moves at a much faster rate (10 - 25 m/sec.) than the weld takes place [5]. High-speed arc rotation, using a magnetic field, is also employed in the plasma torch in order to prevent excessive erosion of the electrodes. [2]

This thesis presents the results of research into low speed arc velocities (less than 0.025 m/sec) and the development of an arc velocity closed-loop control system. The research has been specifically orientated towards future demands of industrial processes, such as seam welding, profile cutting and zone refining, where it is visualised that magnetically-controlled arcs could take the place of present day mechanically-moved electrodes and workpieces. This would present an enormous advantage in specialised processes, such as operation in environment chambers, where mechanical movement would be

impracticable.

The specific terms of reference for the research are:-

1) To consider short d.c. arcs only,using arc currents up to 50 A.
2) To use a transverse magnetic field as the controlling parameter.
3) To only consider arc motion between parallel electrodes using commonly available electrode material of copper and brass.
4) To investigate and control arc velocity in the industrial range (0.005 m/sec to 0.025 m/sec) using commands of the form : velocity v_1 to position x_1 then velocity v_2 to position x_2 etc.
5) To develop an arc velocity feedback system without using an external optical or magnetic sensor.
6) To restrict any computer control found necessary to the low price type of computer commonly available in industry.
7) To develop any hardware to a point where it is almost ready for commercial manufacture.

1.2 The electric arc

Comprehensive reviews of the electric arc are given in the literature[2,6,7] ; this section contains a brief survey of the arc processes.

An electric arc is basically a conduction of current through a gaseous medium between two electrodes.The energy from the discharge is used to heat,dissociate and ionise the gas molecules,thus providing the conducting medium.The discharge is maintained by a flow of electrons from the cathode ;

in the case of a cathode of high vapourisation temperature the electrons are released by thermionic emission,but when a cathode of low vapourising temperature is used the origination of the released cathode electrons is in doubt.It has been shown that thermionic emission cannot account for the current densities observed in cold-cathode arcs,but there is reasonable evidence to show that high electric field intensities close to the surface of the cathode could be responsible [8].

The electric field (or voltage gradient) in the arc is not uniform and can be considered as having three distinct regions:-

1) Cathode fall region.

2) Arc column.

3) Anode fall region.

This is indicated in Fig.1.1

The voltage in the cathode-fall region has been measured at about 15 volts for a cold-cathode arc and the voltage in the anode-fall region at about 10 volts [2].The extent of the anode and cathode fall regions appear to be in the order of 10^{-5} metres,though variations in arc current and electrode material can have an effect on this value [2].

The majority of current carriers are electrons,though the ratio of electrons to positive ions can vary throughout the arc.The anode and cathode roots are of very small cross-section compared with the area of the arc column and high current densities ($\sim 10^{10}$ Amps/metre^2) are required from the electrodes.Electrode vapour occurs in the anode and cathode fall regions and, because of the constriction of these regions,is under pressure.The result is that jets of vapour are projected from the roots into the column.In short arcs the vapour jets can interact and affect the characteristics of the arc,

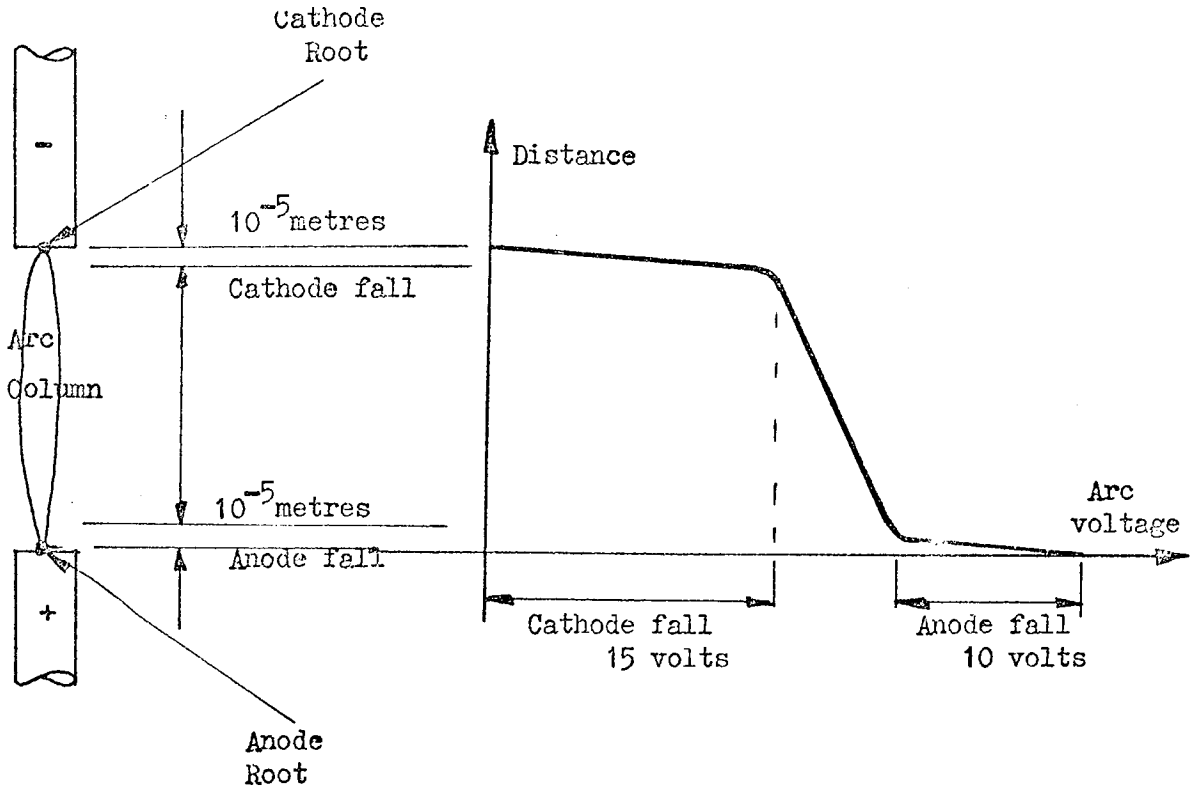

Fig.1.1 The electric arc

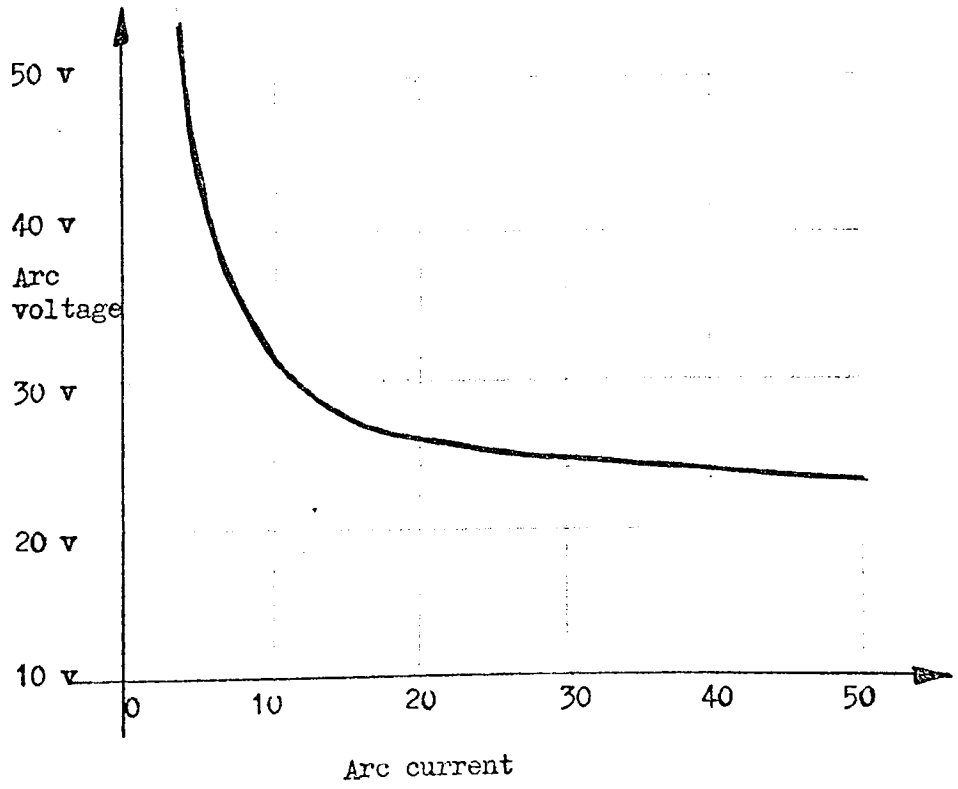

Fig.1.2 Voltage/current curves for a short arc

particularly its motion in a magnetic field[9].

Typical voltage/current characteristics of a short d.c. arc are shown in Fig.1.2. This final 'stable state' of the electric discharge can be seen to have a negative resistance characteristic, the voltage across the arc approaching a constant value as current is increased. Due to the random processes occurring within the arc, associated with the high energy discharge, the arc current is extremely noisy over a very wide frequency range; measurement problems associated with this are discussed in Chapter 2.

1.3 A brief review of recent arc velocity research

Interest in the motion of electric arcs in transverse magnetic fields has accelerated over the past decade. Original research was orientated towards the prediction of the velocity of an arc formed by the interrupt action of a circuit breaker†. The earlier prediction of arc velocity was based on curve fitting experimental results[3,10]; theoretical predictions were made by considering the arc as a solid rod conductor with opposing forces produced by the transverse magnetic field and aerodynamic drag[11]. More recent research has revealed that the motion of an electric arc is dependent upon the mechanisms of the cathode root and its associated fall region[12]. Models of the cathode-fall region have been proposed and seem to fit observed results, particularly the interesting phenomenon of the retrograde motion* of an arc

---

† This was in connection with the rapid extinction of a circuit breaker arc in a magnetic field generated by the current in the breaker contacts.

* Reverse direction to amperian motion.

in a transverse magnetic field at low pressures.[13,14]

Using dimensional analysis, researchers have produced important dimensionless groups to investigate both the velocity characteristics and voltage characteristics of an electric arc[15,16]. By correlating experimental results with theoretical calculations, mathematical models of the high velocity electric arc have been obtained and can predict velocity to within $\pm$ 50%[9,17].

The majority of measurement techniques used in high-velocity arc research have been photographic[32], though with experiments using continuously rotating arcs on a pair of circular electrodes the velocity has been monitored by observations of the arc current[18]. The photographic methods consist of filming the arc at a high speed ($\sim$ 1000 frames/second) and calculating the arc velocity by determining the distance moved by the arc per frame. In some cases, the high-speed cameras have been manufactured by the researchers themselves[19,20]. The use of photographic measurement has also been used to examine various modes of arc motion, especially the discontinuous motion of the arc under certain conditions.[20]

A few experiments have been carried out on the effect of electrode surface conditions on the arc velocity characteristics[21,22]. In all cases, the velocity of an arc was found to achieve a maximum with a small coating of oxide on the electrodes, a condition attained by previously running an arc along the electrodes. It would also appear that the stability of a cold-cathode arc depends very much on the oxide layers at the surface of the cathode electrode[14].

1.4 Structure of the thesis

Fig. 1.3 shows a flow diagram of the structure of the thesis. Chapter 2, 3 and 4 effectively work in parallel to achieve the final arc velocity control system

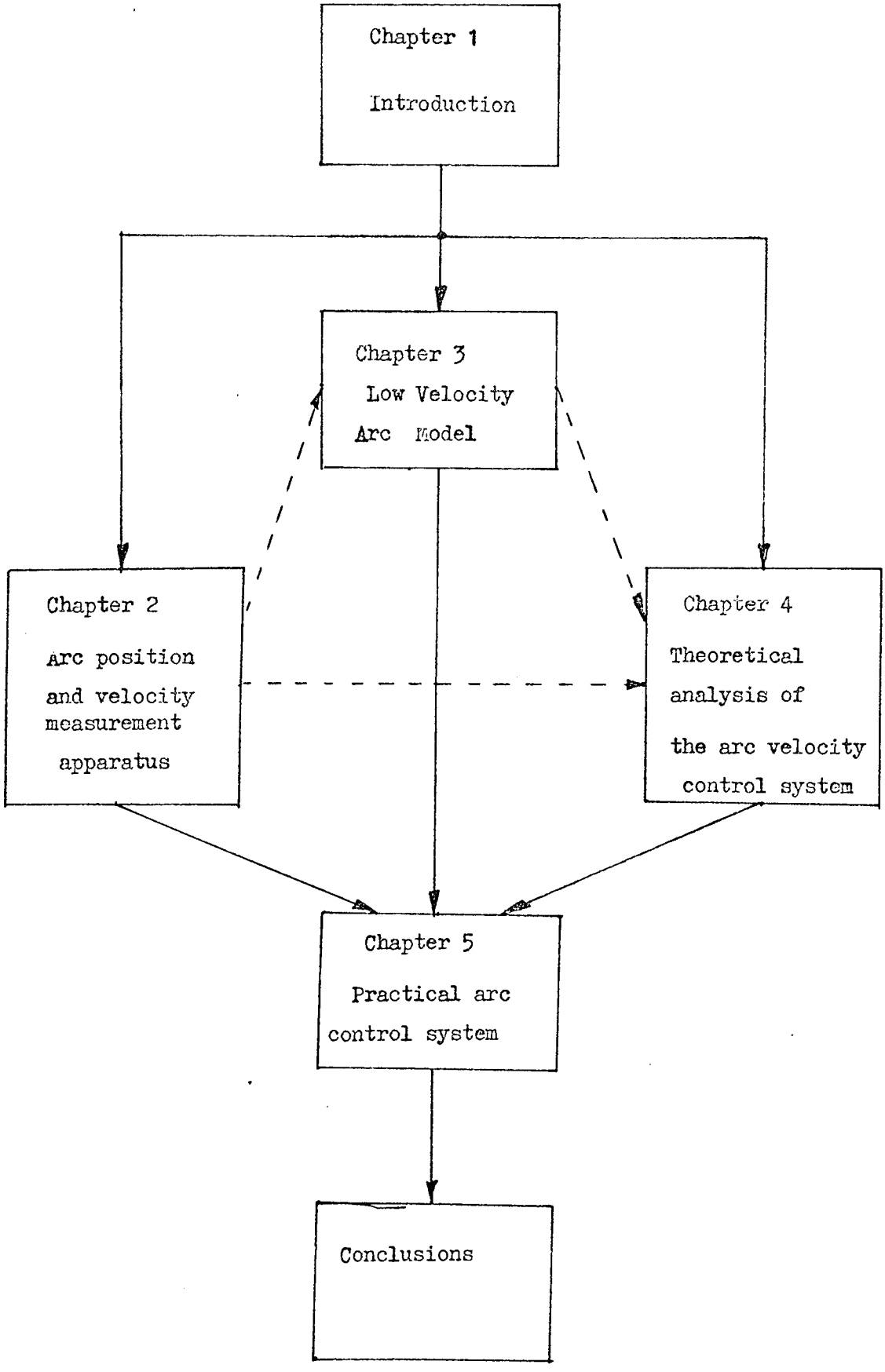

Fig.1.3 Flow diagram of construction of thesis

discussed in Chapter 5. Chapter 2 deals with the instrumentation system associated with the control feedback loop, Chapter 3 investigates the 'arc plant' and produces an approximate mathematical model for the low-velocity arc and Chapter 4 discusses the theoretical aspects of a closed-loop system design.The dotted lines in Fig.1.3 indicate connections between these three Chapters.Measurement techniques produced in Chapter 2 help to investigate low velocity arcs in Chapter 3 and mathematical results from both Chapters are used to produce design calculations in Chapter 4.

CHAPTER 2

Arc Instrumentation

2.1.1 Instrumentation Principles

In order to produce a system to control the velocity and position of a d.c arc along parallel electrodes, electrical feedback signals have to be generated which are proportional to the velocity and position of the arc. If a signal proportional to the position of the arc can be generated then the velocity of the arc can be found by differentiating this signal. The position of the arc can be measured in two ways:

1) By the use of optical or magnetic transducers spaced along the length of the electrode assembly, as shown in Fig. 2.1. Voltages generated by these transducers due to the proximity of the arc are fed into an electronic system which determines, by interpolation methods, the position of the arc relative to the nearest transducer.

2) By using the voltage generated by the arc current flowing through one of the electrodes; as shown in Fig. 2.2. Providing the electrodes are homogeneous the output signal is proportional to:

(Arc Current X Arc Position)

If the arc current is constant, the output signal is proportional to arc position.

2.1.2 A Practical Instrumentation System

Of the two methods outlined in 2.1.1 the second is far more practical for

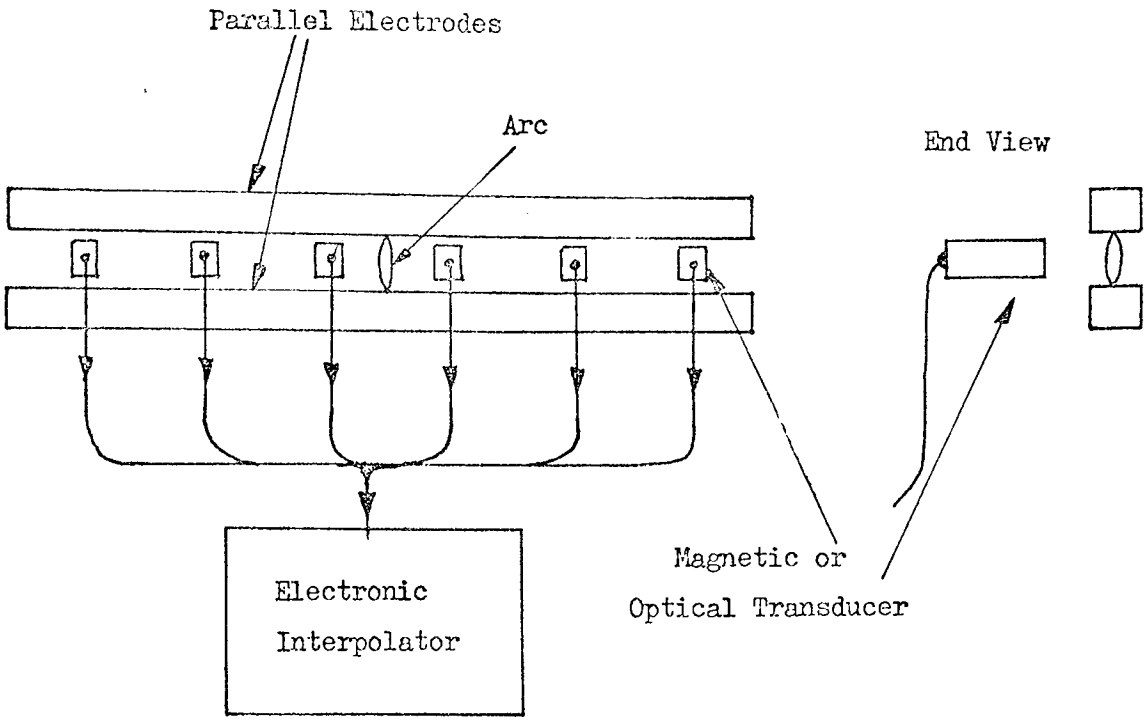

Fig.2.1 Typical measurement system using external transducers

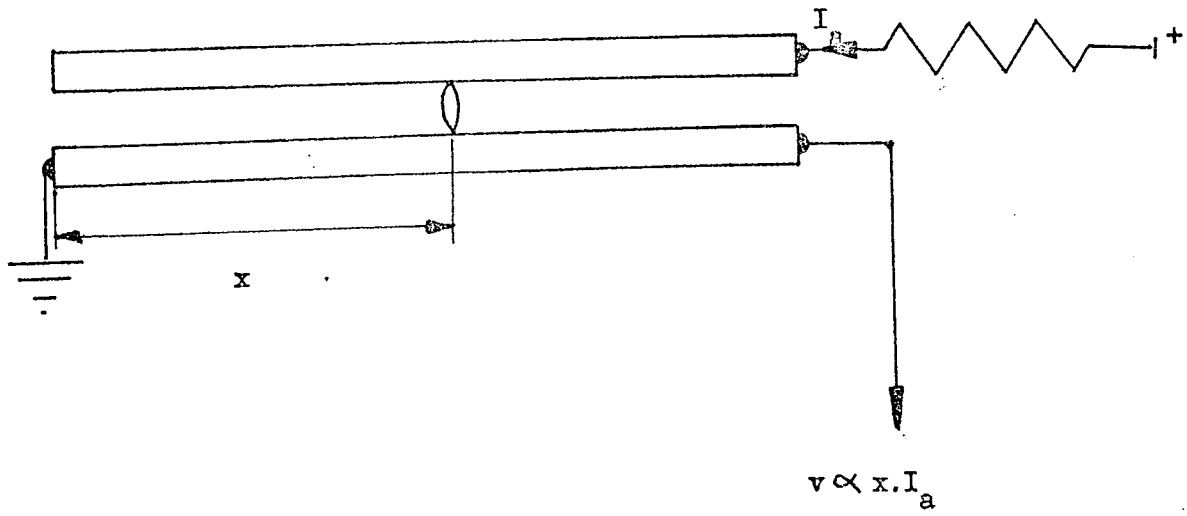

Fig.2.2 Basic system for producing a position signal using the arc current flowing in the cathode

the rugged demands of industry than the first. Since the research was intended as a feasibility study for arc control, the second method was chosen for the generation of the arc-position signal. The mechanical details of the electrode and field generation apparatus are given in 3.1.1 and 3.1.2.

2.2.1 Arc position Signal

(The system analysed in this section is a modification of an original system described in a paper by Roots and Jullien[23])

The position signal, as shown in Fig. 2.1, is dependent on the current flowing through the electrodes. Although it is possible to produce a control system which will endeavour to keep the arc current constant (see Appendix I), high-frequency perturbations (due to random electron noise) and low-frequency perturbations as the arc moves over fluctuating surface conditions (i.e. pitting and oxidation) will be present on the controlled d.c current. The random electron noise may be filtered out, since its frequency will be far higher than the measurement system needs to respond; but the low-frequency fluctuations, which the current control system cannot correct, cannot be successfully filtered out without making the system too sluggish.

By utilising a signal proportional to arc current, v_2, and the arc position signal, v_1, (see Fig. 2.3) we can perform an analogue division $\frac{v_2}{v_1}$, the resulting output being independent of current.

Since v_1 is of very low amplitude (typically less than 5mV depending on arc current and size and material of electrodes) the problem of drift in high-gain d.c amplification becomes appreciable with most types of d.c amplifiers. By 'chopping' v_1 and feeding it through an a.c amplifier, to obtain the gain

required, then de-modulating and recovering the d.c signal the problem of drift at high gains can be eliminated.

2.2.2 The Arc Position Measurement Circuit

The analogue divider consists of an analogue multiplier in the feedback circuit of a d.c amplifier[24]. Such a configuration is shown in Fig.2.4. If the input current is equated to feedback current (this is correct providing the amplifier takes negligable input current) then:

$$\frac{N}{R} = \frac{D.O}{10\,R} \qquad \text{hence,} \qquad O = \frac{10\,N}{D}$$

Thus the output is proportional to the division of one input by the other.

Fig.2.5 outlines the system used for a.c amplification of v_1. The input signal is chopped by two N-channel field-effect transistors, a system used widely in chopper stabilised d.c amplifiers[25]. The signal is amplified by an a.c amplifier and fed into the de-modulator, which clamps the waveform into the negative region on the output side; the square wave is filtered out, leaving the negative d.c component at the output. The transfer function of the de-modulator is:

$$\frac{R_o}{R_i} \left\{ \frac{1}{1 + s\,C_o\,R_o} \right\} \qquad \text{.....(2.1)}$$

In order to analyse the de-modulator consider an input square wave of fundamental frequency ω. Since this square wave is being filtered, the harmonic components can be neglected, this results in an approximate expression for the square wave (amplitude V) :

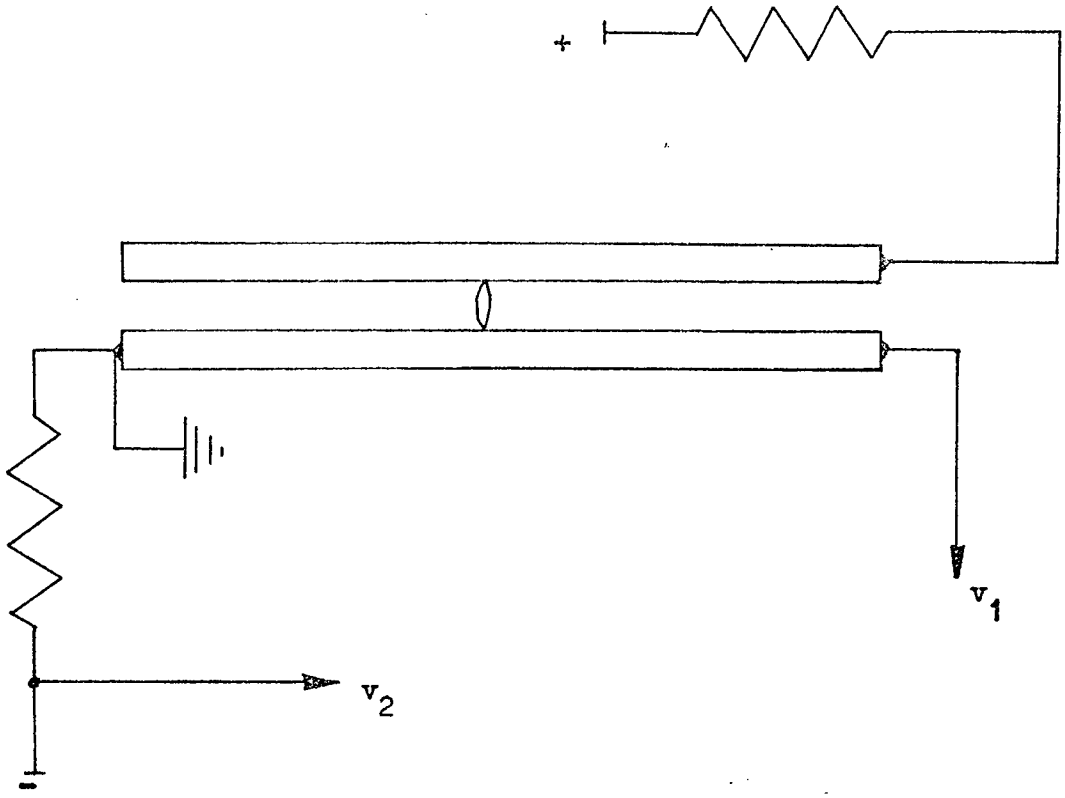

Fig.2.3 Basic system for producing arc position signal (v_1) and arc current signal (v_2) The arc current supply is floating.

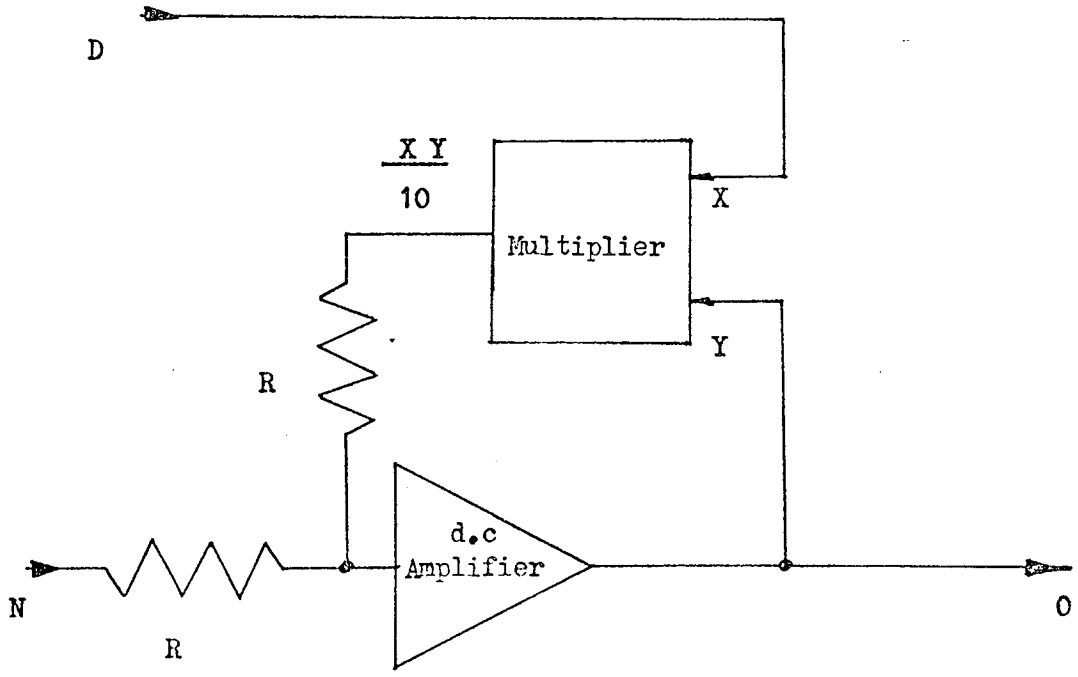

Fig.2.4 Configuration for an analogue divider

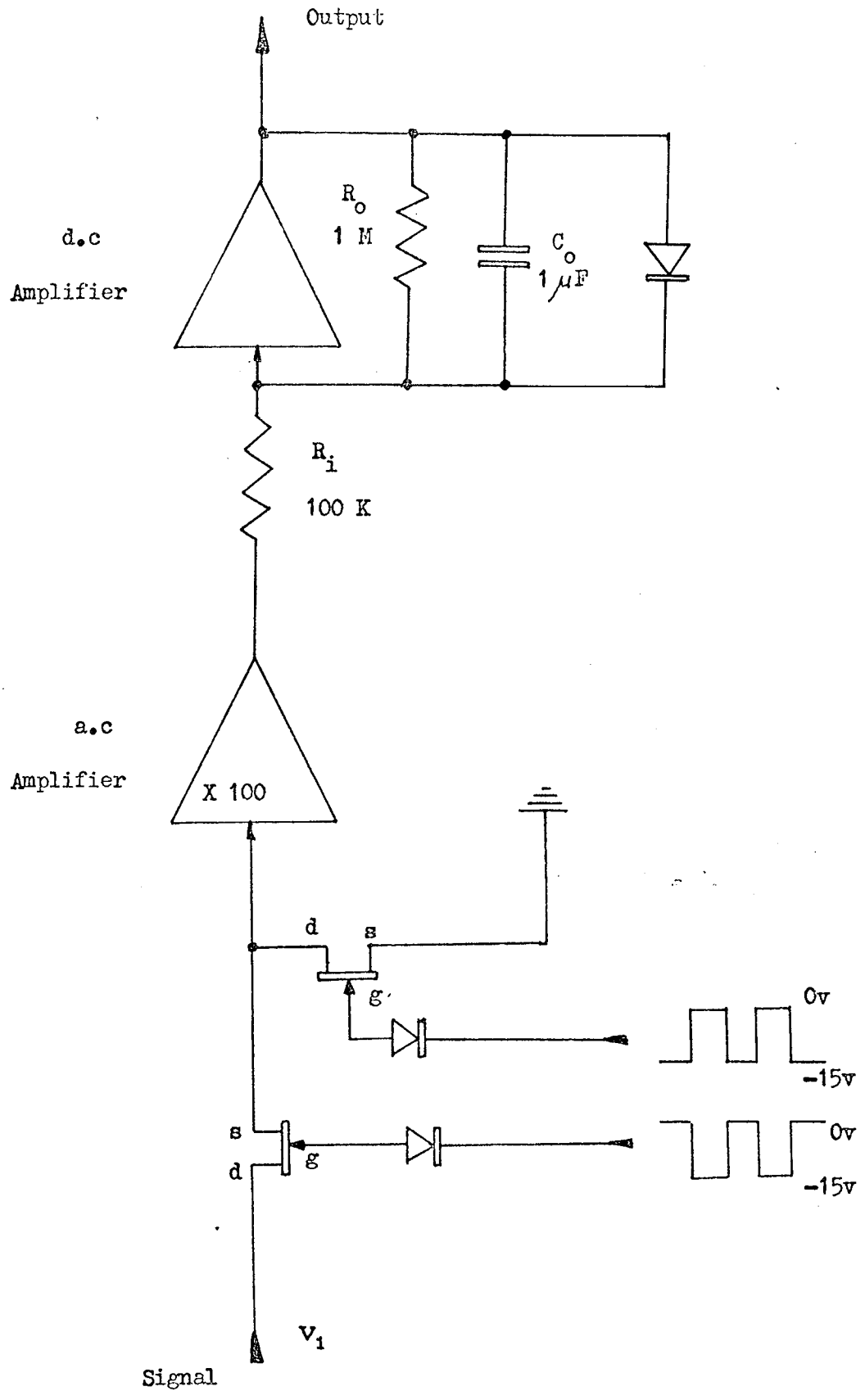

Fig.2.5 Modulation and de-modulation system for removing drift in the d.c amplification of low voltage signals

$$V \left\{ \frac{1}{2} + \frac{2}{\pi} \sin\omega t \right\} \qquad \ldots\ldots\ldots\ldots\ldots\ldots\ldots\ldots\ldots\ldots (2.2)$$

By combining eqn.(2.1) and eqn.(2.2),a ratio of d.c output to fundamental-frequency output,which can be effectively termed a signal-to-noise ratio, is obtained.

$$\text{Signal/Noise ratio} = \frac{V R_o}{2 R_i} \Big/ \frac{2 R_o V}{\pi R_i \omega \tau}$$

where $\tau = C_o R_o$

hence; $$\text{Signal/Noise ratio} = \frac{\pi \omega \tau}{4} \qquad \ldots\ldots\ldots\ldots\ldots\ldots (2.3)$$

providing $\omega\tau >> 1$.

Practical values of ω and τ have been found to be 1000πr/sec. and 1 sec. respectively.The considerations in this choice have been the speed of sampling (if ω is too high the F.E.T's will not switch 'cleanly') and the signal-to-noise ratio of the output,the importance of which will be discussed in a later section.Using these values for ω and τ ,a signal to noise ratio of $250\pi^2$ can be calculated from eqn.(2.3);this is about 68 dB.

The complete measuring system is shown in Fig.2.6.Since the datum point on the electrodes (x = 0) is not at the current input to the electrodes,a voltage bias is present on the output voltage and has to be biassed off in the de-modulator stage,as shown.

The multiplier used in the analogue divider operates on the characteristics of a p.n junction in a transistor and is accurate to within less than 1%.The series resistance used to obtain v_2 is 150 mΩ and so

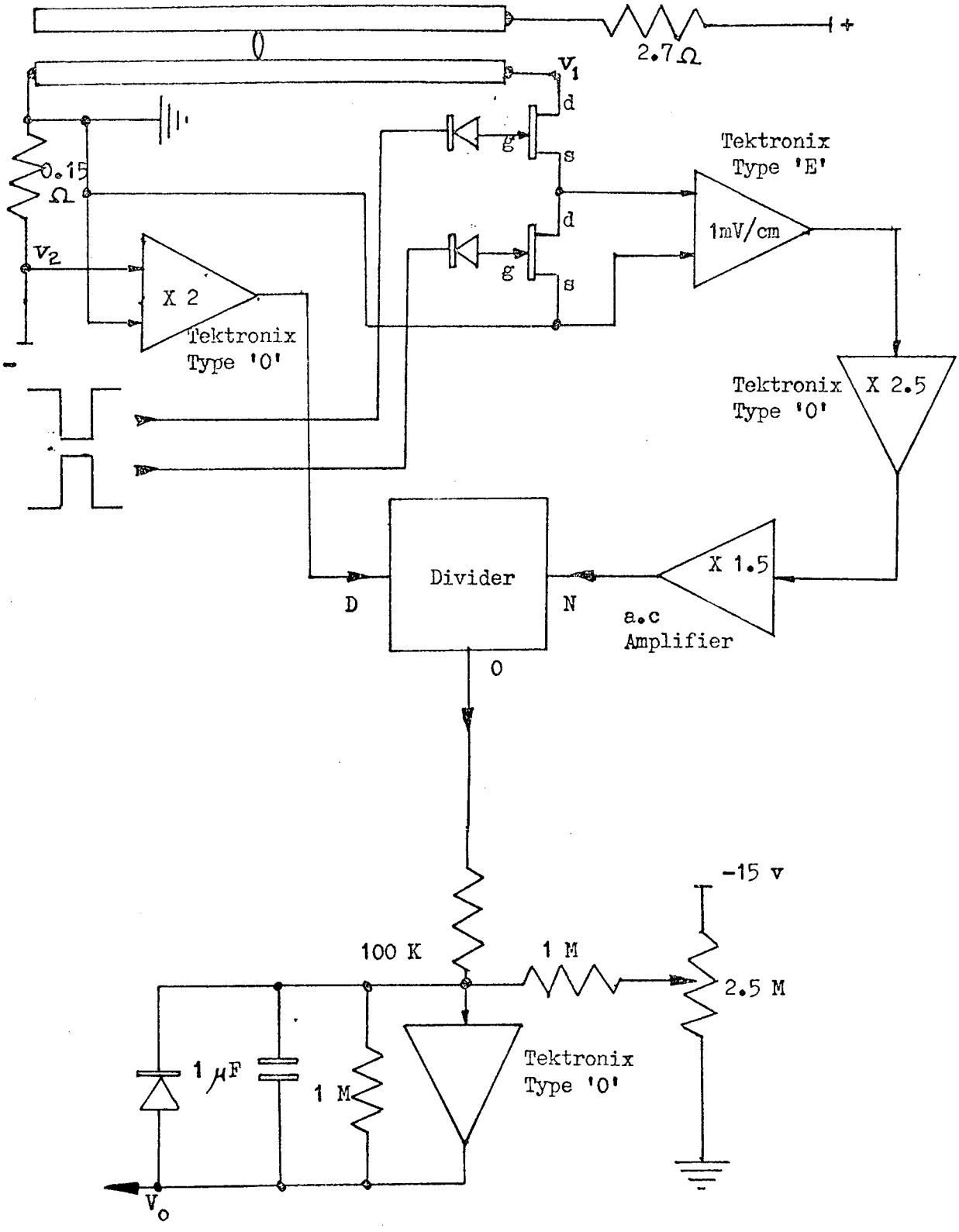

Fig.2.6 Complete arc position measuring circuit

produces a large value of signal that has only to be amplified by a factor of two.This eliminates amplifier drift which would occur at higher gains causing inaccuracies in the output of the divider.The arc current control system(see Appendix I) uses v_2 as a feedback signal so any increase in the 150 mΩ resistor,due to power dissipated in it by the current flowing through,will correspondingly modify the arc current by the same fraction as v_2,thus maintaining the balance.

2.2.3 The Measurement Circuit Performance

In order to justify the use of an a.c system to eliminate drift,both the a.c system (Fig.2.5) and a d.c system,using two amplifiers in cascade,were compared under the same conditions.With a gain of 1000 and an input of 7mV the outputs of both systems were photographed from an oscilloscope.Fig.2.7 (a) is the output of the d.c system and Fig.2.7 (b) the output of the a.c system. In both cases the centre of the graticule indicates 7V amplitude and the scaling in the photographs is:

X-direction	1 division	$\equiv$ 1 second
Y-direction	1 division	$\equiv$ 0.5 volts

Appreciable drift is present on the d.c system and is of a rate of the same order as a typical input signal.The a.c system indicates a little drift, this occurring in the de-modulator stage.Fig.2.8 shows a typical output from the analogue divider before de-modulation.

The effectiveness of the analogue divider is shown in Fig.2.9 which gives the results of arc position output versus arc current,these were tabulated at a distance of 0.12m from the zero datum point.For a $\pm$ 50% current

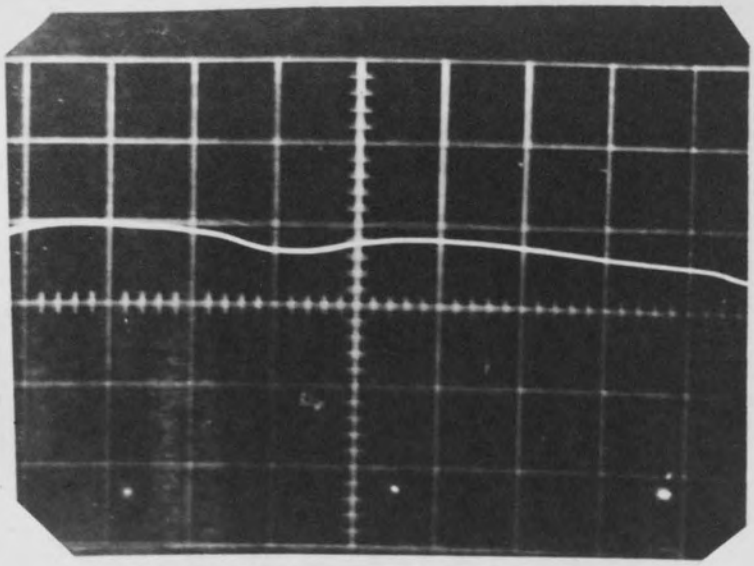

a) Output of d.c system using two d.c amplifiers in cascade

Scaling: X 1 division ≡ 1 second

Y 1 division ≡ 0.5 volts

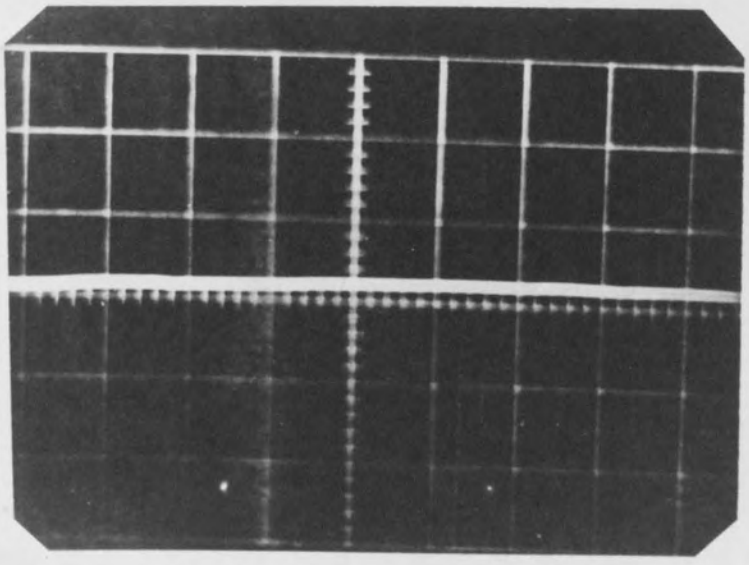

b) Output of a.c system using an input signal modulated carrier and output de-modulator stage

Fig.2.7

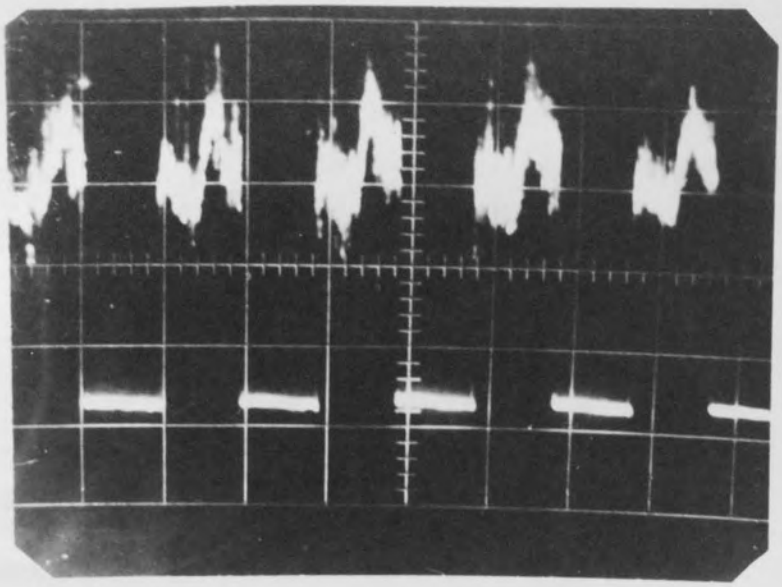

X direction
1 division ≡ 1 mS

Y direction
1 division ≡ 1 volt

Fig.2.8 Typical output from the analogue divider of the measurement system

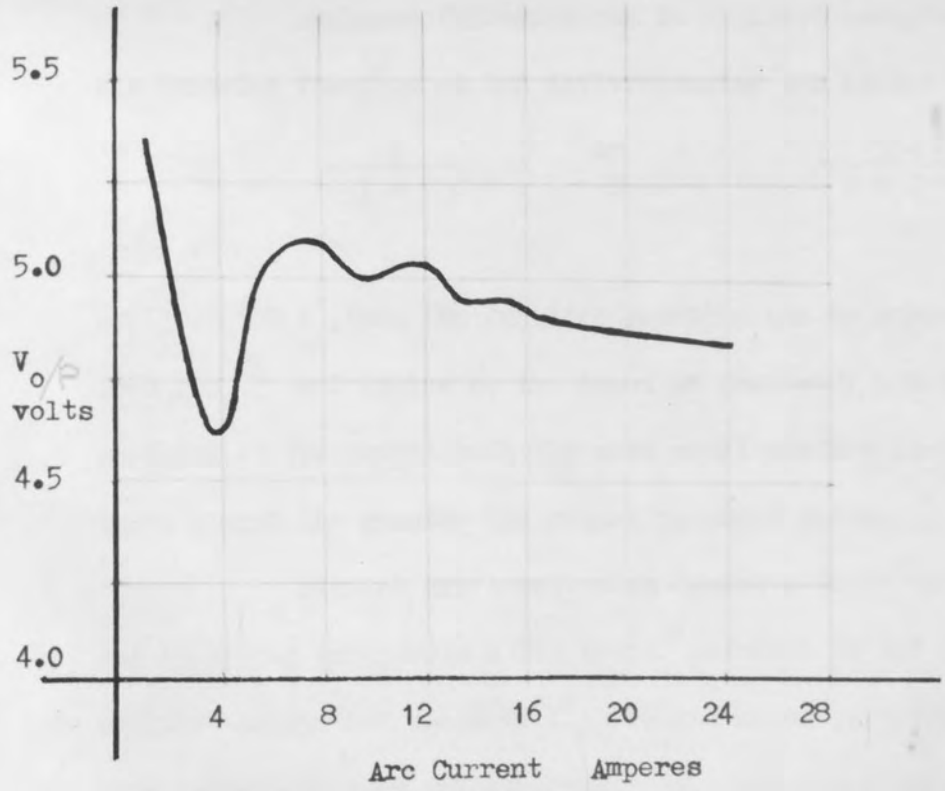

Fig.2.9 Output voltage of position measuring system versus arc current

swing from a nominal 12 Amperes, the total error in output voltage was 4.5% of the nominal 5volts; since there was an effective d.c offset of about 3volts the actual error in output voltage was only 3%.

2.3.1 Arc Velocity Signal

The differentiation of the arc position signal can be accomplished in two ways:

a) Analogue differentiation

b) Digital differentiation

With any form of differentiation, noise present on the input signal will be amplified proportional to its frequency; evidently filtering must be employed to reduce the output noise.

Analogue filtering can be employed using a first order system, the transfer function of the differentiator and filter being:

$$\frac{s}{1 + s\tau} \quad \text{or} \quad \frac{j\omega}{1 + j\omega\tau}$$

If $j\omega\tau >> 1$, then the transfer function can be approximated to $\frac{1}{\tau}$. Thus for $\tau = 1$, noise at the input of frequency $>> 1$ r/sec. will be produced at the output with the same amplitude. The lower the frequency of the input signal the greater the signal to noise ratio.

Digital differentiation (using a first difference approximation) and filtering represents a far better solution to the problem, since it requires no further analogue filters and hence restricts the system to a single-time-constant transfer function. With regard to the control of the arc,

a discrete controller (which can be used in conjunction with the differentiator and filter) is shown to be a far more realistic approach to the problem of arc - velocity control than the use of an analogue system (see Chapter 4).

2.3.2 Principles of a Digital Filter

Digital filtering is accomplished by taking n samples of the amplitude of a signal over a space of time T and finding the average value of these n samples. The output of the filter will be pulses every T seconds, the amplitude of the pulses representing the average value of the signal over the previous T seconds. If a zero-order hold circuit is used after the digital filter then the output of this hold circuit will be steps changing every T seconds, the amplitude of each step corresponding to the amplitude of the input pulse. This is demonstrated in Fig. 2.10. If T is very much greater than $\frac{2\pi}{\omega_{nl}}$, where ω_{nl} is the lowest noise frequency and many samples are taken (say $\not< 10^3$), then adequate filtering of the signal will take place.

If S_m is the value of the mth sample then S_n, the average value of n samples, is:

$$S_n = \frac{\sum_{m=0}^{m=n} S_m}{n} \qquad \text{.....(2.4)}$$

Digital differentiation can be performed by taking the first difference of the sampled (and filtered) signals. Fig. 2.11 demonstrates this method of differentiation. In practice we cannot obtain the average value of the input signal until the end of the period T and this accounts for the delay of

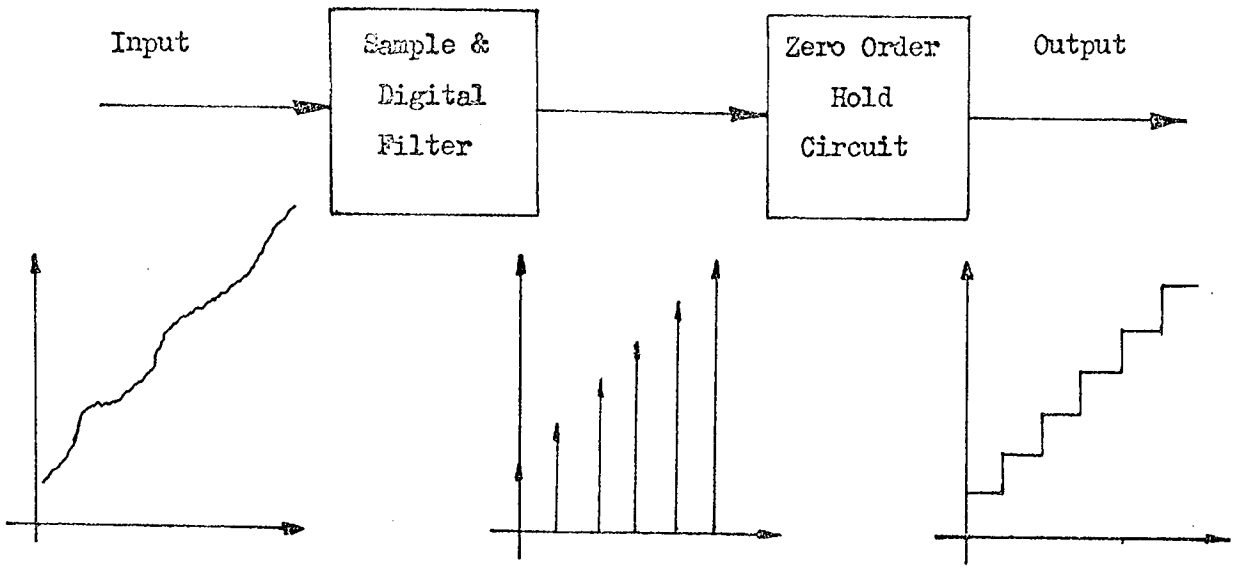

Fig.2.10 Operation of digital filter and output hold circuit

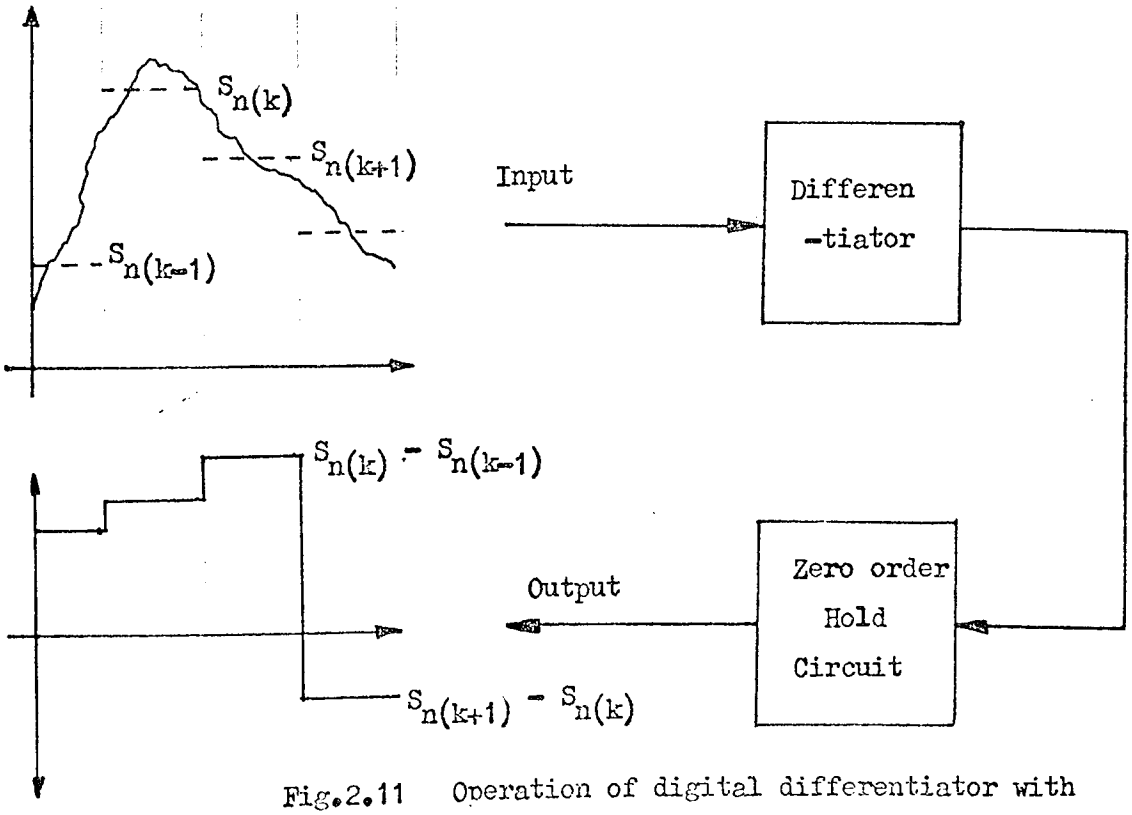

Fig.2.11 Operation of digital differentiator with output hold circuit

the first difference calculation, by time T , in Fig.2.11. This becomes important when considering the control system design (see Chapter 4).

2.3.3 A Practical Digital Filter

A PDP9 computer (typical of the low-priced computer found in industry), with analogue-to-digital and digital-to-analogue conversion facilities, has been used for the digital differentiation and filtering systems. The analogue-to-digital converter can perform a 12-bit (binary) conversion in 35μ seconds which, if we take into account the time for first difference and filtering operations, means that over 1000 samples can be taken in 100 mS. Using $T = 100$ mS and $n = 2^{10} = 1024$ (for ease of computer manipulation), from eqn.(2.4) :

$$S_n = \frac{\sum_{m=0}^{1024} S_m}{1024} = \sum_{m=0}^{1024} \frac{S_m}{1024} \qquad \text{.....(2.5)}$$

Since a division of 1024 is equivalent to shifting S_m (binary) 10 places to the right, by summing S_m (shifted) 1024 times the resultant value will be S_n (from eqn.(2.5)).

The computer operates with an 18 bit register, so a shift of 10 places with a 12-bit number will result in a loss of 4 bits. If, however, we expand eqn.(2.5) to:

$$S_n = \sum_{p=0}^{p=32} \frac{S_p}{32} \qquad \text{where} \quad S_p = \sum_{m=0}^{m=32} \frac{S_m}{32} \qquad \text{.....(2.6)}$$

then we can perform the same averaging function without shifting S_m more than 5 places to the right.

Full details of computer programmes can be found in Appendix II.

2.3.4 Typical Velocity Output Performance

Figs.2.12 a) and b) show typical velocity outputs using the computer; Fig.2.12 a) indicates zero arc velocity and in Fig.2.12 b) the arc is moving at an average velocity of about 0.005 m/sec. Considering the very low velocity in Fig.2.12 b) the results are remarkably good. The fairly rapid change in arc velocity, which can be seen in this photograph, indicates changing surface conditions and is probably the most predominant factor contributing to the non-uniform motion of the arc.

2.4 Summary

1) A system has been developed for measuring arc position along parallel electrodes. This is particularly suited for the industrial arc speeds of up to 0.025 m/sec.

The system is:

a) Virtually free from drift

b) Affected by fluctuations in arc current by a factor of less than 0.05.

2) Differentiation of the arc position signal at welding speeds has been made possible by the use of a digital computer and variations in arc velocity along a pair of electrodes can be monitored.

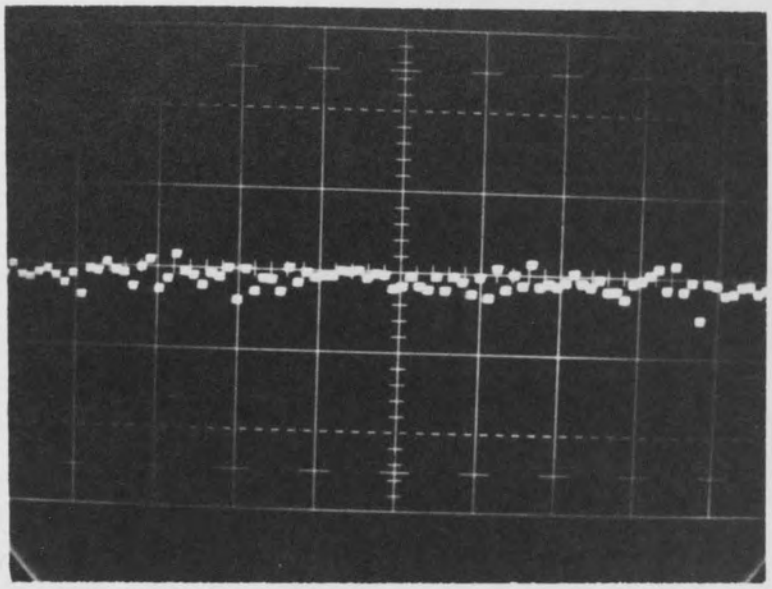

a) Computer output for zero arc velocity

Scaling: X one division ≡ 1 second

Y one division ≡ 1 volt

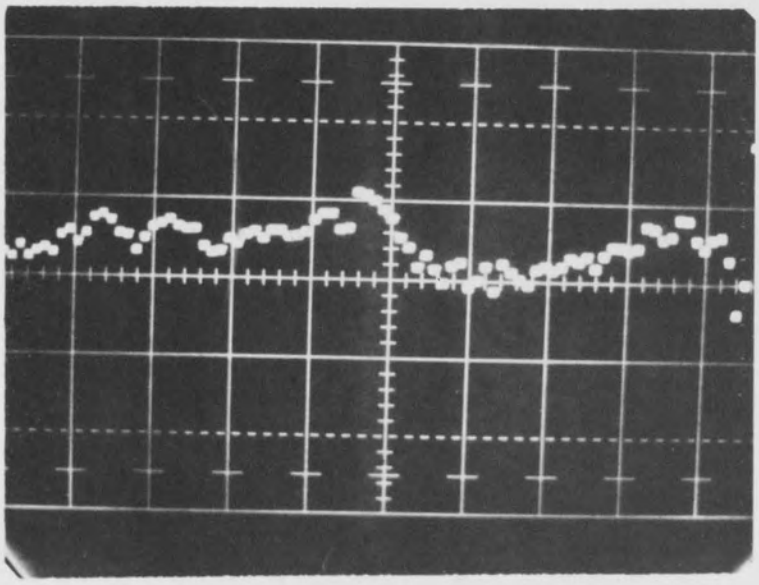

b) Computer output for an average arc velocity of 0.005 m/sec.

Fig.2.12

Chapter 3

Characteristics of low velocity arcs in transverse magnetic fields

3.1.1 Apparatus

The apparatus developed for modelling the slowly moving arc process is shown in Fig.3.1.The arc is run between parallel electrodes in a transverse magnetic field and although this is not a true representation of an industrial process,the basic configuration can be adapted to such processes as seam welding,profile cutting (where the lower electrode is replaced by a moving sheet of metal) and zone refining.

The cathode and anode electrodes are of a square cross section positioned as shown in Fig.3.2.The arc is initiated by a piece of silver foil inserted between the electrodes at one end.

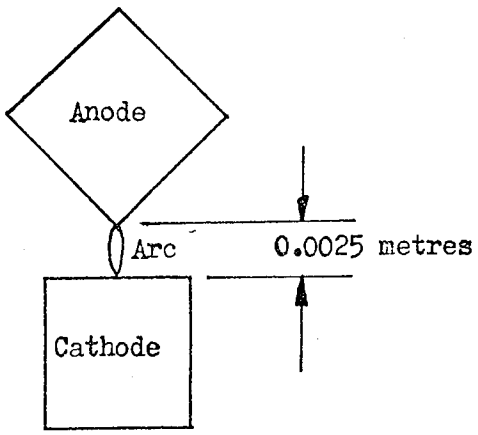

Fig.3.2 Electrode configuration

This electrode configuration is the result of many experiments carried out with various configurations and proves to be the most successful with regard to constraining the arc to one degree of freedom i.e along the length of the electrodes.It is also the most stable with regard to the arc extinguishing itself.These two effects are interlinked,since the latter occurs if the

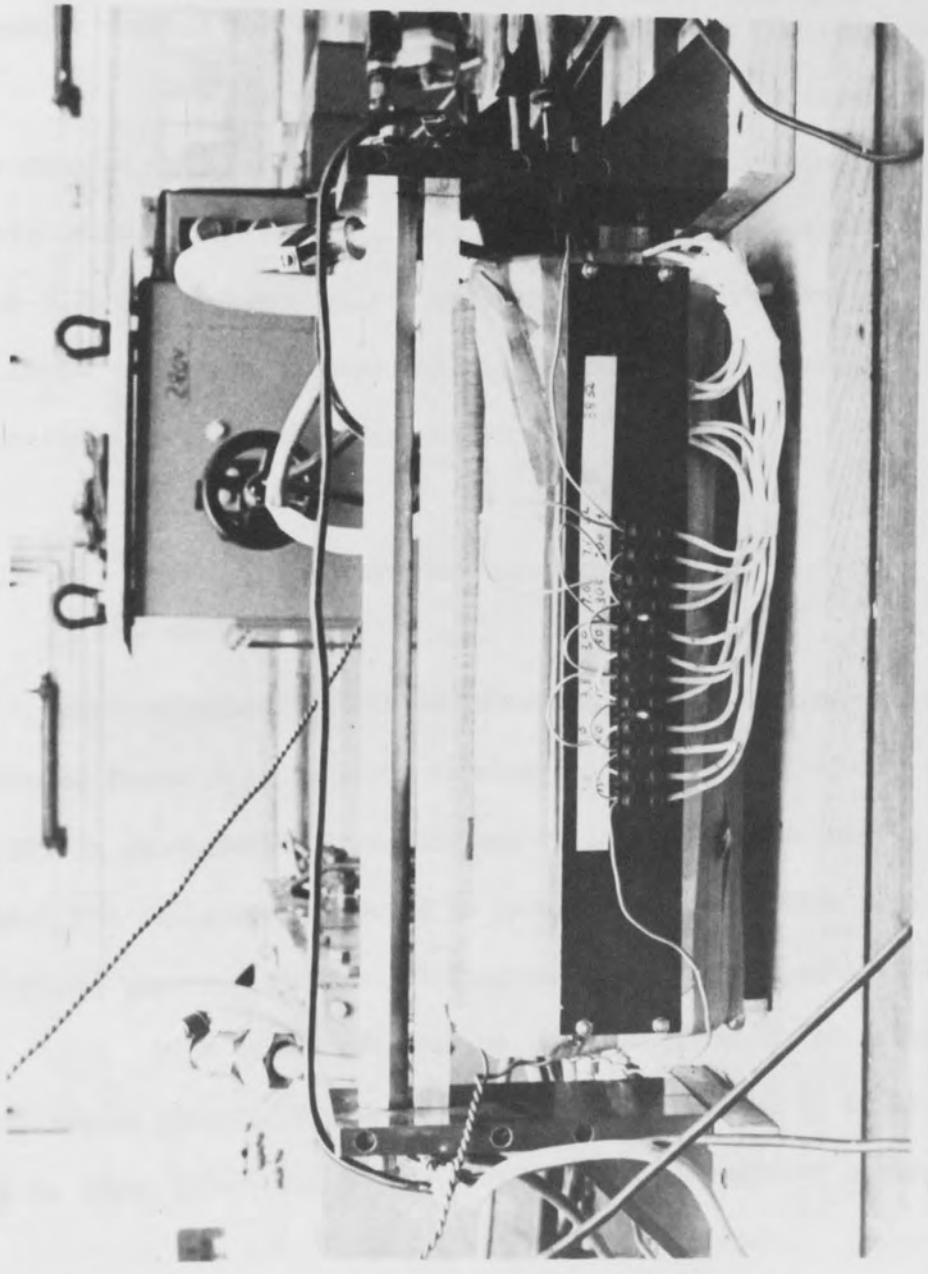

Fig.3.1 Photograph of 'arc plant'

arc moves perpendicular to the length of the electrodes. In such a situation, the arc can increase its length to such an extent that the power supply can no longer provide the voltage necessary to maintain the lengthened arc.†

Both the anode and cathode electrodes are water cooled with a flow rate of 0.23 litres/second and are readily interchangeable when clean electrodes are required. The electrode assembly length is 0.36 metres, of which 0.25 metres are used for the low-velocity arc experiments, this being the length within the linear portion of the field generated by the nickel-iron laminations (see the following section).

3.1.2 The Transverse Magnetic Field

The transverse magnetic field is generated in the air gap of a nickel-iron laminated former, this is shown in more detail in the plan view of Fig.3.3. The MMF is generated by four 300-turn coils wound round the two sides of the former. The coils are connected in parallel and are driven from a power amplifier. The complete circuit diagram is given in Appendix III.

With this configuration, the inductance of the coils and the total series resistance give a time constant ($\tau = \frac{L}{R}$) of 15 mS which, as will be shown later, can be neglected for the purposes of analysis.

3.1.3 The Arc Current Supply

The arc-current power supply is obtained from a variable-impedance mains-frequency voltage supply; this drives into a conventional full-wave rectification

† Instability is particularly noticeable at arc velocities greater than 0.03 metres/second with currents greater than 30 Amperes(see 5.4.3).

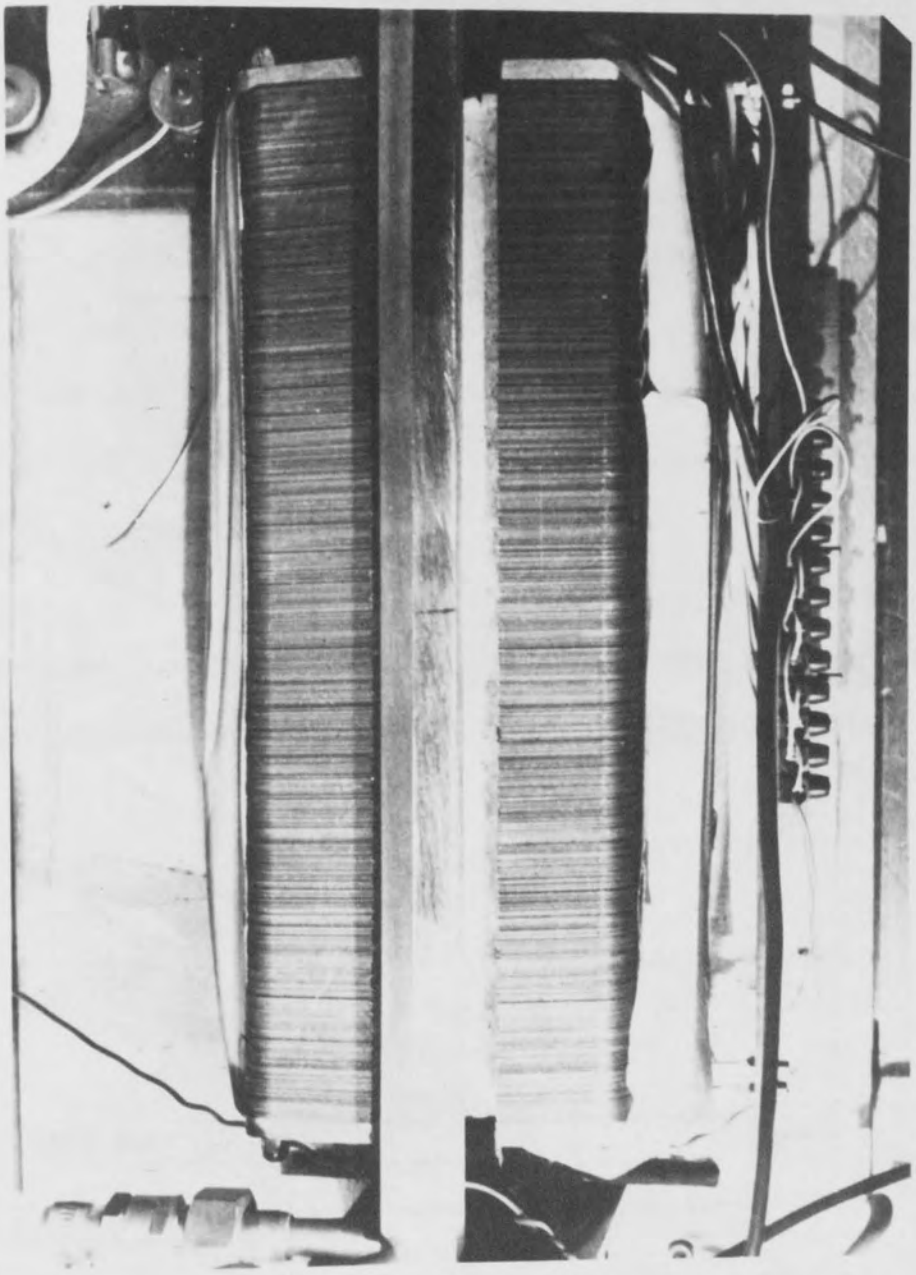

Fig.3.3 Plan view of the 'arc plant'

circuit via an isolation transformer.A variable-inductance transductor is used for the a.c voltage supply and an output current varying from 5 Amperes to 50 Amperes can be produced with an input current variation of a few hundred milliamperes.The transductor has a capacity of 25 KVA.

Using an arc-current feedback signal(see Fig.2.3) and input command signal,driving into the single-ended power amplifier at the input of the transductor,a closed-loop current supply has been built.The system has been designed to minimise low-frequency current fluctuations due to random arc variations.Circuit details and a complete closed-loop analysis are given in Appendix I.

The current is fed to the electrodes as shown in Fig.3.4,this minimises the transverse magnetic field produced by the current flowing in the electrodes,since the fields are of opposite polarity and tend to cancel out.

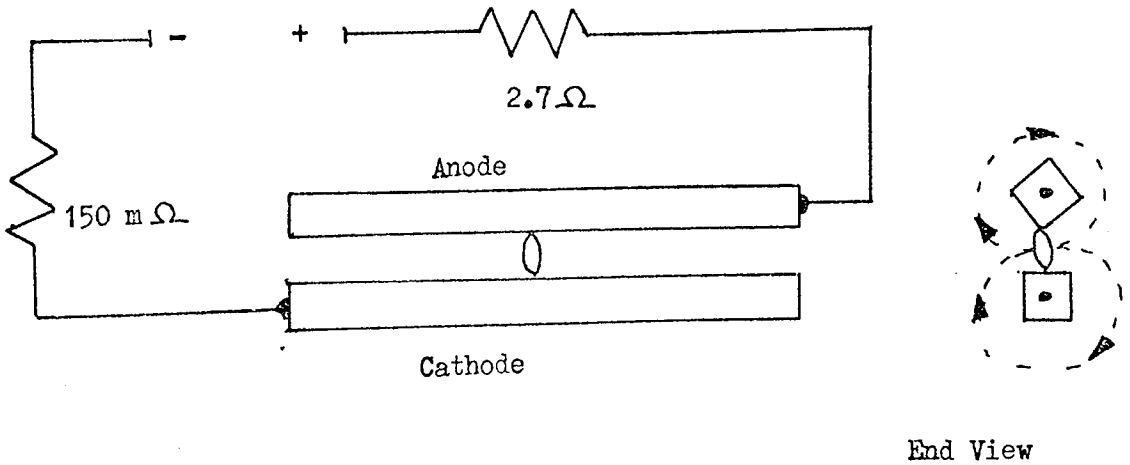

Fig.3.4 Direction of current feed to the electrodes

3.1.4 Open-loop Position Measurement

For open-loop measuring purposes, the arc position instrumentation system (see Chapter 2) is used in conjunction with a Hewlett-Packard X/Y plotter. The plotter has a passive filter on the input and this is used as the de-modulator filter. The input to the plotter is fed from the output of the analogue divider via a diode and resistor de-modulator network as shown in Fig.3.5.

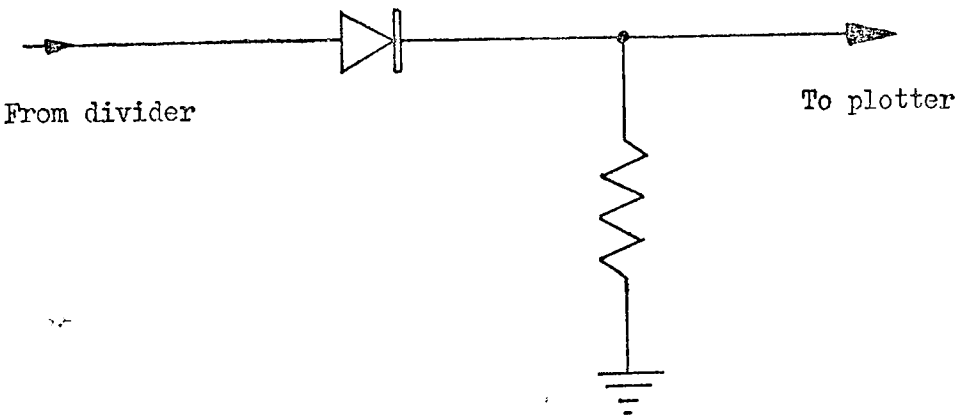

Fig.3.5 De-modulator network to chart plotter

A time-base unit is fitted on to the X input of the plotter giving a time-base variation of from 0.5 seconds/inch to 50 seconds/inch. Typical results of arc position verus time, for slowly-moving arcs, are shown in Fig.3.6 for a time base of 5 seconds/inch and a vertical deflection of 1 inch/0.05 metres of arc movement.

3.2.1 Experimental Results

Using the apparatus discussed in 3.1.1 to 3.1.4, experiments have been carried

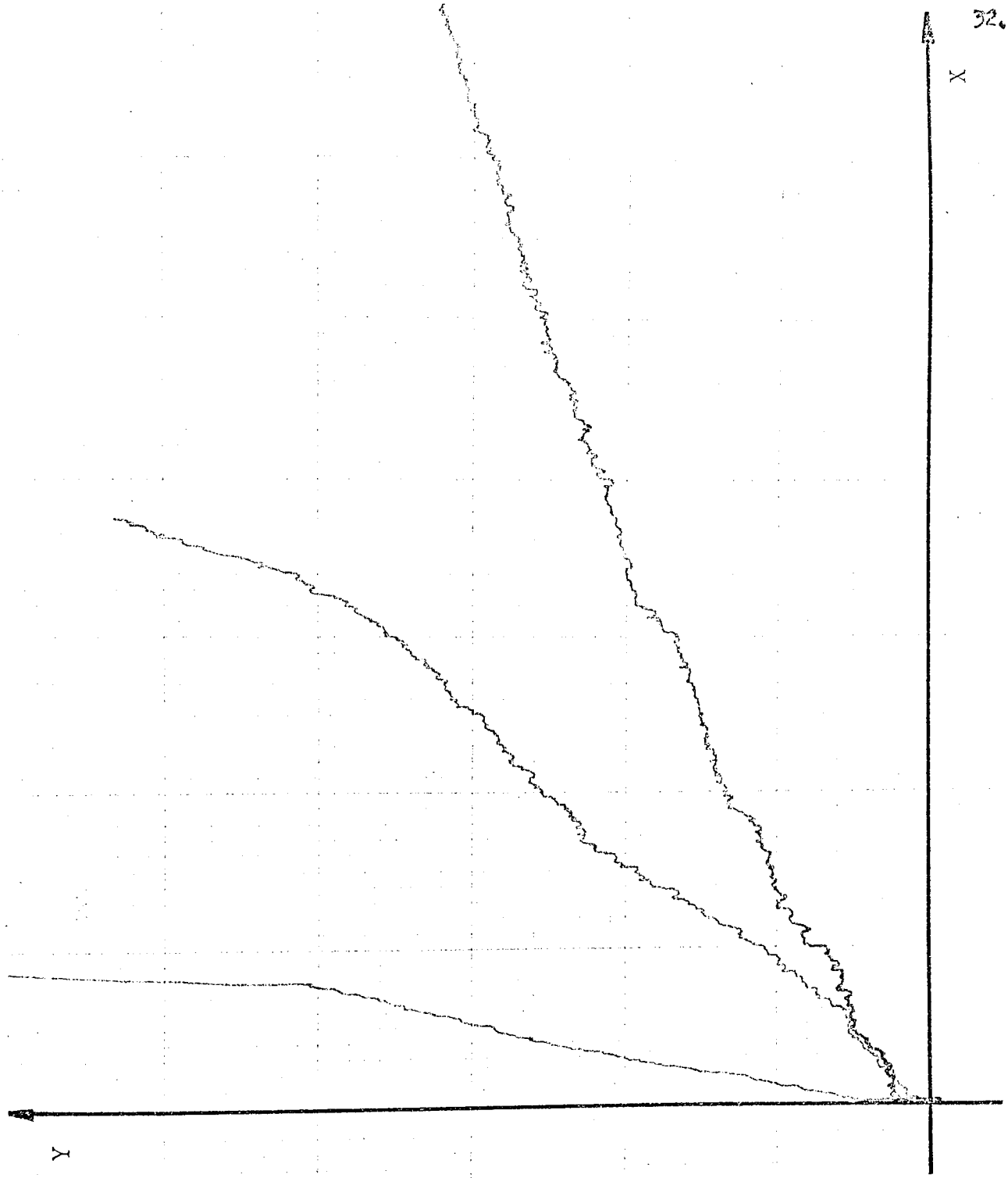

Scaling: X direction 1 inch ≡ 5 seconds

Y direction 1 inch ≡ 0.05 m of arc movement

Fig.3.6 Typical outputs from the chart plotter

out to determine a mathematical model for the low-velocity motion of arcs in a transverse magnetic field.Using a constant electrode gap (0.0025 metres), the velocity of the arc depends upon three variables:arc current,transverse magnetic field and electrode surface conditions.This latter parameter indicates the roughness of the surface (pitting,scratches etc.) and the amount of oxide on the surface.† Both are caused by the movement of an arc across the electrodes.

For each set of conditions applied to the arc,three arc runs were made;the average velocity of the arc was found from the slopes of these runs. The small field produced by the arc current in the electrodes was biassed off by generating an equal and opposite field in the air gap of the laminated former.The bias field was adjusted for a stationary arc.All field measurements were made with a Bell and Howell flux meter ,the probe being positioned in the electrode gap.

3.2.2 Arc Velocity Characteristics

Fig.3.7 shows the results of velocity versus transverse magnetic field for various surface conditions on brass electrodes and Fig.3.8 gives results of velocity versus field for various arc currents under constant surface conditions. In order to produce a practical method of measuring surface conditions,albeit approximate,the degree of roughness is measured from the number of times a 10 ampere arc is run down the electrodes in a field of 6×10^{-4} Tesla.Previous workers[21,22] have carried out tests with varying surface conditions, but these conditions have been produced by introducing a carefully measured coating of oxide on to the electrodes.The author feels that although this method

† It has been found[21,22] that the maximum velocity of an arc is reached when a small coating of oxide is present on the cathode surface.As the coating is increased,so the arc velocity decreases.The importance of the oxide coating would seem to originate from the properties of such a coating in affecting the field emission of electrons from the cathode surface.

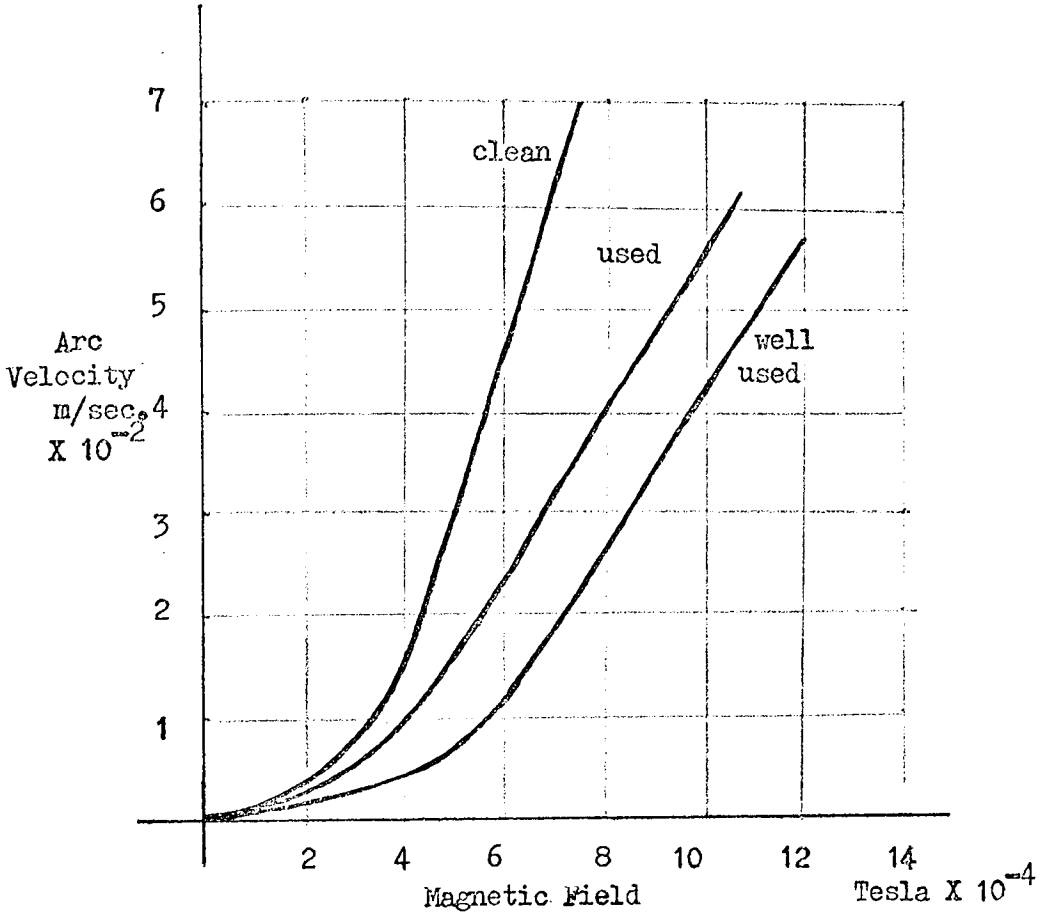

Fig.3.7 Arc velocity versus transverse magnetic field for different electrode surface conditions

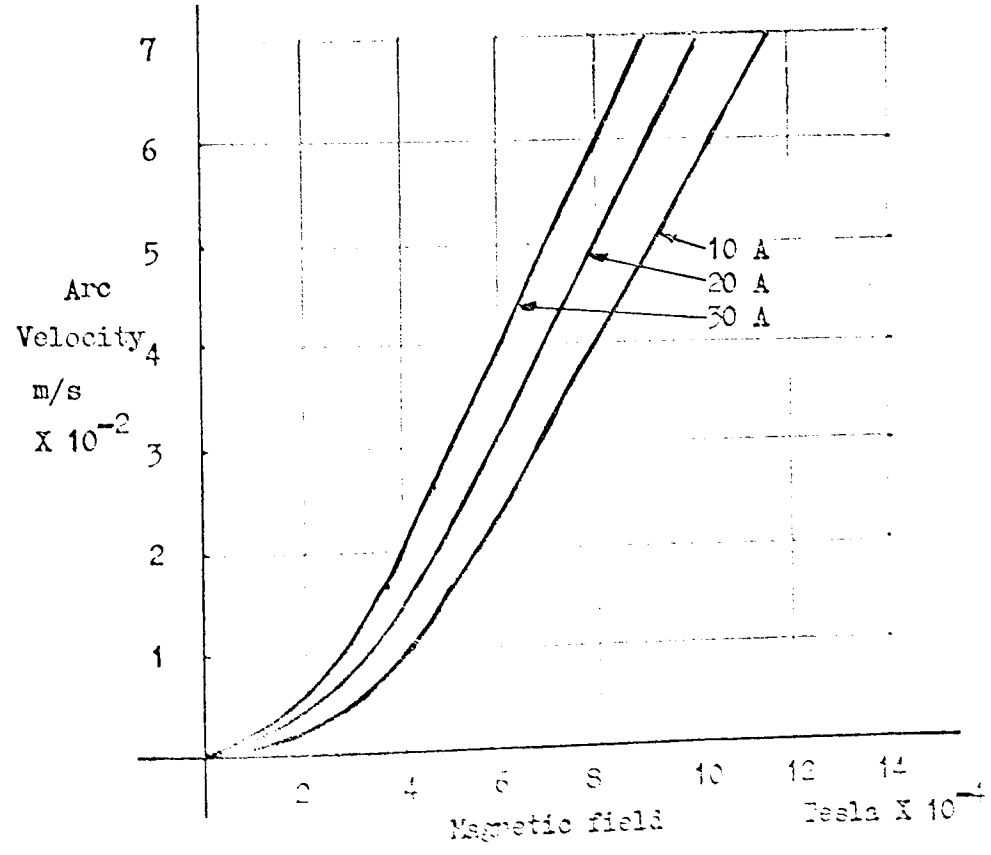

Fig.3.8 Arc velocity versus transverse magnetic field for different arc currents

of measuring degree of roughness is far more precise than the method proposed, its practical application is limited, since carefully-controlled oxide layers do not occur in practice. Furthermore, pitting of the electrodes cannot be produced in this way and pitting contributes heavily in determining the arc motion characteristics.

All results of arc runs, as indicated in section 3.2.1, are taken from the slope of a position-versus-time curve. Superimposed on this average slope is a random variation of arc velocity which, from observations, seems to be dependent on:

1) Surface conditions

2) Random movement of cathode and anode spots.

Such variations have been reported and discussed by workers in the field of high-velocity arc research.[21,22,26]

Since the arc has negligible inertia, very high acceleration and deceleration is possible so that 1) and 2) above produce immediate changes in velocity which impart to the arc a discontinuous mode of motion. This effect is more noticeable at very low fields (less than 3×10^{-4} Tesla), where it is quite possible for the arc velocity to suddenly drop to zero or even reverse its direction. As an illustration of the effects of varying surface conditions over the electrodes, an arc was run on fairly clean electrodes but with well-used conditions over a short length at the centre of the electrodes. The well-used conditions were obtained by maintaining a motionless arc at the required position for a few seconds. Fig. 3.9 shows an oscilloscope trace photograph of the output of the position-measuring system for this run. The effect of the sudden change in surface conditions can be clearly seen and for this particular run the arc dwells on the rough surface conditions for almost half the total run time.

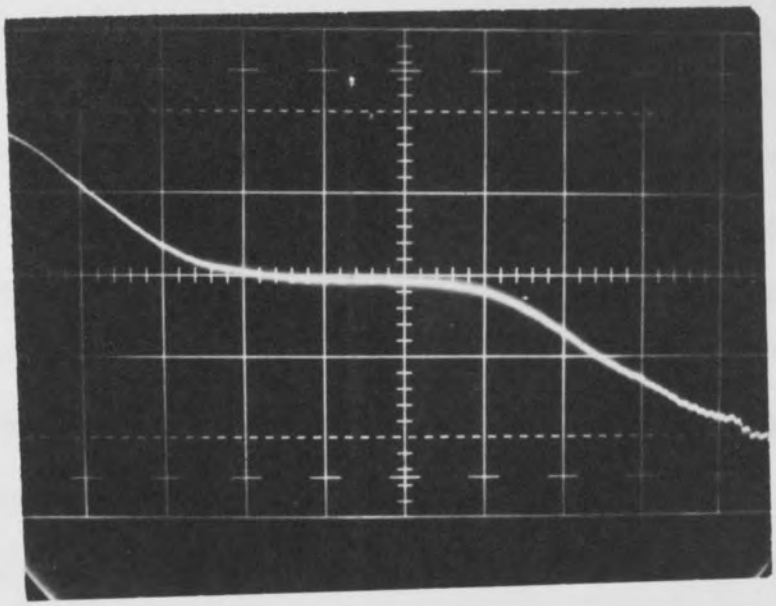

Fig.3.9 Output of arc position measuring system for conditions described in section 3.2.2

The scaling of Fig.3.9 is:

X 1 division ≡ 2 seconds

Y 1 division ≡ 0.05 metres

3.2.3 Electrode Surface Conditions

If one compares Fig.3.7 with Fig.3.8 ,varying the surface conditions can be seen to have far more effect on the velocity-versus-field curves than varying the arc current from 10 to 30 Amperes.'Used' electrodes are defined by two arc runs at 10 Amperes,'Well Used' defined by twenty arc runs,both at a field of 6×10^{-4} Tesla.After twenty arc runs the characteristics of the arc do not change noticeably for successive runs.At higher fields (greater than 5×10^{-4} Tesla) variations in surface conditions have far

more effect on clean electrodes than with well used electrodes;below 5 X 10^{-4} Tesla this effect does not occur.A possible explanation for this is that, as the arc is moving at very low velocities,the oxide deposits taking place around the cathode root (the predominant root in the arc motion process) have time to build up sufficiently to slow the arc down as it progresses through them.Thus at low fields the arc generates its own 'Used' surface conditions on an initially clean electrode.This is certainly a possible hypothesis,since an initially clean electrode,which has had one arc run at less than 0.01 m/second (less than 4 X 10^{-4} Tesla),has very high deposits of oxide on the arc track.

Burkhard[21] found that an arc moved faster on thinly-oxidised electrodes† than on clean electrodes and concluded from this that an arc would move faster on tracks left by a previous arc than on no arc tracks.No evidence has been found from low-velocity arc experiments that the arc moves faster on slightly-oxidised electrodes;but this is probably because a thin coating could not be obtained with low velocity arcs.In support of the above claim,however,it has been found that an arc has a tendency to move along previous arc tracks;this is particularly noticeable on tracks left by an arc that has extinguished itself by running out of the gap(see 3.1.1).In such circumstances,if this track is not removed there is a high probability of successive arcs also extinguishing themselves at this point.On 'Well Used' electrodes the oxide coating can cover the whole width of the electrodes; this causes the arc to wander to one side or other of the gap,through the oxide path,tending to extinguish itself and for this reason the arc model becomes more unstable as the surface conditions on the electrodes deteriorate.

With the apparatus described in 3.1.4,there is no way of measuring

† See 3.2.1

the velocity of an arc as it extinguishes itself; but it may well be that the velocity is greater when the arc runs along previous arc tracks than on a clean surface, as Burkhard suggests.

3.2.4 Arc Velocity Characteristics with Various Electrode Materials

Fig.3.10 gives velocity versus field curves for all combinations of brass, copper and stainless steel electrodes†. The apparatus used for this experiment is shown in Fig.3.11. The electrodes are not water cooled (in order to allow easier removal) and the gap is adjustable. The electrode configuration is shown in Fig.3.12. Although this configuration is not as stable as the previous one for all surface conditions, under relatively clean conditions its stability is quite high.

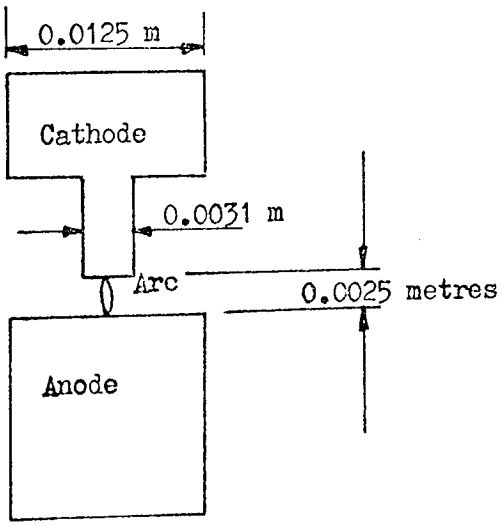

Fig.3.12 Alternative electrode configuration

All experiments were carried out with electrodes whose surface conditions corresponded to two ten-ampere arc runs at a field of 6×10^{-4} Tesla; the electrode gap was 0.0025 metres and the arc current ten amperes. The electrodes

† Results of high-velocity arcs on varying materials can be found in the literature [28,29,30,31].

Key

Trace	Cathode Material	Anode Material
1	Copper	Copper
2	Stainless Steel	Brass
3	Stainless Steel	Copper
4	Brass	Copper
5	Copper	Brass
6	Brass	Stainless Steel
7	Brass	Brass
8	Stainless Steel	Stainless Steel
9	Copper	Stainless Steel

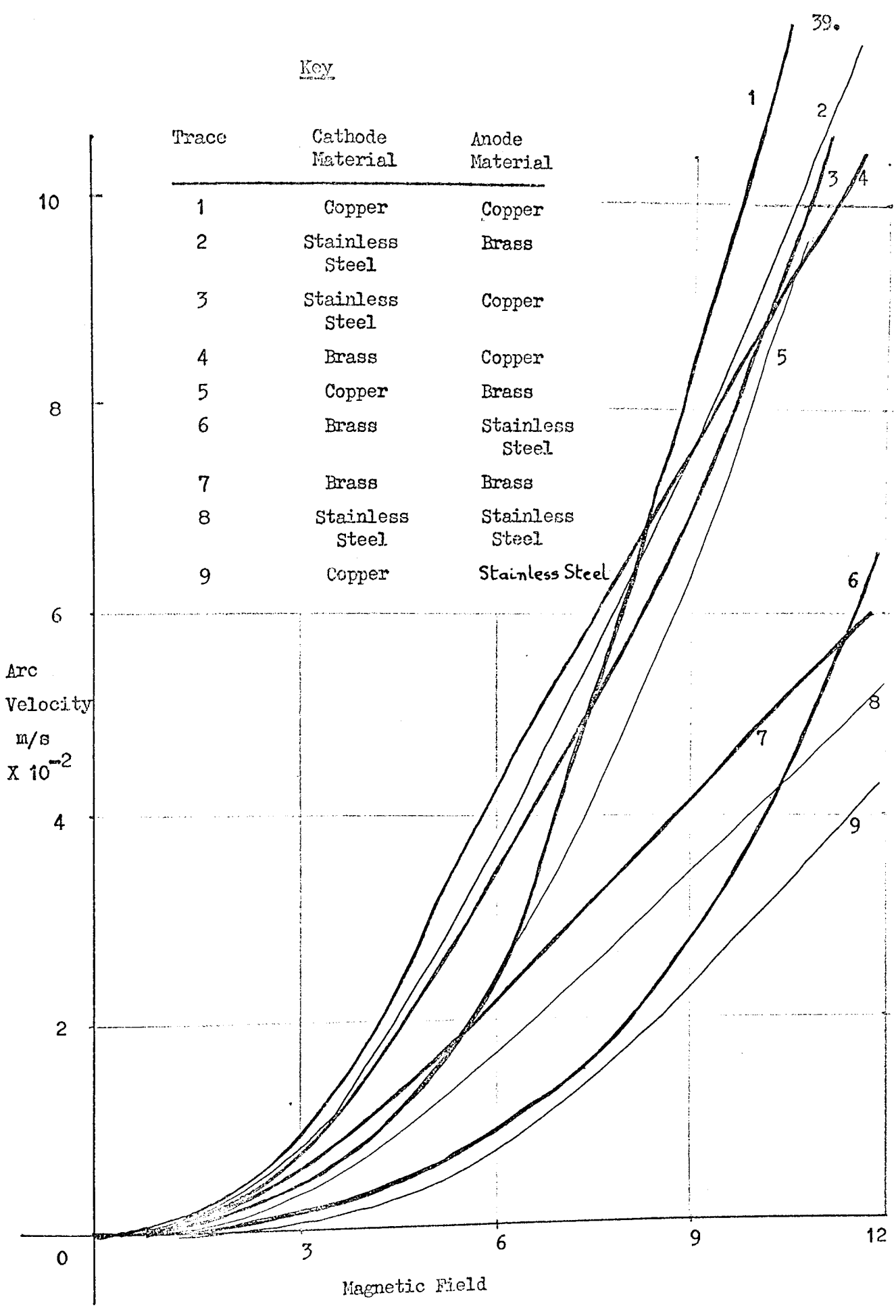

Fig.3.10 Arc velocity versus transverse magnetic field for varying electrode materials

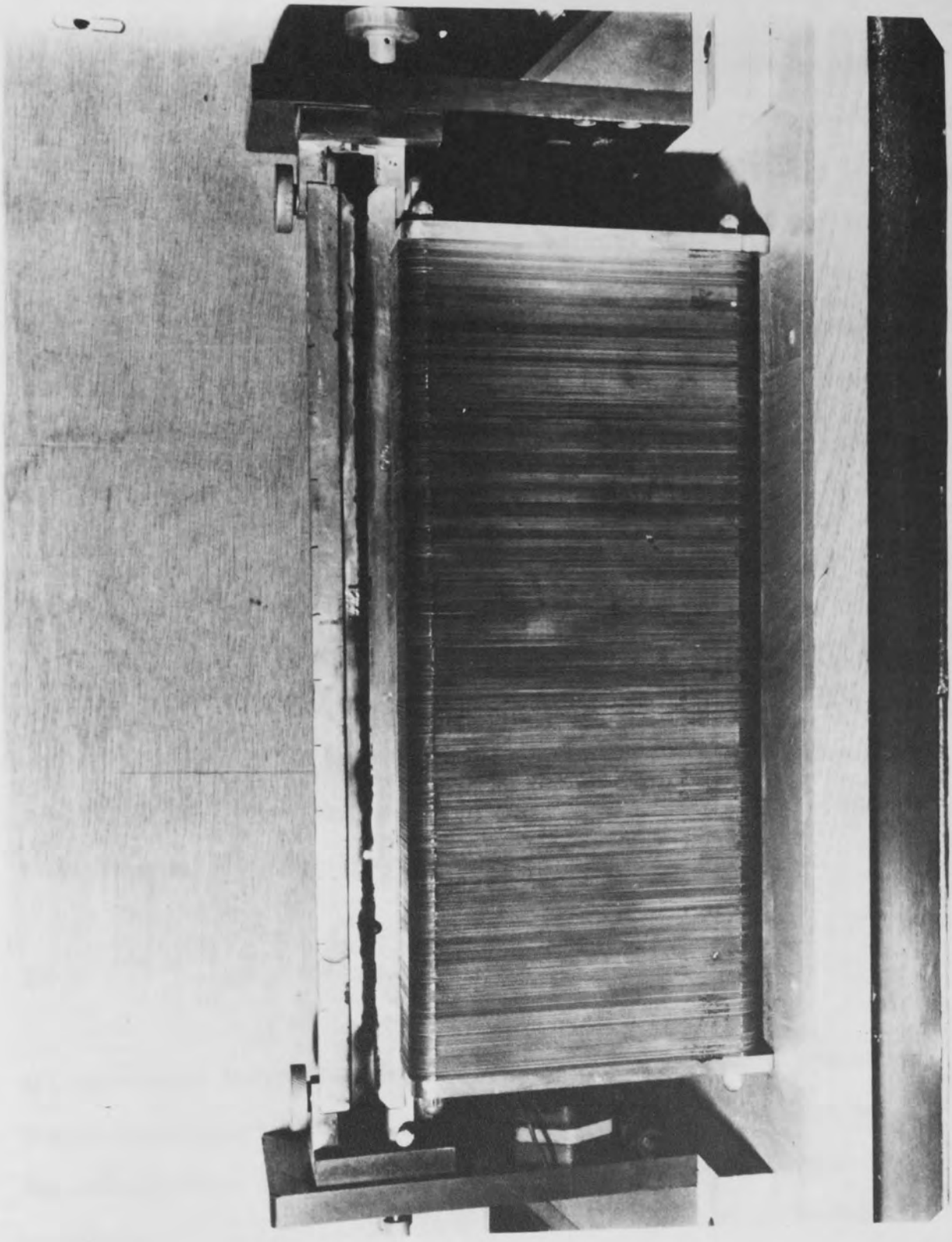

Fig.3.11 'Arc plant' used for changing electrode materials

were initially at room temperature before each arc run and each run was short enough in time to prevent the electrodes from heating up to too high a temperature; this was done to preserve, as nearly as possible, the same conditions as used with the water cooled electrodes. Experiments have shown that the arc motion can be affected by the temperature of the surface over which it is moving[26]. The electrode materials used for the various tests are indicated by the key in Fig. 3.10 and close examination reveals that the electrode materials can be classified in to two main sections:

a) High velocity systems

b) Low velocity systems

Table 3.1 lists the electrode materials and their classification.

The copper seems predominant in the high velocity systems and the stainless steel predominant in the low velocity systems. Although the cathode root has been observed as the predominant root in the arc movement mechanism, the material of the cathode electrode does not seem to be predominant as a factor influencing the arc velocity versus field characteristics.

3.2.5 Electrode Polarity Reversal

All experiments discussed so far have been performed with the cathode as the bottom electrode, but if the polarity is reversed (so that the anode is below the cathode) erratic arc movement occurs which rapidly leads to the arc extinguishing itself. This effect is very noticeable on clean electrodes but the arc is more stable on used electrodes. Fig. 3.13 shows a comparison between the arc tracks left on:

a) A cathode electrode in the lower position

b) An anode electrode in the lower position.

HIGH VELOCITY SYSTEMS	
Cathode Material	Anode Material
Brass	Copper
Copper	Copper
Stainless Steel	Copper
Stainless Steel	Brass
Copper	Brass

LOW VELOCITY SYSTEMS	
Cathode Material	Anode Material
Brass	Brass
Brass.	Stainless Steel
Stainless Steel	Stainless Steel
Copper	Stainless Steel

Table 3.1 Classification of electrode materials

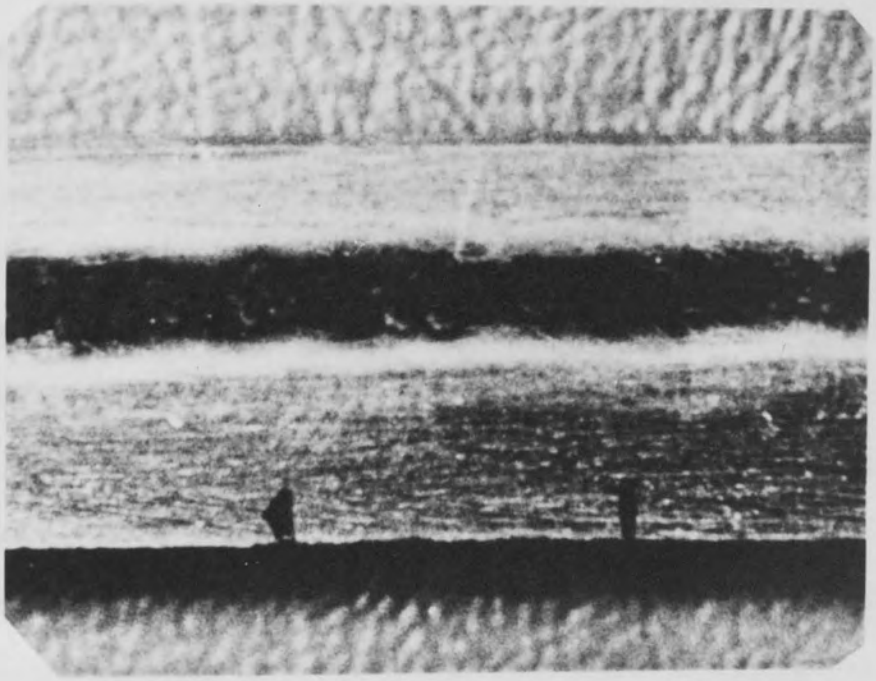

a) Arc track on cathode electrode with cathode underneath anode

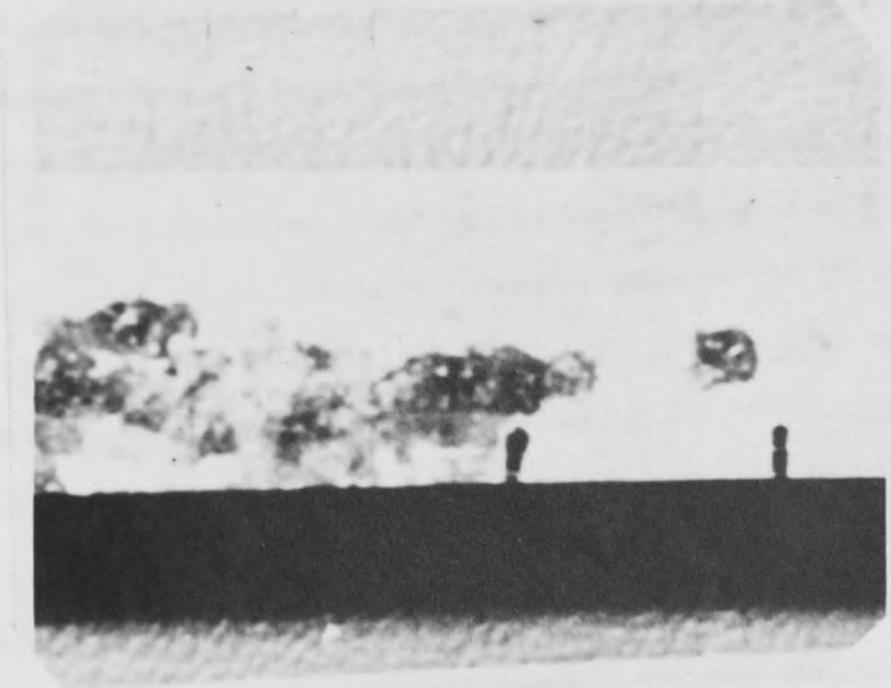

b) Arc track on anode electrode with anode underneath cathode

Fig.3.13

In Fig.3.13 the electrode configuration is maintained for both a) and b), whilst the polarity is reversed.The same effect of erratic arc motion was observed on configurations of both Fig.3.2 and Fig.3.12. A comparison between a) and b) of Fig.3.13 reveals that,although the arc track of a) is relatively continuous,the arc track of b) indicates large jumps of the anode root.The phenomenon of discrete anode root motion is not unknown and has been reported previously[20],but no mention of electrode configuration,with reference to the stability of arc motion,has been recorded.The mechanism of this erratic movement has not been thoroughly studied since this represents a digression from the main research,but certain work has been carried out and is presented below.

A ten-ampere arc running on brass electrodes in a field of 6×10^{-4} Tesla was filmed at approximately 3000 frames per second using a Fastax camera.Fig.3.14 shows a small section of the film demonstrating the discrete motion of the anode (upper) root.The cathode (lower) root is stationary over the two frames shown and,infact, is stationary over about ten frames in the vicinity of the section shown.The anode root can be seen to jump from a position to the left of the cathode root to a new position to the right of the cathode root.Previous research into the discrete motion of the anode root seems to indicate that the phenomenon is due to the arc column being attracted to the anode electrode and 'shorting out' the existing root,so forming a new root.This can also explain the double root clearly visible on the anode electrode of Fig.3.14;however,since the cathode exhibits multiple roots (far more closely spaced than those of the anode), this phenomenon of 'shorting out' cannot be the only explanation.One hypothesis offered by the author and others[27] is that a single emission site is not sufficient to maintain the arc and so more than one root is necessary

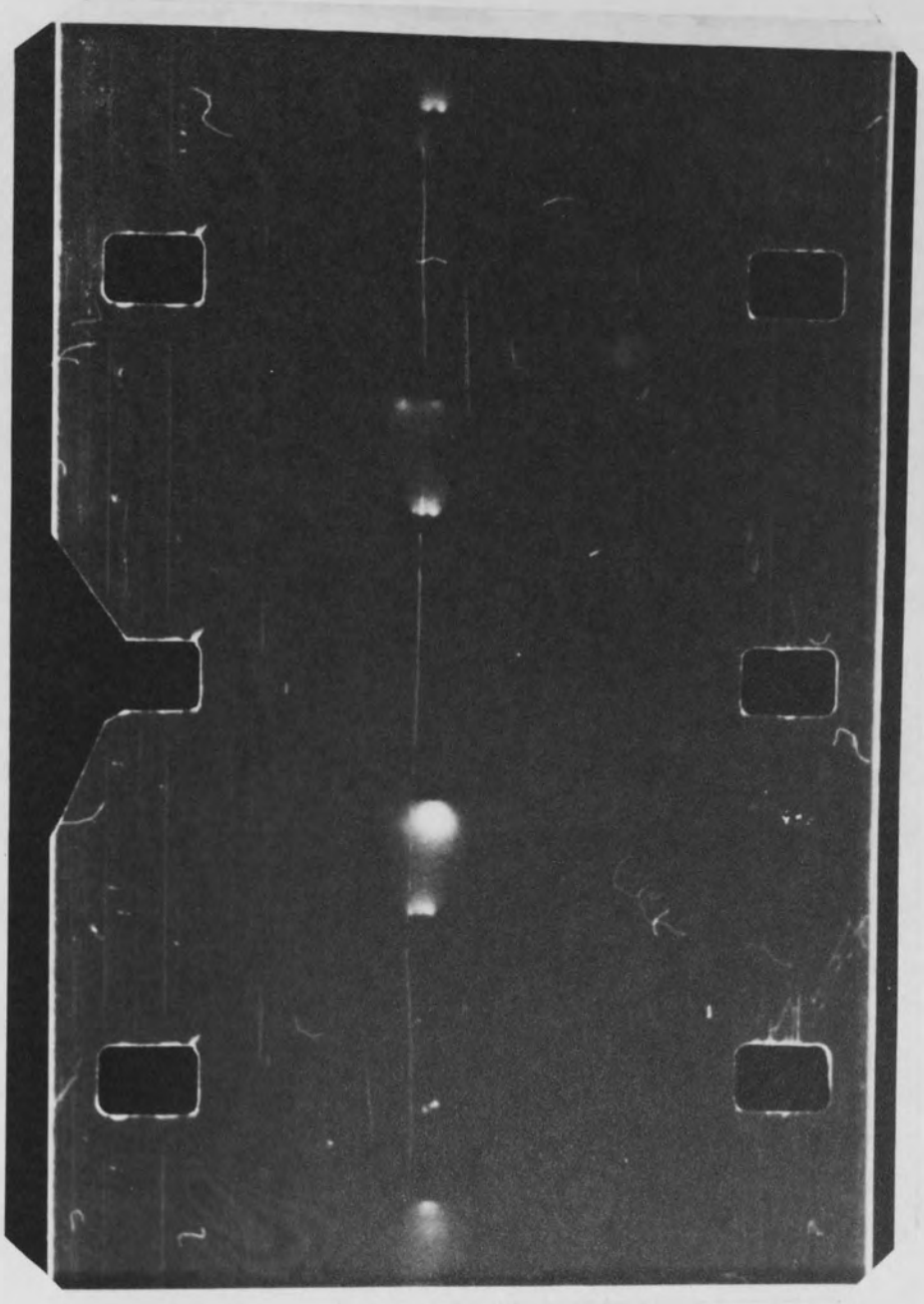

Fig.3.14 Section of film taken by a Fastax camera(at about 3000 frames per second) of a 10 Ampere arc running between brass electrodes

for the existance of the arc. Depending on their position, these could appear as multiple or single roots.

In both configurations of electrodes used, the upper electrode restricts the arc to movement along its length, whereas the lower electrode allows movement over both its width and length. With the anode on the lower electrode far more random movement is possible than in the upper position and so this could give rise to the erratic movement observed. Fig. 3.13 b) indicates a large anode movement over the width of the electrodes.

3.3.1 Mathematical Model

Several papers on the correlation of experimental results for arc velocities in transverse magnetic fields have been written[9,16,17]. Dautov and Zukhov[15] have applied dimensional analysis to the electric arc and have produced a set of dimensionless groups from which the following equation has been obtained:

$$\frac{\rho^{1/2} U d}{\mu_o^{1/2} I} = f\left\{\frac{\mu_o I}{B d}, \frac{B^2}{\mu_o p}, \frac{L}{d}\right\} \quad \ldots\ldots\ldots (3.1)$$

where:

ρ = Ambient gas density

p = Ambient gas pressure

L = Characteristic surface width on which the arc moves

U = Velocity of the arc

I = Arc current

d = Electrode gap

B = Transverse magnetic field

μ_o = Permeability of free space

From experimental results correlated with eqn.(3.1) it has been found that[17] the dependence of eqn.(3.1) on $\frac{B^2}{\mu_o p}$ and $\frac{L}{d}$ is negligible and so the dominant form of the equation can be written:

$$\frac{\rho^{1/2} U d}{\mu_o^{1/2} I} = f\left\{\frac{\mu_o I}{B d}\right\} \qquad \ldots\ldots\ldots\ldots\ldots\ldots (3.2)$$

Since μ_o is constant and, if ρ is constant, then from eqn.(3.2) :

$$\frac{U d}{I} = f\left\{\frac{I}{B d}\right\} \qquad \ldots\ldots\ldots\ldots\ldots\ldots (3.3)$$

Guile and Naylor[17] have also obtained a similar relationship using the magnetic and aerodynamic forces acting on an arc column.

By correlating experimental data with eqn.(3.3), an approximate equation for an arc moving in air at atmospheric pressure has been found to be:

$$\frac{U d}{I} \simeq 4.6 \left\{\frac{I}{B d}\right\}^{-0.6} \qquad \ldots\ldots\ldots\ldots (3.4)$$

Results have also been obtained[17] for arcs burning in argon and helium and

for arcs held by a magnetic field against an argon flow.[17] The equation for the mean line for both helium and argon is:

$$\frac{U\,d}{I} \simeq 4.0 \left\{ \frac{I}{B\,d} \right\}^{-0.6} \qquad \ldots\ldots\ldots\ldots\ldots\ldots (3.5)$$

From eqn.(3.4) and eqn.(3.5) a general trend can be observed. The experimental results hold for arcs running on either clean or used electrodes with velocities not lower than 1.3 metres/second.

3.3.2 A Modification to the Existing Arc Model

In order to examine the usefulness of eqn.(3.4) the following parameters were used:

$$B = 6 \times 10^{-4} \text{ Tesla}$$

$$I = 10 \text{ Amperes}$$

$$d = 2.5 \times 10^{-3} \text{ metres}$$

From eqn.(3.4) :

$$U \simeq \frac{4.6\,I}{d} \left\{ \frac{I}{B\,d} \right\}^{-0.6}$$

or

$$U \simeq \frac{4.6\,I^{0.4}\,B^{0.6}}{d^{0.4}} \qquad \ldots\ldots\ldots\ldots\ldots\ldots (3.6)$$

Substituting the parameters into eqn.(3.6) gives:

$$U \simeq 1.5 \text{ metres/second} \qquad \ldots\ldots\ldots\ldots\ldots\ldots (3.7)$$

Using the same parameters on Fig.3.7 we obtain a velocity of:

$$U \simeq 2.5 \times 10^{-2} \text{ metres/second} \quad \ldots\ldots\ldots\ldots\ldots\ldots (3.8)$$

(for used electrodes)

There is a multiplying error of 60 between eqn.(3.7) and eqn.(3.8) and from this we must conclude that eqn.(3.4) is not valid for the conditions given. Adams et al[9] indicate that eqn.(3.4) does not take into account vapour-jet interactions, which arise mainly at very low spacings, and the degree of oxidation of the electrodes. The latter consideration can also have an effect on clean electrodes for low velocity arcs (as indicated in 3.2.3) and probably, to a lesser extent, on the higher arc velocities considered in this research.

If we assume that eqn.(3.3) still holds for the low velocity arc model, then we can calculate the value of constant and index required to produce the form of equation:

$$\frac{U\,d}{I} = K\left\{\frac{I}{B\,d}\right\}^{n} \quad \ldots\ldots\ldots\ldots\ldots\ldots (3.9)$$

Fig.3.15 gives a log/log plot of $\frac{U\,d}{I}$ versus $\frac{I}{B\,d}$ for the curves shown on Fig.3.7 and Fig.3.8. From Fig.3.15 we can see:

a) That the points approximate to a set of straight lines indicating the validity of eqn.(3.9)

b) The slopes of these lines are almost constant at a value of -2.

Hence:

$$\frac{U\,d}{I} \simeq K\left\{\frac{B\,d}{I}\right\}^{2} \quad \ldots\ldots\ldots\ldots\ldots\ldots (3.10)$$

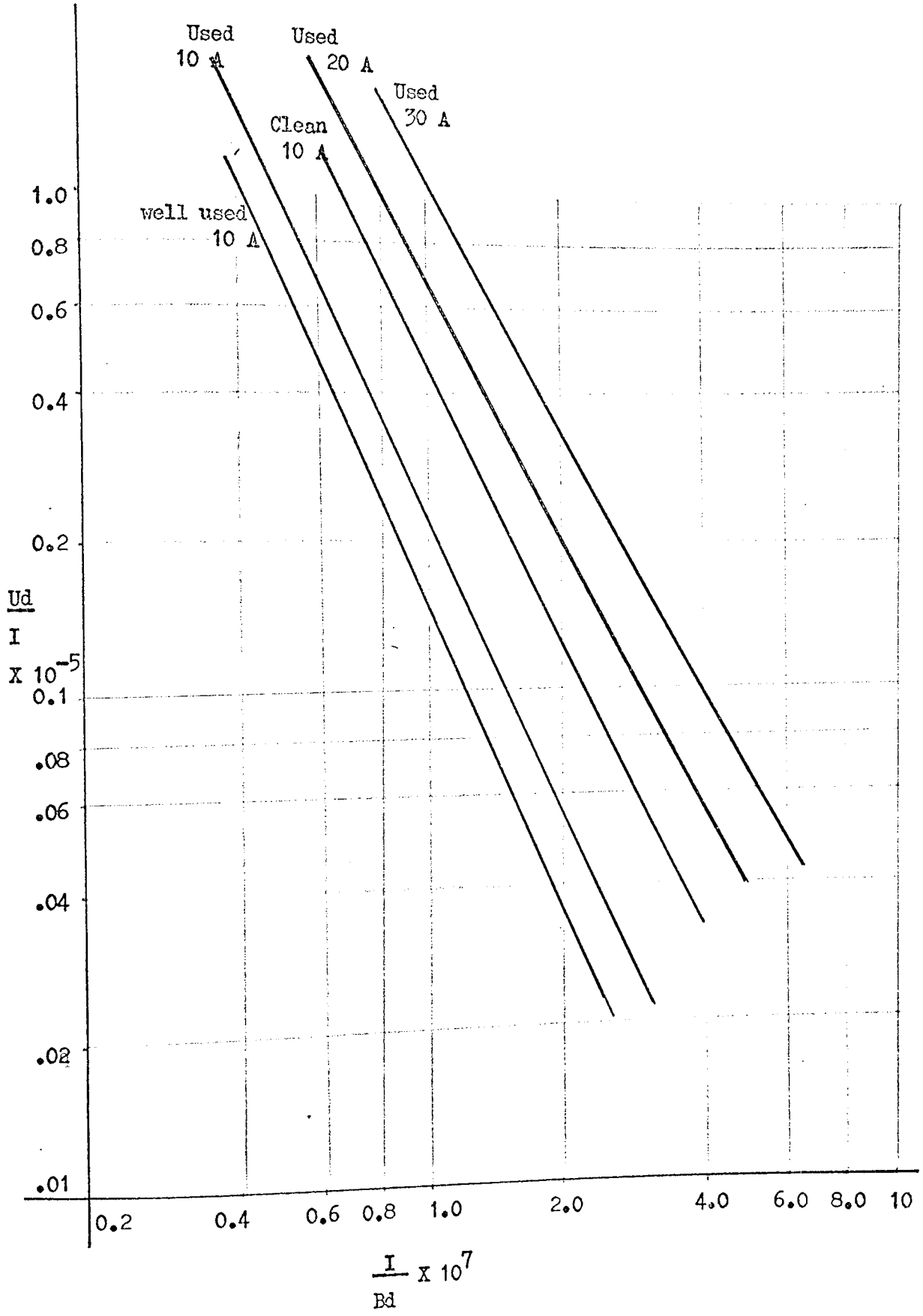

Fig.3.15 $\frac{Ud}{I}$ versus $\frac{I}{Bd}$ plotted on log/log coordinates for varying arc currents and electrode surface conditions

Fig.3.16 shows a plot of $\frac{U\,d}{I}$ versus $\left\{\frac{B\,d}{I}\right\}^2$ for conditions presented in Fig.3.7 and Fig.3.8. From the slopes of these graphs values of K have been obtained for different surface conditions and arc currents and these are listed in Table 3.2.

Electrode Surface Conditions	Arc Current	K
Clean	10 Amperes	0.5×10^9
Used	10 Amperes	0.25×10^9
Well Used	10 Amperes	0.16×10^9
Used	20 Amperes	0.65×10^9
Used	30 Amperes	1.0×10^9

Table 3.2 Values of K for different surface conditions and arc current

For used electrodes with arc currents of 10,20 and 30 Amperes $\frac{K}{I}$ is almost constant and:-

$$K \simeq 0.3 \times 10^8 I \quad \ldots\ldots\ldots\ldots\ldots\ldots\ldots\ldots (3.11)$$

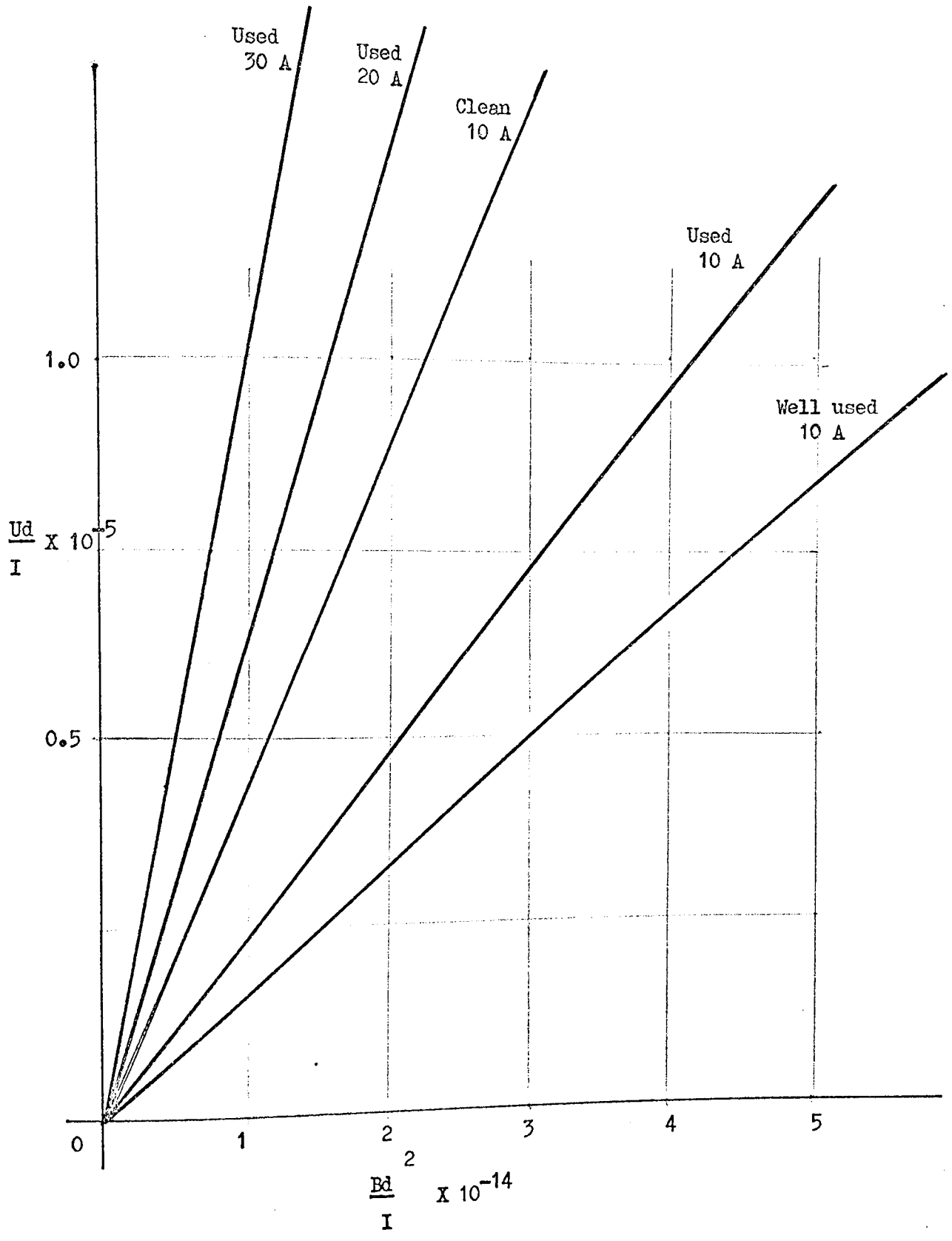

Fig.3.16 $\frac{Ud}{I}$ versus $\frac{Bd^2}{I}$ for various arc currents and electrode surface conditions

Substituting eqn.(3.11) in eqn.(3.10) :

$$\frac{U\,d}{I} \simeq \frac{0.3 \times 10^{8}}{I} (B\,d)^{2}$$

this can be re-arranged to give:

$$U \simeq 7.5 \times 10^{4} B^{2} \qquad \text{.....(3.12)}$$

(d = 0.0025 metres)

Eqn.(3.12) is plotted in Fig.3.17 together with the experimental curves of Fig.3.7 and Fig.3.8.

3.3.3 A Mathematical Representation of Electrode Surface Conditions

From Fig.3.17 it can be seen that, although eqn.(3.12) agrees well with the results for 10, 20 and 30 Ampere arcs on used electrodes, the results for 10 Ampere arcs on clean and well used electrodes do not match eqn.(3.12). Clearly eqn.(3.12) must be modified to include variations in electrode surface conditions. Section 3.2.2 details an experimental method of defining surface conditions, but this cannot be applied directly to a mathematical arc model. The simplest solution is to define a 'gain' Ψ which has a value of 1.0 for clean electrodes and zero for 'infinitely rough' electrodes, i.e conditions upon which the arc is unable to move. Using the results given in Table 3.2 and eqn.(3.12), an approximate arc model may be derived:

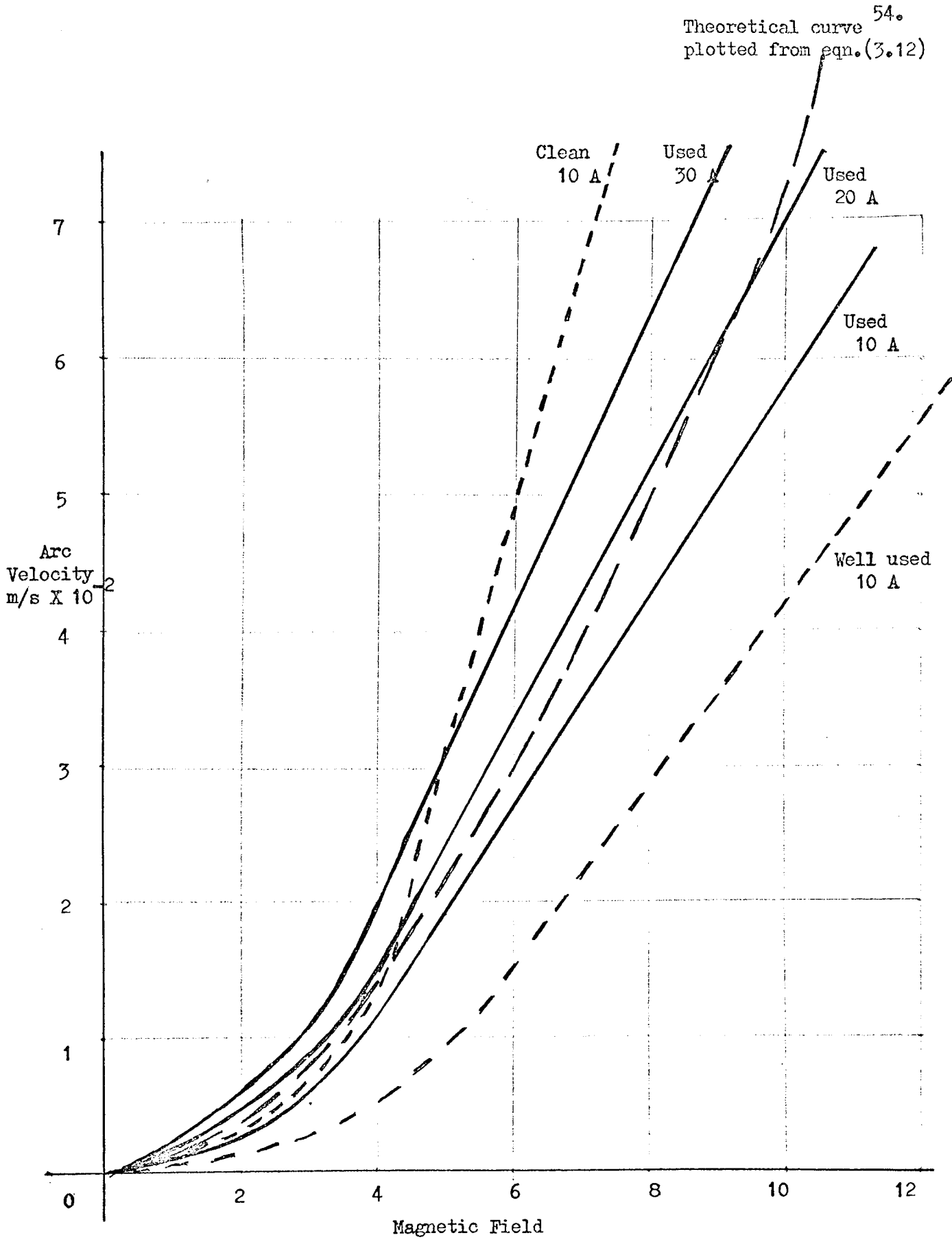

Fig.3.17 Comparison of approximate arc model with experimental results

$$U \simeq \Psi \; 0.15 \; B^2 \times 10^6 \quad \ldots\ldots\ldots\ldots\ldots\ldots\ldots\ldots\ldots\ldots (3.13)$$

Table 3.3 gives values of Ψ for varying surface conditions.

Electrode Surface Conditions	Ψ
Clean	1.0
Used	0.5
Well Used	0.3

Table 3.3 Values of Ψ for varying surface conditions

The figures quoted in Table 3.3 are derived for average surface conditions. The instantaneous value for Ψ fluctuates about the average value and can fall to zero especially on well used electrodes. An attempt to express Ψ in terms of number of arc runs n (see 3.2.2) results in an expression:

$$\Psi \simeq 0.3 + 0.7 \; e^{-n/2} \quad \ldots\ldots\ldots\ldots\ldots\ldots (3.14)$$

Eqn.(3.14) is plotted in Fig.3.18 together with the three experimental points for clean, used and well-used electrodes. Although three points cannot give a true representation of a characteristic curve, eqn.(3.14) fits the points given and concentrates the important variation in Ψ to the first five arc runs, which agrees with experimental observation.

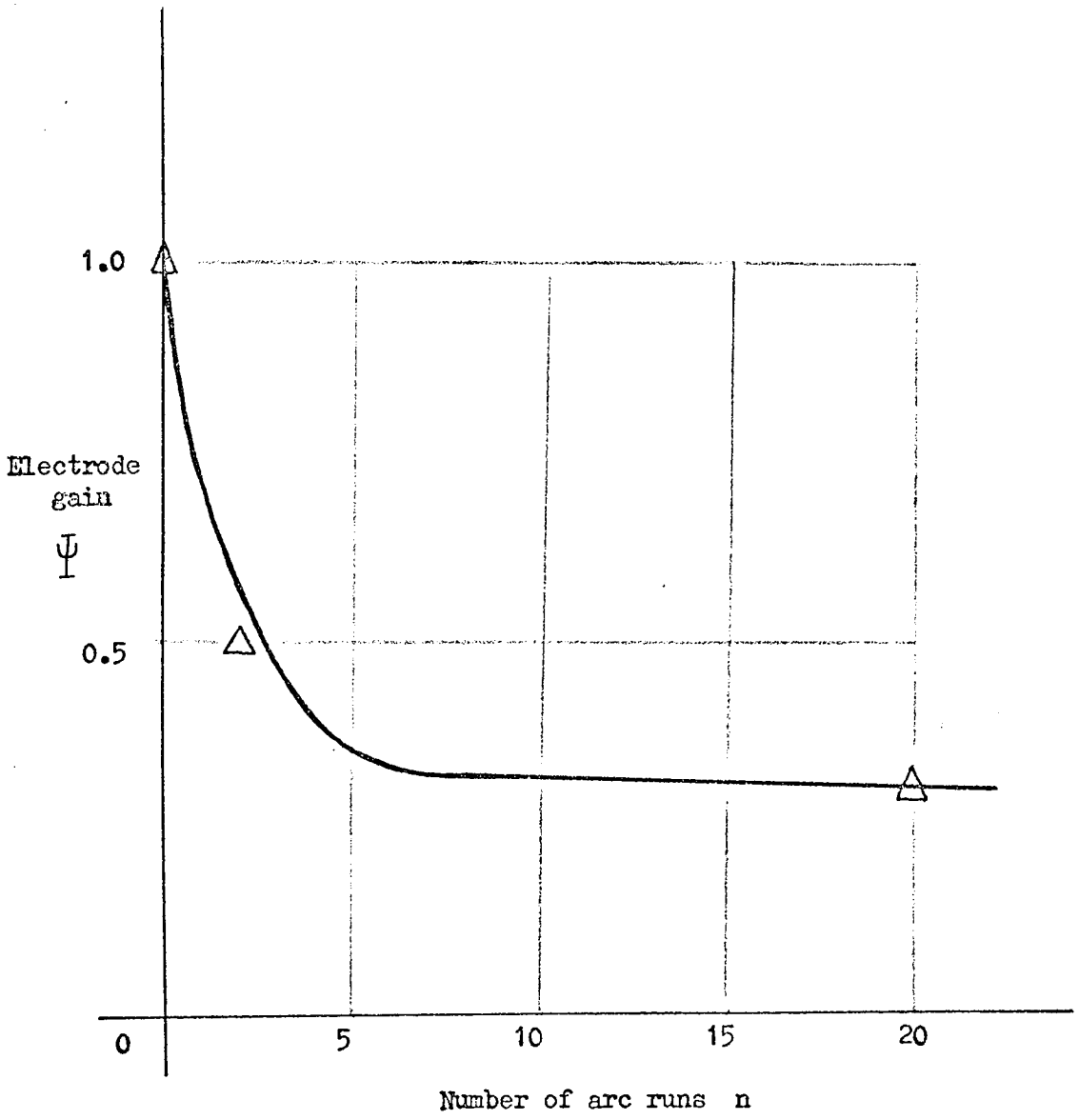

Theoretical curve plotted from eqn.(3.14)

△ Experimental results

Fig.3.18 Electrode gain plotted against number of arc runs

3.4 Summary

A simple arc model, based on typical industrial processes of seam welding, profile cutting and zone refining, has been developed and various arc motion characteristics of arc velocity versus transverse magnetic field have been obtained.

From experimental observation and correlation of data, the low-velocity arc can be represented by a zero-order transfer function (no time constants) of output velocity to input transverse magnetic field. The non-linear gain of the system is dependent on :

a) The input field

b) The electrode surface conditions.

By combining eqn.(3.13) and eqn.(3.14), it is possible to predict arc velocity to within $\pm$ 30% using readily attainable parameters; this is perfectly acceptable if one considers the randomness associated with the electrode surface conditions.

The time constant of the field coil is 0.15 seconds and so the final arc model transfer function can be written:

$$\frac{V_o}{v_i}(s) = \frac{G}{1 + 0.015s} \qquad \text{.....(3.15)}$$

where $G = f(v_i, \Psi) \simeq K v_i \Psi$ (i.e a square law output)

V_o = Arc velocity

v_i = Input voltage to bias winding amplifier

K = Gain constant of the system

Ψ = 'Gain' of electrode surface conditions

CHAPTER 4

Control System Analysis

4.1.1 The uncompensated arc velocity control system

In order to create an industrially usable system of arc control, one must be able to control both the velocity and position of the arc. Both controlled parameters, however, can be associated with velocity control, since it is visualised that the only useful position control is one where the arc is moved from position A to position B at a certain velocity decided by the control command. Position control, therefore, can be associated with velocity control, the command of the controller depending upon the position of the arc. Since the velocity of the arc is obtained from the position signal this type of control is readily available. Both analogue and digital feedback signals can be used, the analogue signal generated as explained in 2.3.1 and the digital signal as in 2.3.1 and 2.3.2. For the purposes of this feasibility study, the digital control has been decided on for three main reasons:

1) The feedback transfer function is more complex with analogue filtering at the differentiator (see 2.3.1)
2) Command changes with position can be easily accomodated by a digital controller.
3) Means of adapting the system to changes in surface conditions are far more realistic with digital control.

4.1.2 The Control System Block Diagram

The block diagram of the computer (digital) control system without any form of compensation is given in Fig. 4.1. The output of the first difference

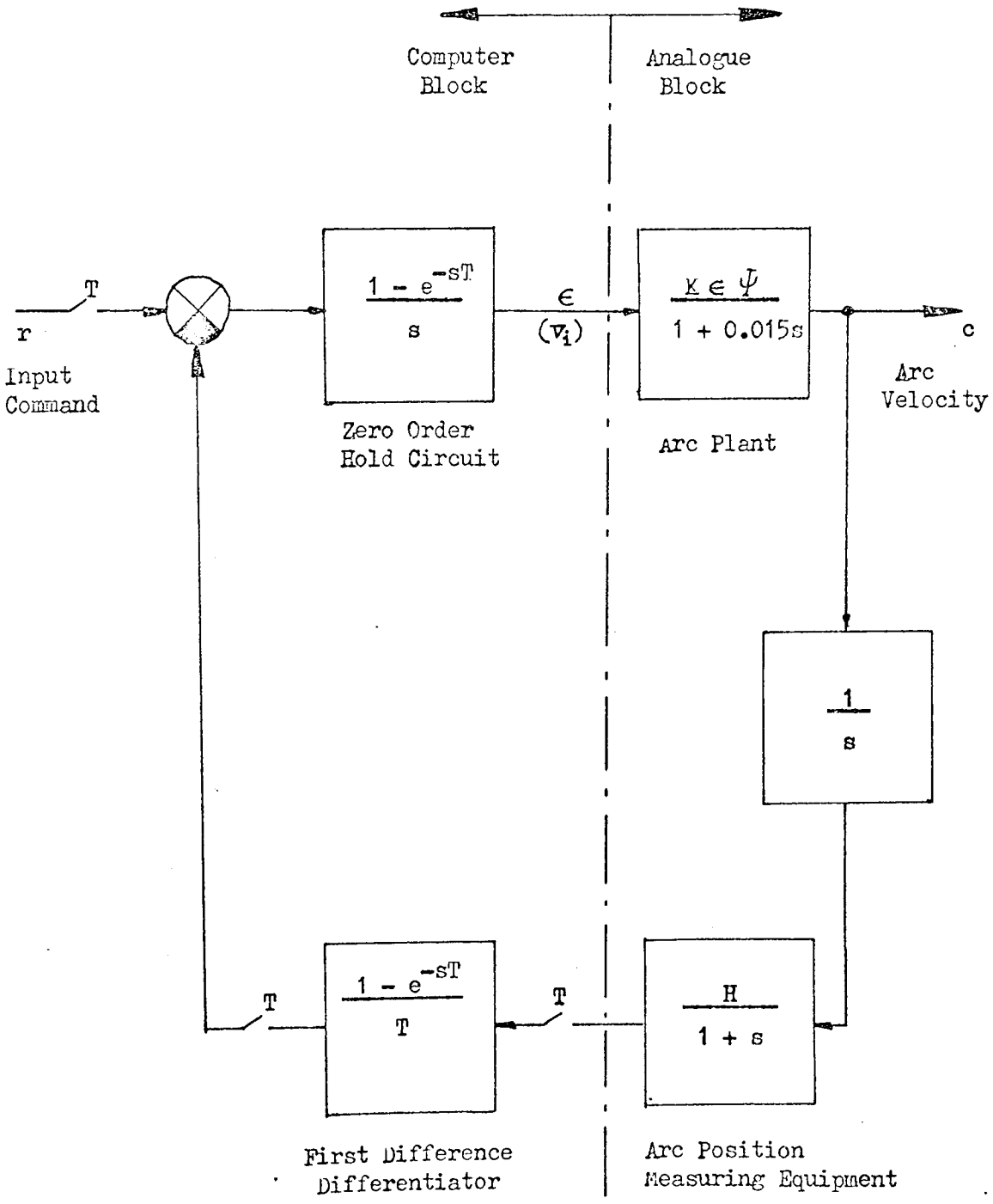

Fig.4.1 Block diagram of control system without compensation

calculator is delayed by T as shown in 2.3.2 and is divided by T in order to produce a transfer function gain of 1. Brief details of the zero-order hold circuit are given in 2.3.2; the 'arc plant' transfer function is taken from eqn.(3.15). The dependence of the arc plant gain on its input can be eliminated by a square root function on the computer output.

If the input to the square root function is ϵ then the output is $(\epsilon)^{1/2}$ and the output of the 'arc plant' is:

$$\left\{ \frac{K \epsilon^{1/2} \Psi}{1 + 0.015s} \right\} \epsilon^{1/2} = \frac{K \epsilon \Psi}{1 + 0.015s} \quad \ldots\ldots\ldots\ldots (4.1)$$

Fig.4.2 a) shows the linearised block diagram of the controller and Fig.4.2 b) gives the simplification of this block diagram.

4.1.3 An Analysis of the Uncompensated System

Consider the control system shown in Fig.4.3.

From this:

$$\epsilon^*(z) = r^*(z) - \epsilon^*(z) \left\{ G(s)\, H(s) \right\}^*(z) \quad \dagger$$

or

$$\epsilon^*(z) = r^*(z) - \epsilon^*(z)\, GH^*(z) \quad \ldots\ldots\ldots\ldots\ldots (4.2)$$

and

$$c^*(z) = \epsilon^*(z)\, G^*(z) \quad \ldots\ldots\ldots\ldots\ldots\ldots\ldots (4.3)$$

---

† For details of the sampled data analysis presented in this and later sections see Jury[33].

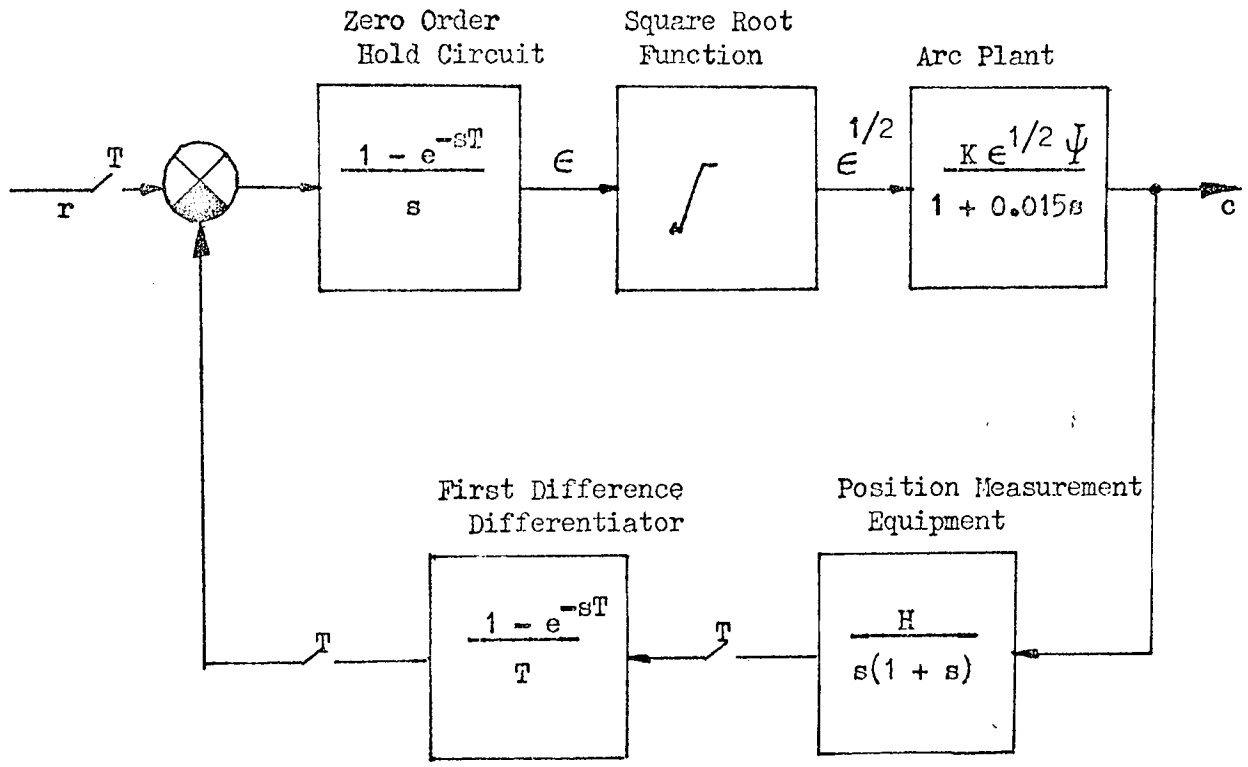

a)

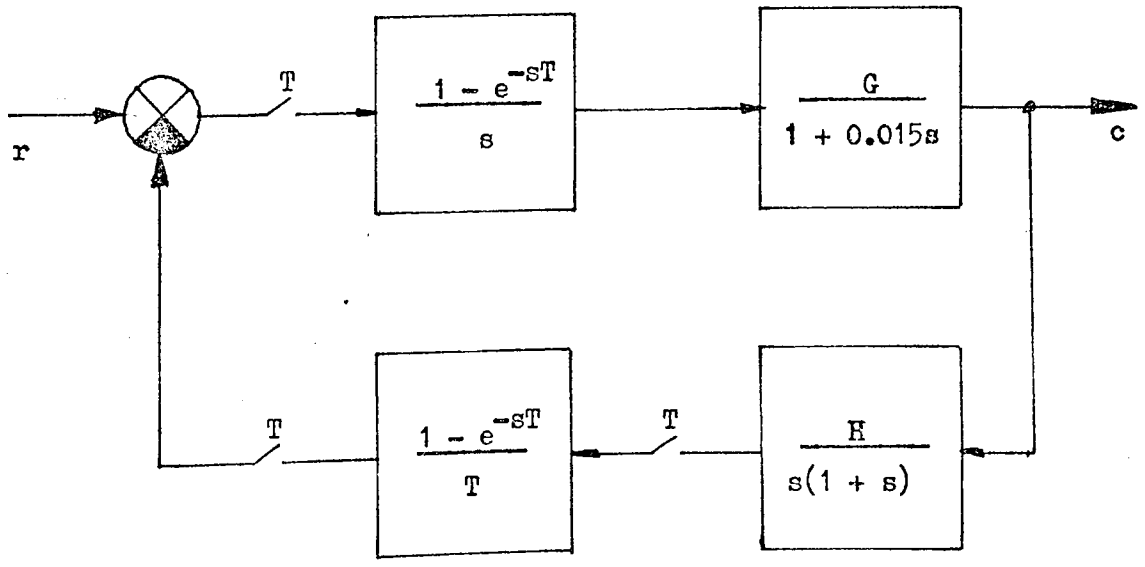

b)

Fig.4.2 Block diagram simplification

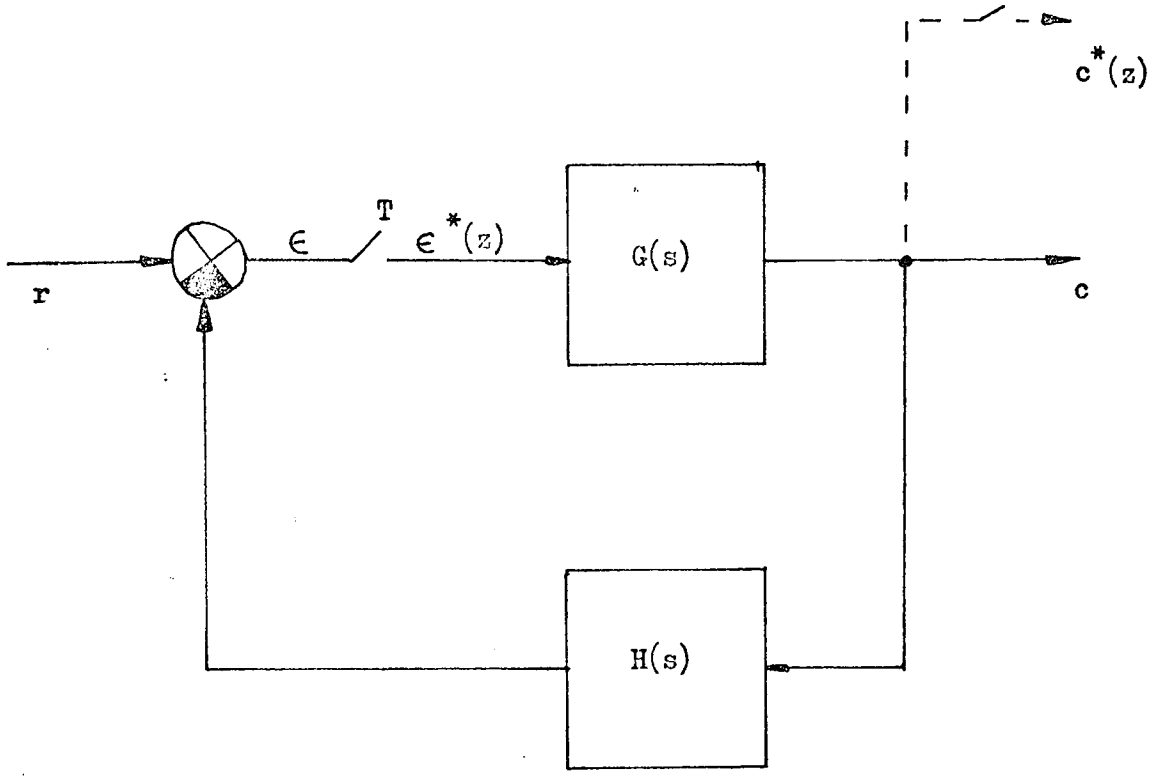

Fig.4.3 Basic sampled data control system

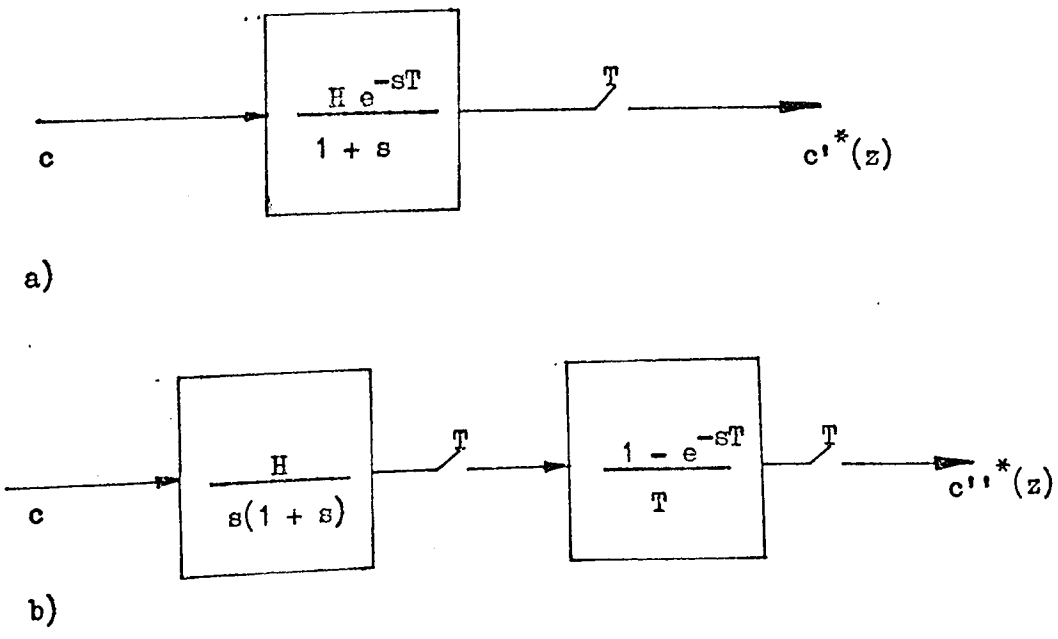

Fig.4.4 Control system feedback paths

From eqn.(4.2) $$\epsilon^*(z) = \frac{r^*(z)}{1 + GH^*(z)} \quad \text{.....(4.4)}$$

Substituting eqn.(4.4) into eqn.(4.3)

$$c^*(z) = \frac{r^*(z)\, G^*(z)}{1 + GH^*(z)} \quad \text{.....(4.5)}$$

This result cannot be applied directly to Fig.4.2 b) because of the complications in the feedback loop; however, since the feedback loop is in effect measuring the output signal c (arc velocity) with a time delay T via a first order 'lag' circuit †, it seems reasonable to replace the feedback loop by the transfer function of Fig.4.4 a). If this is now compared with the original feedback loop of Fig.4.4 b); using the z-transform technique:

$$c'^*(z) = H\left\{\frac{c(s)\, e^{-sT}}{1 + s}\right\}^*(z) \quad \text{.....(4.6)}$$

and $$c''^*(z) = \frac{(z-1)}{zT} H\left\{\frac{c(s)}{s(1 + s)}\right\}^*(z) \quad \text{.....(4.7)}$$

Eqn.(4.6) can be modified to:

$$c'^*(z) = \frac{H}{z}\left\{\frac{c(s)}{1 + s}\right\}^*(z) \quad \text{.....(4.8)}$$

The presence of $\frac{1}{s}$ in a transfer function with simple poles will give rise to a $\frac{T}{(z-1)}$ factor in its z-transform (this can be seen by checking tables of z-transforms)[33].

† See section 2.3.2

Removing this factor outside the brackets of eqn.(4.7) and cancelling, the multiplying factor reduces to $\frac{H}{z}$, which is the same as that for eqn.(4.8). The remaining transformed expression, contained within the brackets of eqn.(4.7), and the transformed expression within the brackets of eqn.(4.8), will have identical denominators; but in their numerators certain coefficients of unity in eqn.(4.8) will be replaced by coefficients of $\frac{(1-e^{-T})}{T}$ in eqn.(4.7). (e.g. Using $c(s) = \frac{1}{s}$ the expression in eqn.(4.8) is $z\left\{\frac{(z-e^{-T}) - (z+1)}{(z-1)(z-e^{-T})}\right\}$ and in eqn.(4.7) $z\left\{\frac{(z-e^{-T}) - \frac{(1-e^{-T})}{T}(z+1)}{(z-1)(z-e^{-T})}\right\}$)

For $T \to 0$, $\frac{(1-e^{-T})}{T} \longrightarrow 1$ and so for small values of T† the feedback of Fig.4.4 a) can be justified. The control system can now be shown as in Fig.4.5 a).

Using eqn.(4.5) :

$$c^*(z) = \frac{r^*(z)\left\{\frac{G(1 - e^{-sT})}{s(1 + 0.015s)}\right\}^*(z)}{1 + \left\{\frac{GH\, e^{-sT}(1 - e^{-sT})}{s(1 + s)(1 + 0.015s)}\right\}^*(z)} \qquad \text{.....(4.10)}$$

The presence of $\frac{1}{1 + 0.015s}$ in the forward loop of Fig.4.5 a) will introduce factors of $\frac{1}{z - e^{-T/0.015}}$ into eqn.(4.10). If T† is 0.1 or greater then $e^{-T/0.015}$ can be neglected and this reduces eqn.(4.10) to:

$$c^*(z) = \frac{r^*(z)\left\{\frac{G(1 - e^{-sT})}{s}\right\}^*(z)}{1 + \left\{\frac{GH\, e^{-sT}(1 - e^{-sT})}{s(1 + s)}\right\}^*(z)} \qquad \text{.....(4.11)}$$

This corresponds to the control system of Fig.4.5 b). The unit step response

† In the control system $T = 0.1$ and $\frac{(1-e^{-T})}{T} \simeq 0.95$

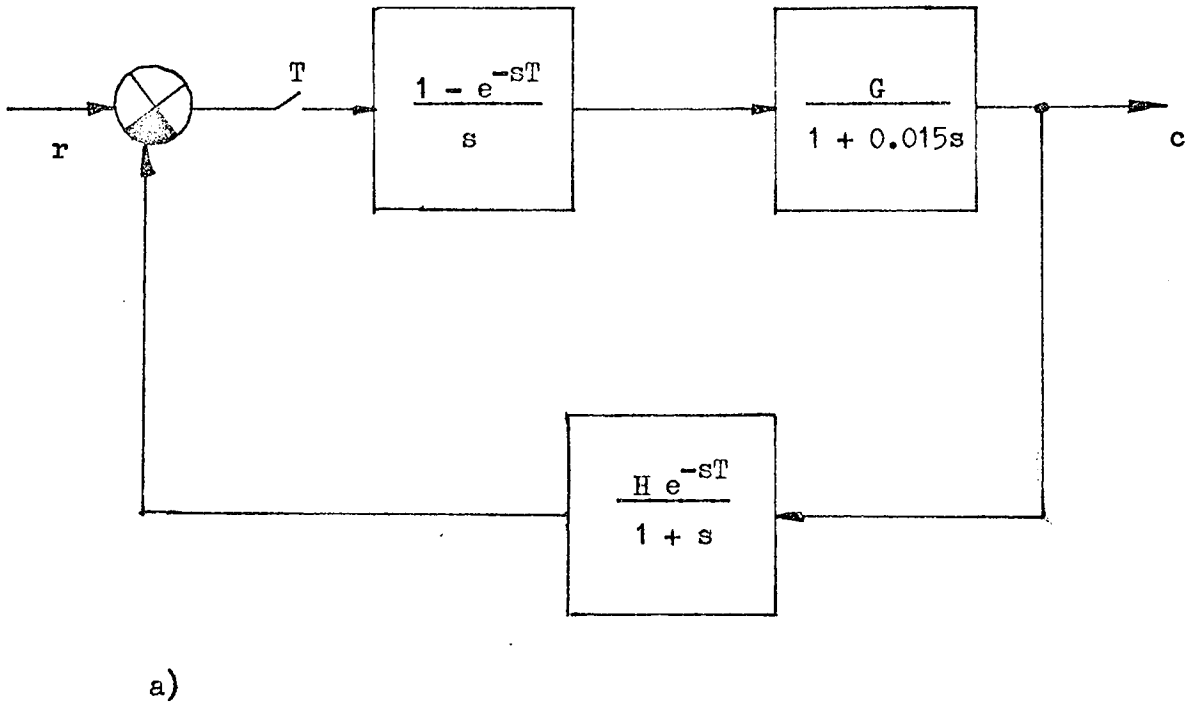

a)

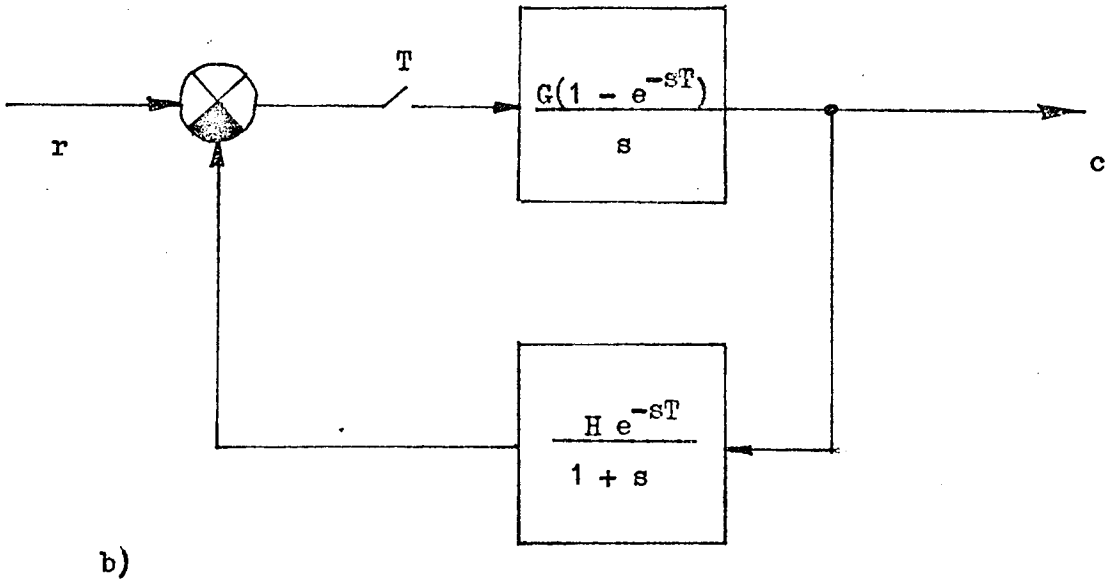

b)

Fig.4.5 Final simplification of the control loop

of eqn.(4.11) can be calculated by letting $r^*(z) = \frac{z}{(z-1)}$ (unit step);

using z-transform techniques:

$$c^*(z) = \frac{G\,z^2\,(z - e^{-T})}{z(z-1)(z-e^{-T}) + (z-1)(1-e^{-T})\,GH}$$

or

$$c^*(z) = \frac{G\,z^2\,(z - e^{-T})}{(z-1)(z-\alpha)(z-\beta)} \qquad \text{.....(4.12)}$$

where:

$$\begin{matrix}\alpha \\ \beta\end{matrix} = \frac{e^{-T}}{2} \pm \sqrt{\frac{e^{-2T}}{4} - GH(1 - e^{-T})}$$

Inverting eqn.(4.12) gives:

$$c(nT) = G\left\{\frac{(1-e^{-T})}{(1-\alpha)(1-\beta)} + \frac{\alpha^{(n+1)}(\alpha - e^{-T})}{(\alpha-1)(\alpha-\beta)} + \frac{\beta^{(n+1)}(\beta - e^{-T})}{(\beta-1)(\beta-\alpha)}\right\}$$

.....(4.13)

Eqn.(4.13), the system unit-step response, has been plotted using a computer programme (see Appendix II), and Fig.4.6 gives the results of this programme for T = 0.1, H = 1.0, G = 1.0 and G = 0.5. The large overshoot, at n = 0 with G = 1.0, is to be expected since initially there is zero feedback signal.

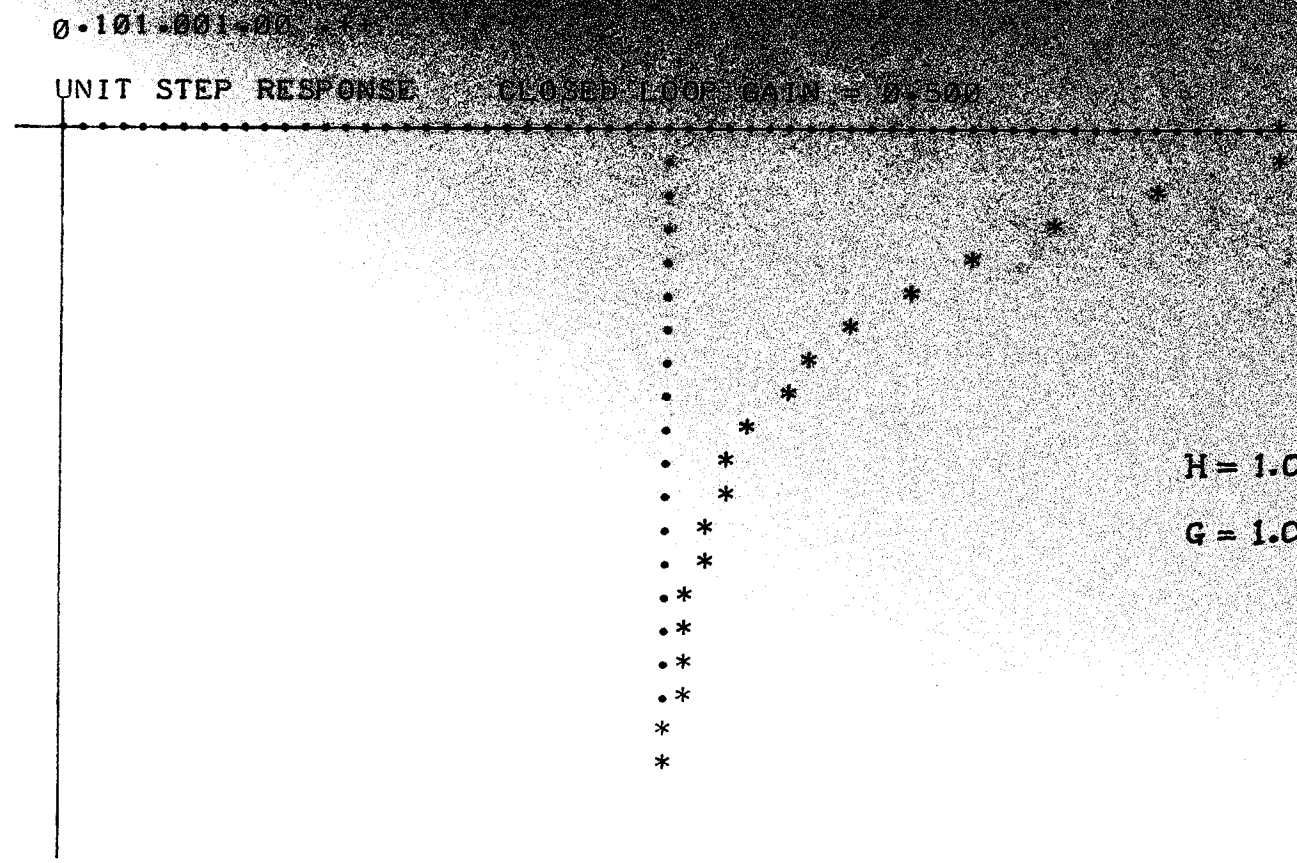

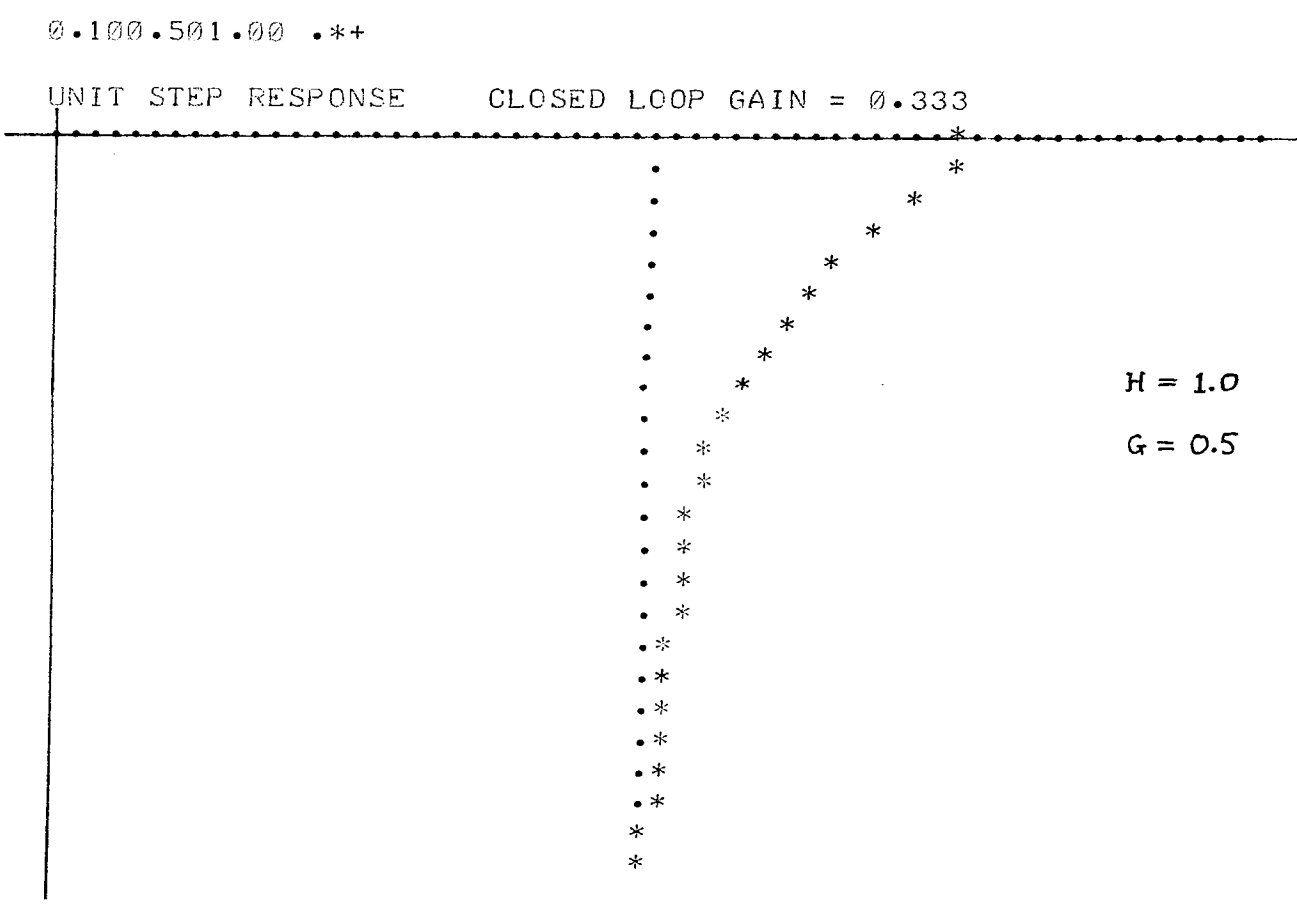

Fig.4.6 Unit step response of uncompensated control system

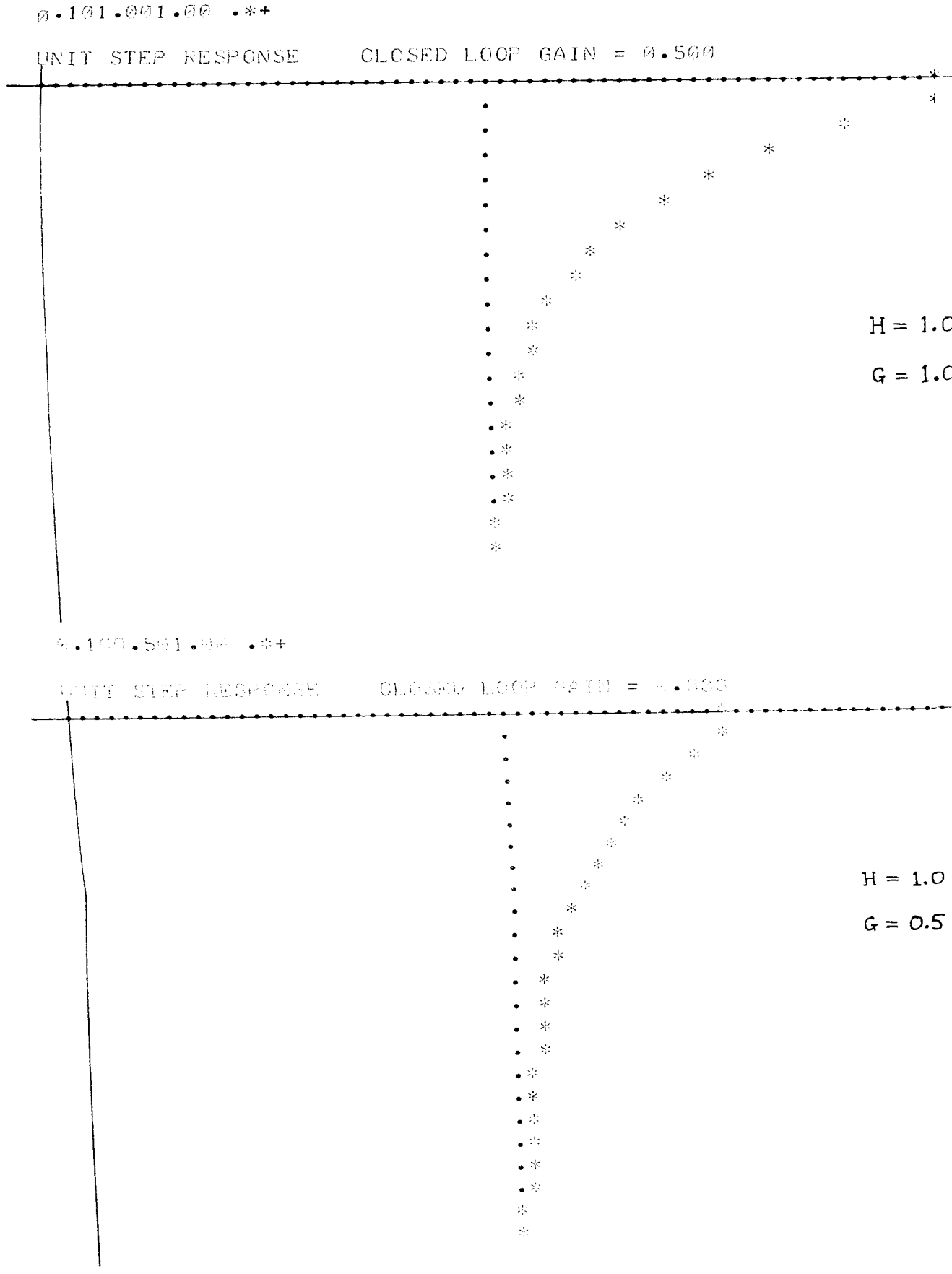

Fig.4.6 Unit step response of uncompensated control system

Fig.4.6 Unit step response of uncompensated control system

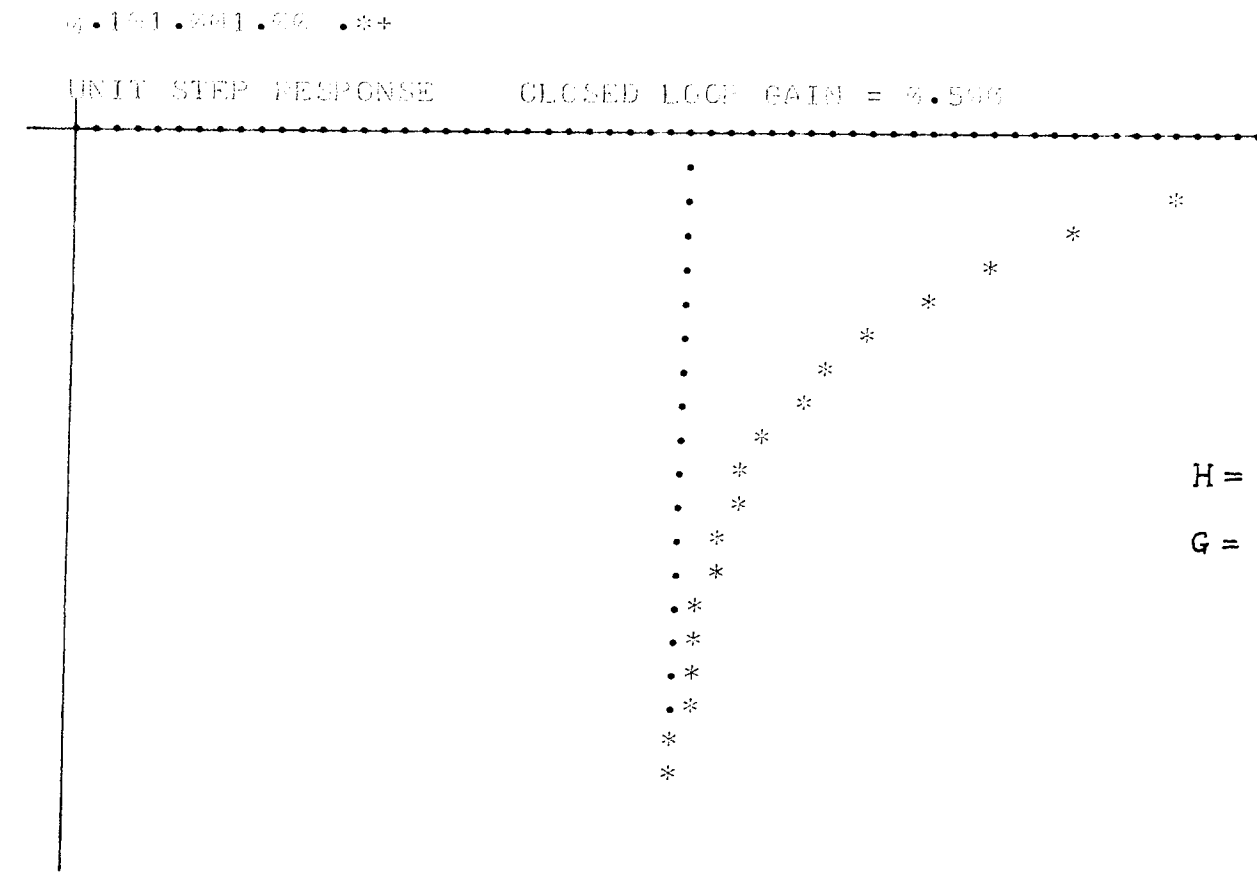

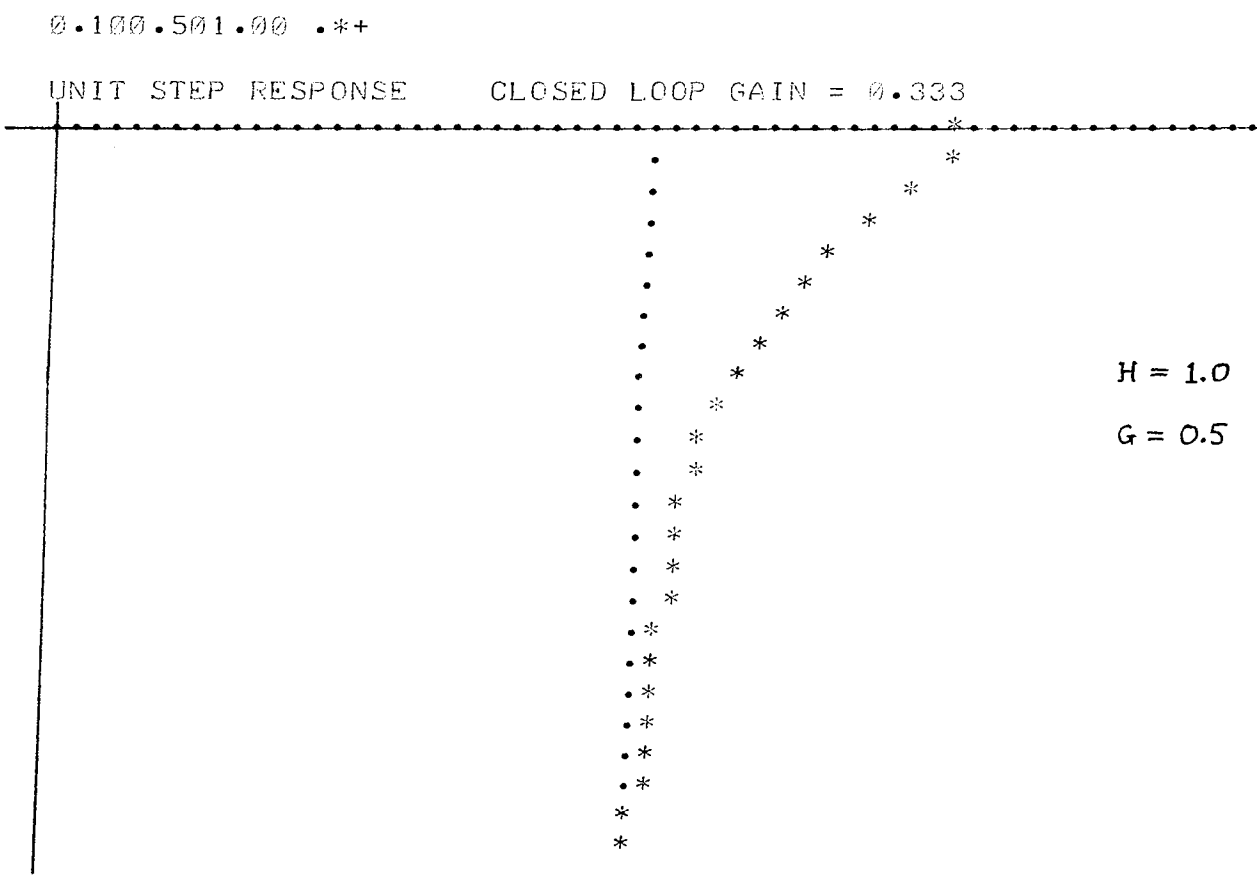

Fig.4.6 Unit step response of uncompensated control system

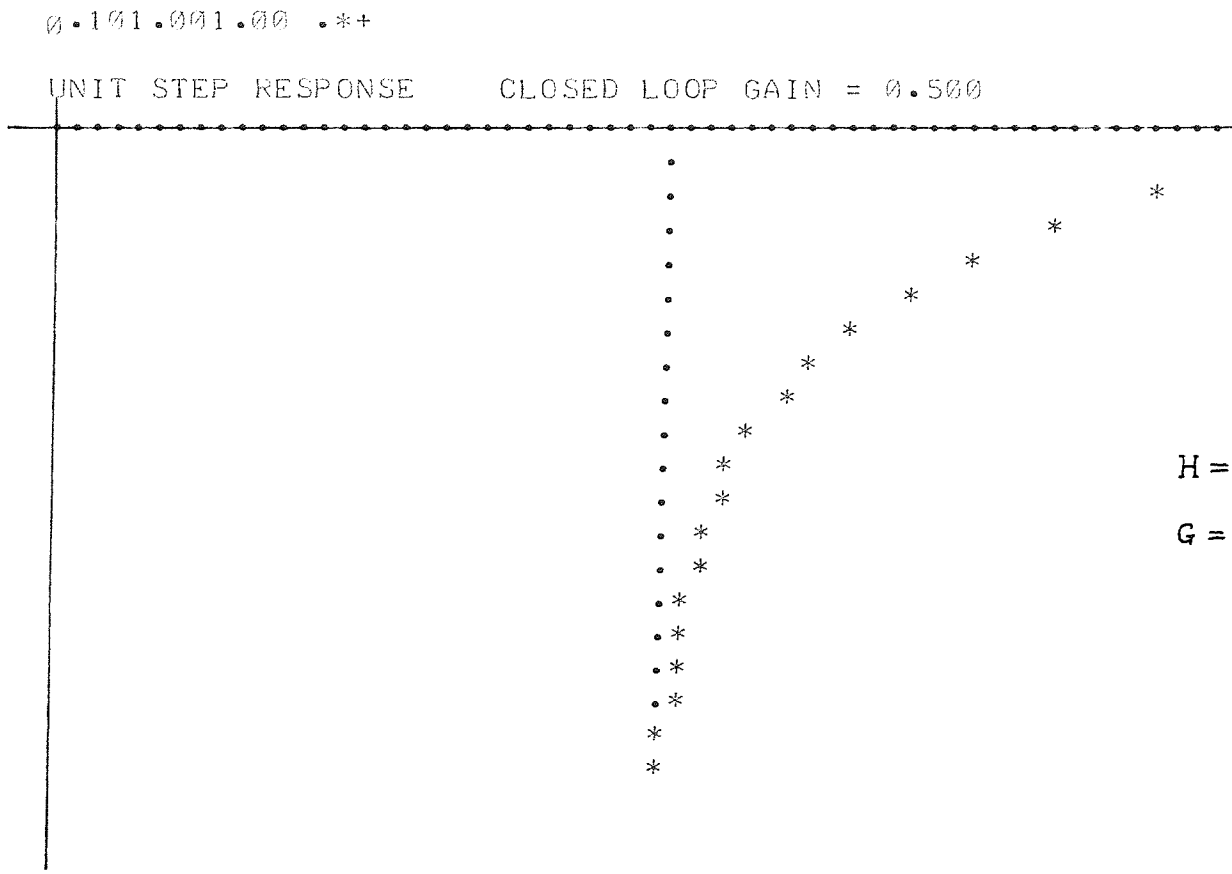

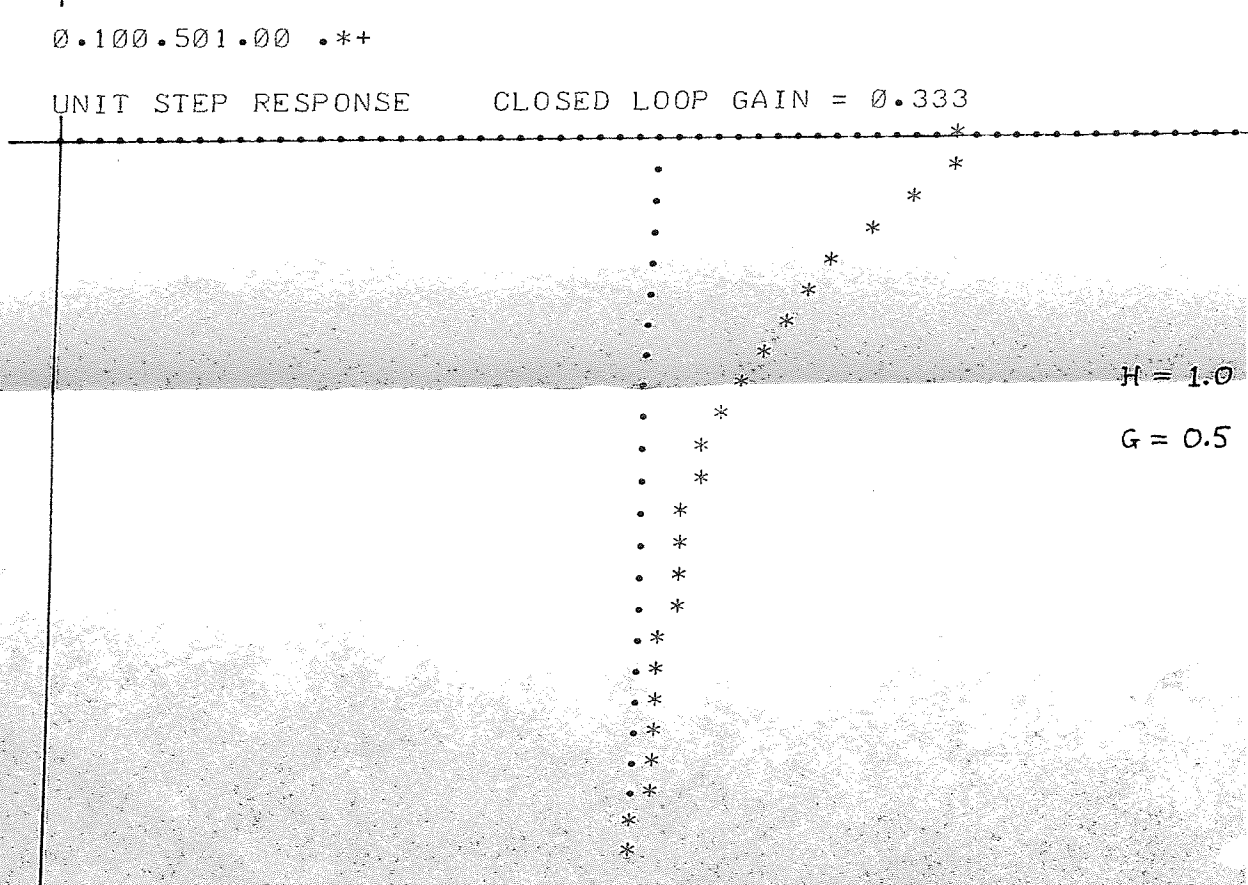

Fig.4.6 Unit step response of uncompensated control system

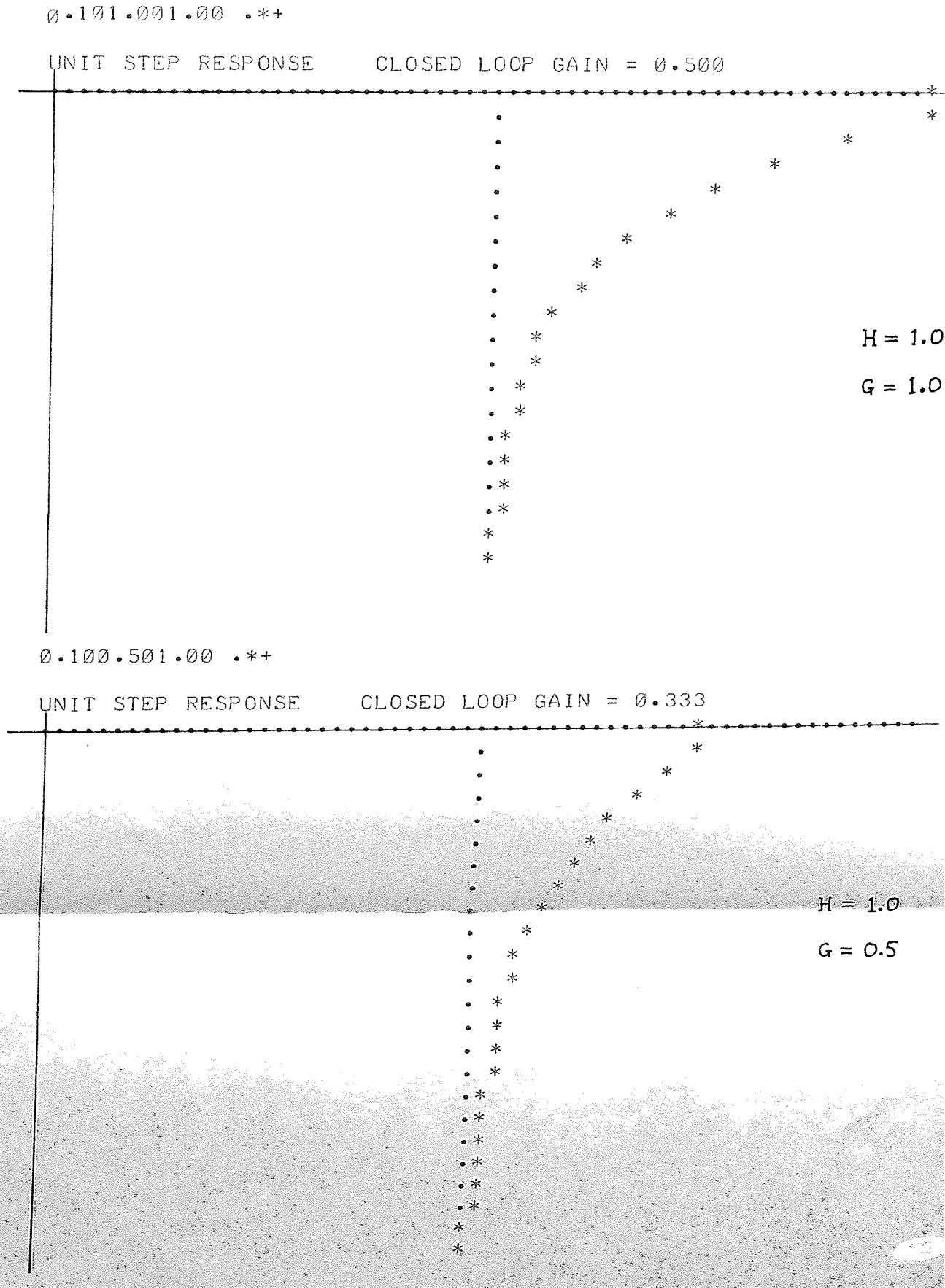

Fig.4.6 Unit step response of uncompensated control system

As G is reduced, the overshoot decreases until at the limit ($G \to 0$) the overshoot is zero (but with zero output). The steady-state closed-loop gain of the system is given by:

$$\frac{G}{1 + GH} \qquad \ldots\ldots\ldots\ldots\ldots\ldots\ldots\ldots\ldots\ldots (4.14)$$

and for $GH \longrightarrow 0$ the closed-loop gain of the system approaches G. Since G is constantly varying with the electrode surface conditions, the arc velocity will vary proportionally and the purpose of the control system will be lost. By making $GH \gg 10$ the closed-loop gain of the system approaches $\frac{1}{H}$ and

so variations in G will not affect the steady-state arc velocity (there will be gain-change transients, however). With such a large open-loop gain, the initial overshoot is prohibitive (1000% in this case). A compensation network is needed which will perform two functions:

a) Reduce the step-response overshoot

b) Maintain the steady-state closed-loop gain if G varies.

The next two sections give alternative methods of compensating the control loop.

4.2.1 Analogue compensator

It is possible to design analogue compensators by sampled-data techniques but, because of the simplicity of the basic control system and the small sample time involved, little error is obtained in this case if the compensator is designed by continuous techniques.

A continuous system approximation to the sampled data loop of Fig.4.3 is shown in Fig.4.7. The additional block in the forward path is the analogue compensator C(s).

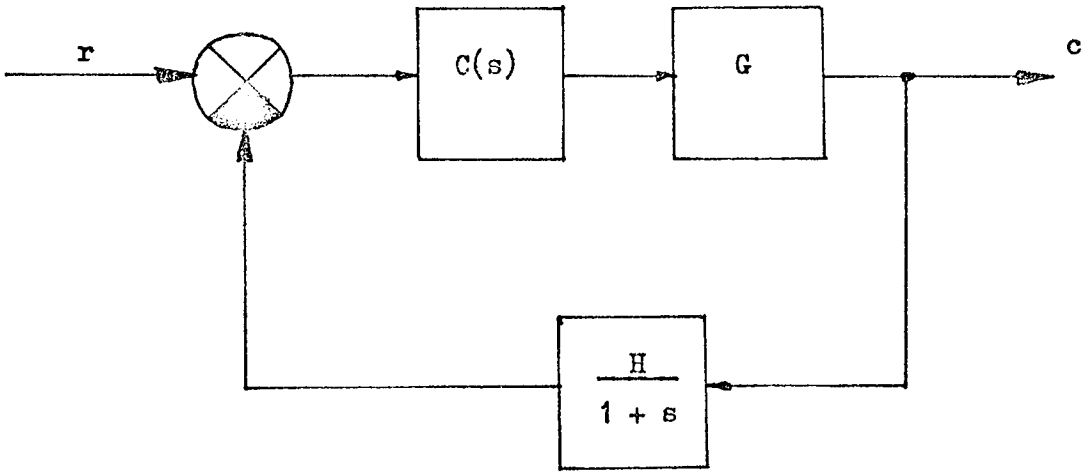

Fig.4.7 Continuous system approximation for the control loop with analogue compensator added

Because of the basic simplicity of the 'arc plant' and feedback transfer functions,it is possible to produce a simple compensator network (C(s)) which will perfectly compensate the system,i.e. create a closed-loop transfer function with no time constants.Such a network has the form:

$$\frac{1 + s}{1 + \tau s} \qquad \text{.....(4.15)}$$

where $\tau = GH + 1$

The gain of the system is determined from eqn.(4.14) and so for complete independence of closed-loop gain on the value of G, G should be much greater than one.

If this analogue compensator is now applied to the sampled data loop of Fig.4.3, eqn.(4.5) becomes:

$$c^*(z) = \frac{r^*(z)\left\{\frac{G(1-e^{-sT})}{s} \cdot \frac{(1+s)}{(1+\tau s)}\right\}^*(z)}{1 + \left\{\frac{GH\, e^{-sT}(1-e^{-sT})}{s(1+\tau s)}\right\}^*(z)} \quad \ldots(4.16)$$

Using z-transform techniques and inverting, an expression similar to eqn.(4.13) can be obtained. This has been plotted using a computer programme and typical results are given in Fig.4.8. For these results, $H = 1.0$, $\tau = 11$ and $T = 0.1$. For these values of H and τ, ideal compensation in a continuous system is obtained with $G = 10$, but the sampled-data system, Fig.4.8, indicates an overshoot of 10% of the steady-state value. This, however, is of little consequence in a control system. With $G = 15$ there is an overshoot of just over 50% of the steady state value and with $G = 5$ an undershoot of 50%. For a nominal value of $G = 9$, a $\pm$ 50% variation in G will only produce +3.5% and -9% change in closed-loop gain. With analogue compensation, therefore, large changes in gain of the forward path will only have a small effect on the closed loop gain of the system, providing the criterion $GH \gg 1$ is adhered to. Changes in gain about a nominally ideally compensated gain will, however, produce changes in the transient response of the system; an increase in gain produces transient overshoot and a decrease in gain, undershoot.

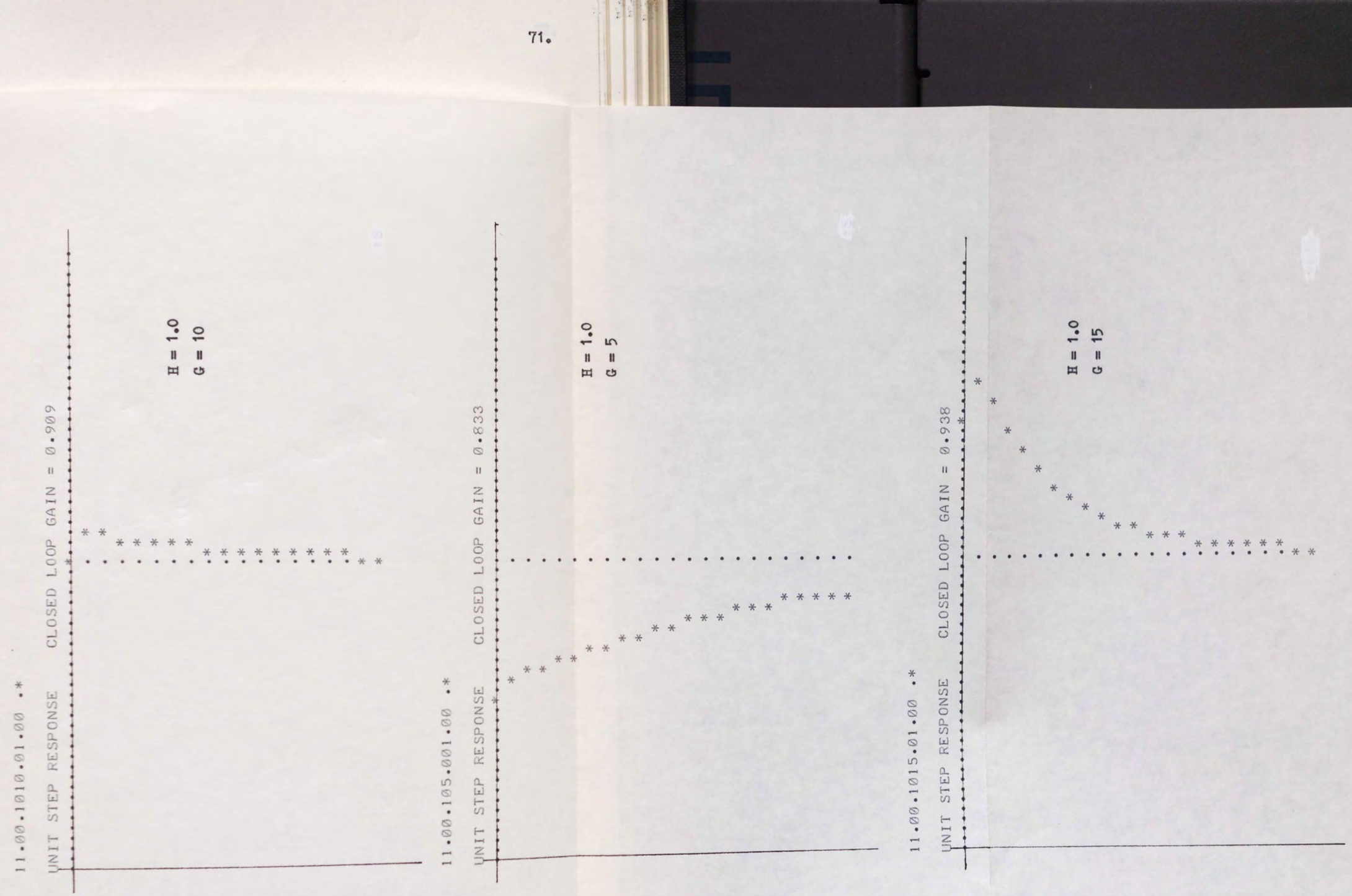

Fig.4.8 Unit step response using analogue compensation

4.2.2 Digital compensation

The presence of a digital computer in the sampled data system allows a form of discrete compensation to be carried out by the computer. The form of the compensation is evaluated using z-transform techniques and can be readily adapted to the time domain for use in computer compensation (see 5.1.1).

The usual way in which the compensation is evaluated is by expressing the desired output of the control system in the time domain and then choosing a discrete compensator as a polynomial in powers of z^{-1}. It is possible to evaluate the coefficients of this polynomial and so determine the form of discrete compensation. Since there are no poles or zeros in the forward path of the control loop, it is possible to obtain a perfect system response (as demonstrated in the last section). If the following closed-loop transfer function is used as a criterion:

$$\frac{c^*(z)}{r^*(z)} = 1 \qquad \text{.....(4.17)}$$

it should be possible to evaluate a realisable discrete compensator which will give the system such a closed-loop transfer function.

Fig.4.9 shows the block diagram of the control system with a discrete compensator $D_c^*(z)$ in the forward path.

From Fig.4.9

$$\epsilon^*(z) = r^*(z) - \epsilon'^*(z) \left\{ \frac{GH\, e^{-sT}(1 - e^{-sT})}{s(1 + s)} \right\}^*(z) \qquad \text{..(4.18)}$$

$$\epsilon'^*(z) = D_c^*(z)\, \epsilon^*(z) \qquad \text{.....(4.19)}$$

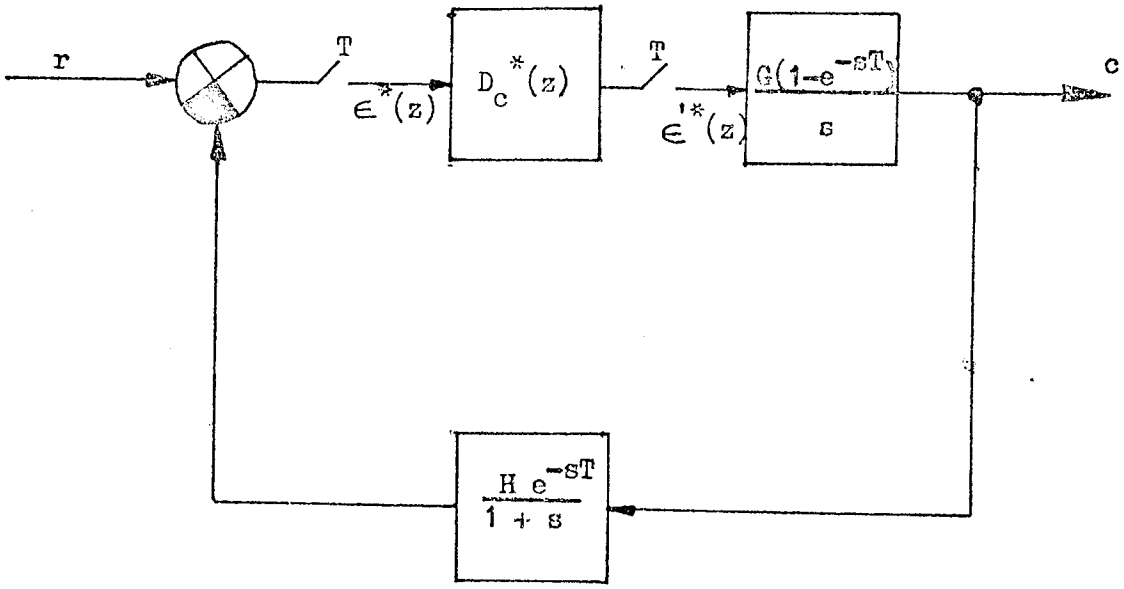

Fig.4.9 Block diagram of the control loop using discrete compensation

$$c^*(z) = \epsilon'^*(z) \left\{ \frac{G(1-e^{-sT})}{s} \right\}^*(z) \quad \text{.....(4.20)}$$

Substituting eqn.(4.18) into eqn.(4.19) to find $\epsilon'^*(z)$ and substituting this into eqn.(4.20), we obtain the expression:

$$c^*(z) = \frac{r^*(z) D_c^*(z) \left\{ \frac{G(1-e^{-sT})}{s} \right\}^*(z)}{1 + D_c^*(z) \left\{ \frac{GHe^{-sT}(1-e^{-sT})}{s(1+s)} \right\}^*(z)} \quad \text{.....(4.21)}$$

Using eqn.(4.17) and applying z-transform techniques, we obtain an expression for $D_c^*(z)$:

$$D_c^*(z) = \frac{1}{G}\left\{\frac{z^2 - ze^{-T}}{z^2 - ze^{-T} - (1-e^{-T})}\right\} \quad \text{.....(4.22)}$$

In this expression, H is taken as unity and will be so for all future analysis.

In order to assess the affects of changing the system gain, whilst the compensated gain G in eqn.(4.22) is held constant, the gain in eqn.(4.21) is changed to G' and eqn.(4.22) is substituted into eqn.(4.21). Using a computer programme, the unit-step response of the system is plotted for G = 10 and G' = 5, 10 and 15; the results are shown in Fig.4.10.

The $\pm$ 50% variation in forward-path gain produces no difference in the closed-loop gain of the system and, infact, the forward path gain can be taken from 0.1 to 10 without any variation in the closed-loop gain. This is the first obvious advantage over the analogue compensation method. As with analogue compensation, the changing gain of the system produces differing transient responses to a step input, as seen in Fig.4.10. It would be desirable to include some method by which the forward-path gain of the system could be measured and the compensator modified accordingly. This leads to the second advantage the discrete compensator has over the analogue compensator, since it is easier to monitor gain and correct the digital compensator to the changing system gain. The next section presents a method of implementing such an adaptive controller.

4.2.3 Adaptive control

In order to monitor the gain of the arc process G', we have to use signals

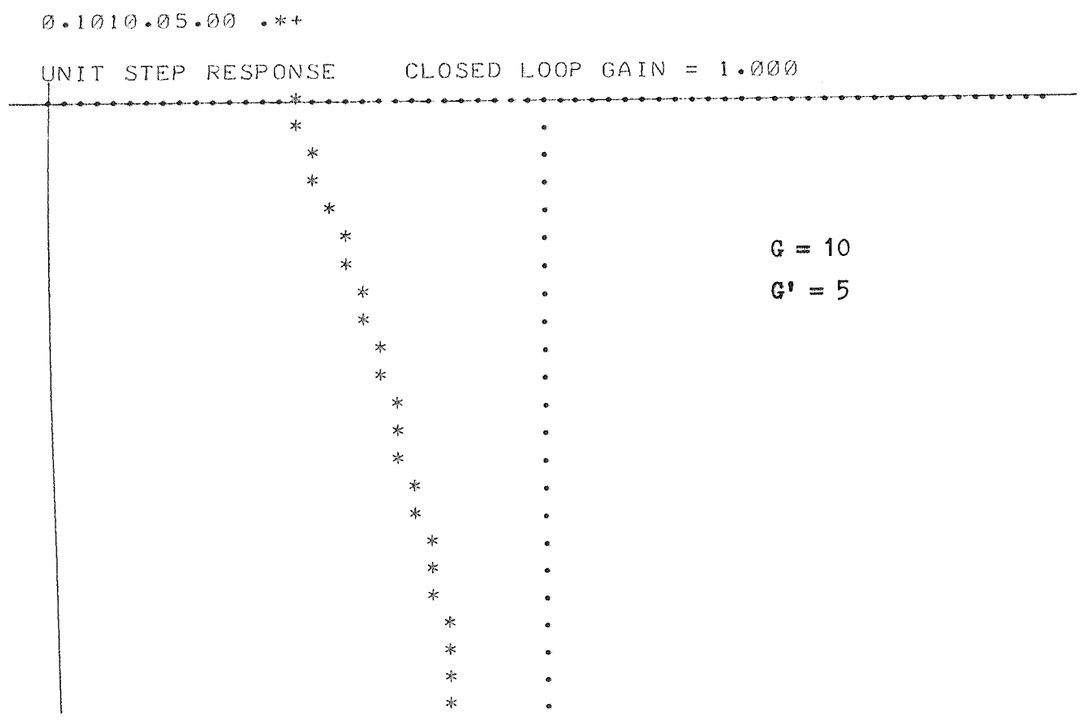

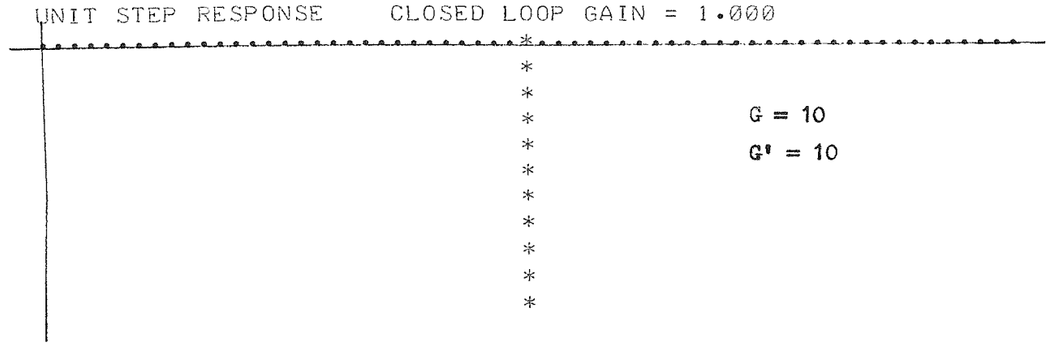

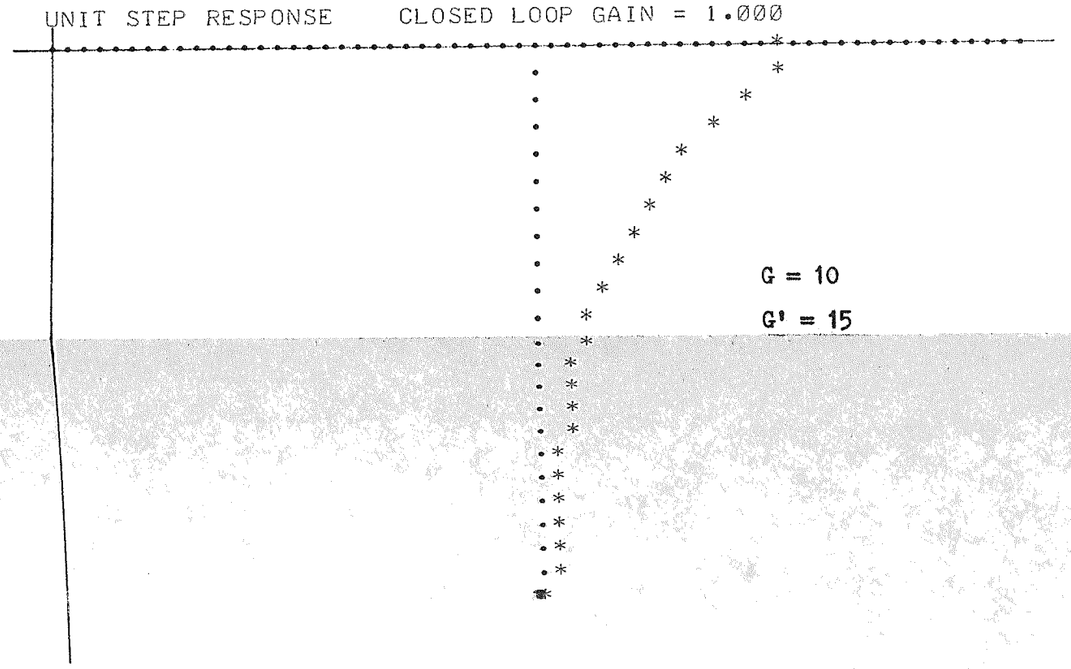

Fig.4.10 Unit step response using digital compensation

which are handled by the computer. Consider the block diagram shown in Fig.4.9. Using the signals r and ϵ' and changing the system gain from G to G', as in the previous section, the following expression can be determined:

$$\frac{\epsilon'^*(z)}{r^*(z)} = \frac{D_c^*(z)}{1 + D_c^*(z)\, G' \left\{ \frac{e^{-sT}(1-e^{-sT})}{s(1+s)} \right\}^*(z)}$$

Substituting for $D_c^*(z)$ from eqn.(4.22) :

$$\frac{\epsilon'^*(z)}{r^*(z)} = \frac{\frac{1}{G} \left\{ \frac{z^2 - ze^{-T}}{z^2 - ze^{-T} - (1-e^{-T})} \right\}}{1 + \frac{G'}{G} \left\{ \frac{z^2 - ze^{-T}}{z^2 - ze^{-T} - (1-e^{-T})} \right\} \left\{ \frac{e^{-sT}(1-e^{-sT})}{s(1+s)} \right\}^*(z)}$$

Using z-transform techniques, we obtain the final expression:

$$\frac{\epsilon'^*(z)}{r^*(z)} = \frac{1}{G} \left\{ \frac{z(z - e^{-T})}{z^2 - ze^{-T} - (1 - \frac{G'}{G})(1 - e^{-T})} \right\} \quad \ldots\ldots\ldots\ldots (4.23)$$

If the system is ideally compensated, i.e. $G' = G$, then $\frac{\epsilon'^*(z)}{r^*(z)} = \frac{1}{G}$

and the gain of the plant can be monitored immediately. If G' suddenly changes, then a transient will occur the form of which is determined by the step change of G' from G.

The transient behaviour can be analysed by letting:

$$r^*(z) = \frac{R\,z}{(z-1)} \qquad \text{(a step function of amplitude } R\text{)}$$

in eqn.(4.23).This produces a time domain expression:

$$\frac{\epsilon'}{R}(nT) = \frac{1}{G}\left\{\frac{(1-e^{-T})}{(1-\alpha)(1-\beta)} + \frac{\alpha^{(n+1)}(\alpha-e^{-T})}{(\alpha-1)(\alpha-\beta)} + \frac{\beta^{(n+1)}(\beta-e^{-T})}{(\beta-1)(\beta-\alpha)}\right\} \qquad \text{.....(4.24)}$$

where:
$$\begin{matrix}\alpha \\ \beta\end{matrix} = \frac{e^{-T}}{2} \pm \sqrt{\frac{e^{-2T}}{4} - (1-e^{-T})\left(\frac{G'}{G}-1\right)}$$

The steady-state value of eqn.(4.24) is given by:

$$\lim_{n\to\infty}\frac{\epsilon'}{R}(nT) = \frac{1}{G}\,\frac{(1-e^{-T})}{(1-\alpha)(1-\beta)} = \frac{1}{G'}$$

i.e. the inverse of the final plant gain.The initial value of eqn.(4.24) is given by:

$$\frac{\epsilon'}{R}(nT)_{n=0} = \frac{1}{G}\left\{\frac{(1-e^{-T})}{(1-\alpha)(1-\beta)} + \frac{\alpha(\alpha-e^{-T})}{(\alpha-1)(\alpha-\beta)} + \frac{\beta(\beta-e^{-T})}{(\beta-1)(\beta-\alpha)}\right\}$$

$$= \frac{1}{G} \qquad \text{i.e. the inverse of the initial plant gain.}$$

For gain increases giving $\frac{G'}{G} > 3$, α and β become complex and produce

damped oscillatory transients. Such large step changes in gain are not, however, anticipated. Assuming an ideally-compensated gain of 1, the inverse of eqn.(4.24) has been plotted by computer for step changes of gain $G' = 1 \rightarrow 2$ and $G' = 1 \rightarrow 0.5$; the results are shown in Fig.4.11. It is obvious that the system as it stands will not respond to rapid fluctuations in gain but will monitor long-term gain changes, for example the slow build-up of oxide, and hence reduction of the gain of the electrodes for consecutive arc runs.

Since the adaptive element of the control system is designed to correct the forward-path gain in order to produce a perfect step response, it is only necessary to modify the compensator (eqn.(4.22)) immediately before a step change in input. If, however, the compensator is continually modified by the gain calculated from eqn.(4.24), different gain change transients can be expected from those shown in Fig.4.11. The continuously-compensated gain transient is difficult to analyse theoretically, since for each time interval T the discrete compensator has to be modified and the initial conditions of the system, at the beginning of T, have to be taken into account. The solution of this problem by simulation techniques, on a hybrid analogue/digital computer configuration, represents a far easier way of producing the adaptive gain change transients, and this is demonstrated in the next chapter.

4.3 Summary

A theoretical control system has been developed which can use either analogue

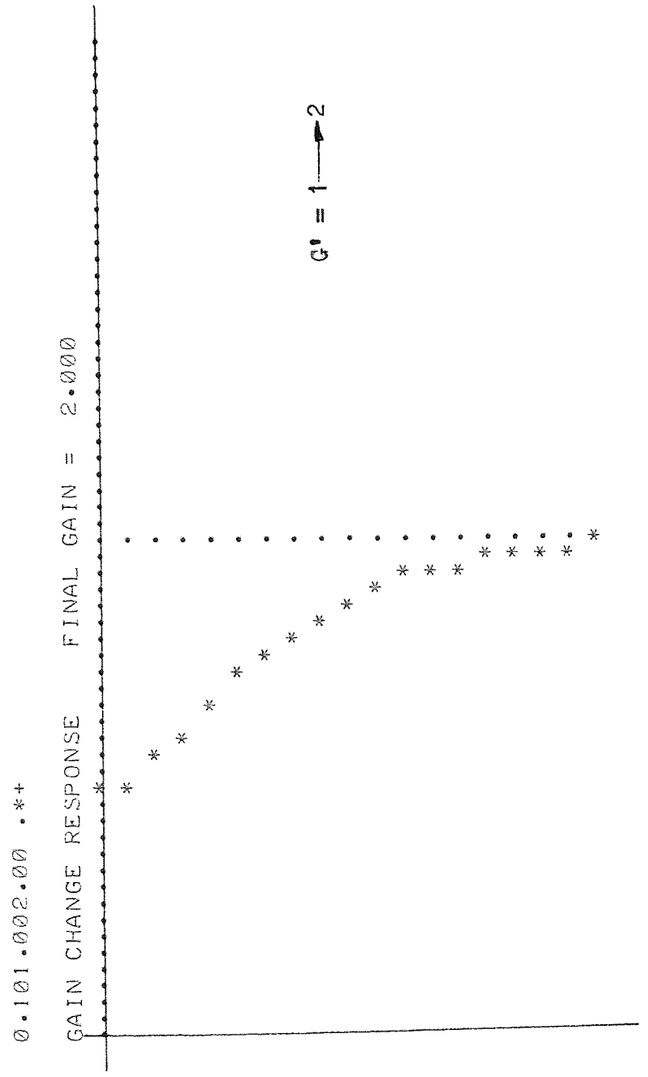

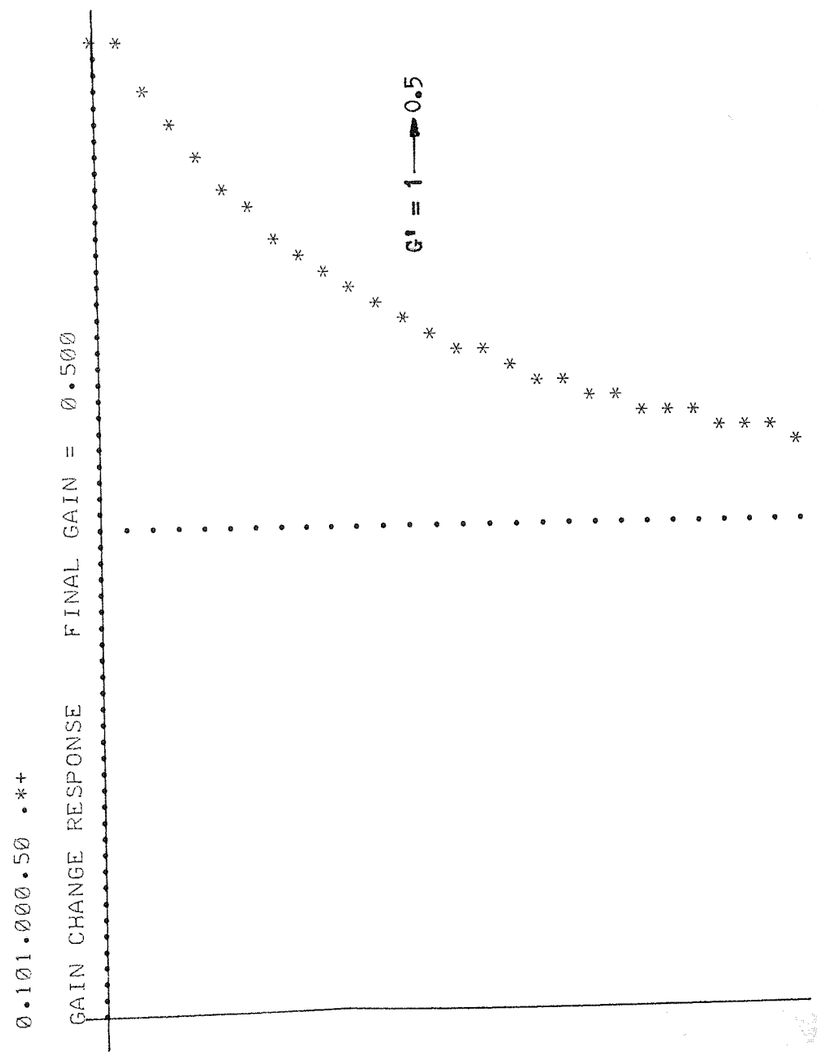

Fig.4.11 System gain change response

or digital compensators.With a known 'arc plant' gain the system has a perfect step response, i.e. the closed-loop transfer function is unity.For both methods of compensation,the system output is independent of gain changes in the moving arc process for a wide range of gains.With digital control an adaptive controller has been developed which monitors the gain of the arc process and continuously modifies the discrete compensator.This creates a very versatile control system able to adapt itself to any system gain within a very large range.

CHAPTER 5

The arc velocity control system

5.1.1 Discrete compensator

The theoretical analysis of the ideal discrete compensator is given in 4.3.2. This is in terms of the variable z which can be related to the complex variable s by the relation

$$z = e^{sT} \qquad \ldots\ldots\ldots\ldots\ldots\ldots\ldots\ldots\ldots\ldots (5.1)$$

T is the period of time between successive samples in the system under investigation. From eqn.(5.1) we can see that z^n is a time delay or advance operator depending on the sign of n. Since, in practice, time advance is not possible, realisable functions have to be expressed in terms of z^{-n}. We can thus rewrite eqn.(4.22) as:

$$D_c^*(z) = \frac{1}{G}\left\{\frac{1 - z^{-1}e^{-T}}{1 - z^{-1}e^{-T} - z^{-2}(1-e^{-T})}\right\} \ldots\ldots (5.2)$$

A further criterion for realisability is that the order of the denominator of the polynomial, in z^{-n}, is the same or higher than the numerator. From this criterion, eqn.(5.2) is realisable.

Using the relation obtained from Fig.5.1,

$$D_c^*(z) = \frac{E_2^*(z)}{E_1^*(z)}$$

eqn.(5.2) can be rewritten as:

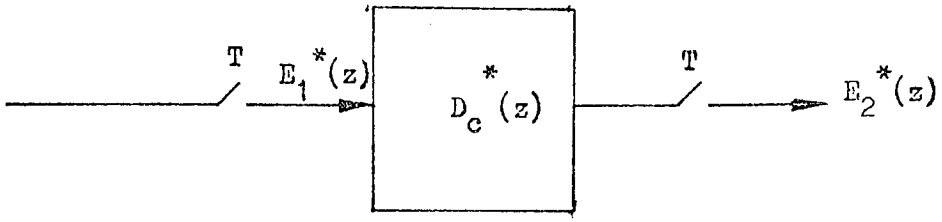

Fig.5.1 Input and output to the digital compensator

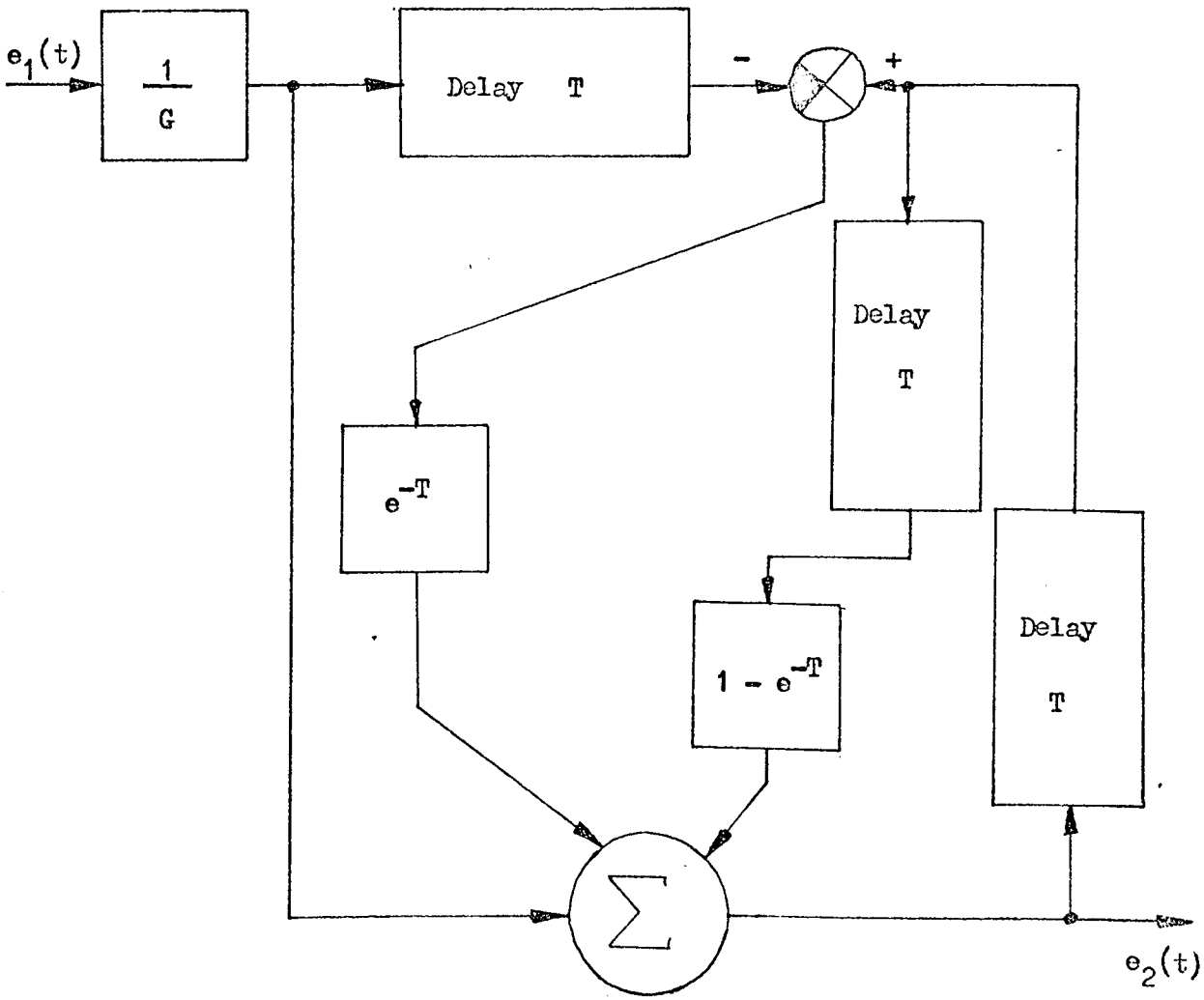

Fig.5.2 Block diagram of the digital compensator for computer representation

$$G\left\{E_2^*(z) - z^{-1}E_2^*(z)\,e^{-T} - z^{-2}E_2^*(z)(1-e^{-T})\right\} = E_1^*(z) - z^{-1}E_1^*(z)e^{-T}$$

This can be expressed in the time domain as:

$$G\left\{e_2(t) - e_2(t-T)e^{-T} - e_2(t-2T)(1-e^{-T})\right\} = e_1(t) - e_1(t-T)e^{-T}$$

or:

$$e_2(t) = \frac{1}{G}\left\{e_1(t) - e_1(t-T)e^{-T} + Ge_2(t-T)e^{-T} + Ge_2(t-2T)(1-e^{-T})\right\}$$

.....(5.3)

Fig.5.2 gives eqn.(5.3) in block diagram form and is used for synthesising the compensator by computer programme.

5.1.2 Computer Implementation

The PDP9 computer used for this research has software to handle two languages, MACRO9 and FORTRAN IV .The first is a basic computer language which allows direct control of the computer hardware,the second is a more sophisticated scientific language.

The sampling and compensating programme has been written in both languages by the use of sub-programmes.In this way,it is possible to perform the sampling and digital filtering operations using MACRO9 and the more complex compensation proceedures using FORTRAN IV.The use of this latter language means a large proportion (greater than 10%) of T is used for calculation purposes rather than sampling and filtering.It would be possible

to write the compensation programme in MACRO9 ,in order to reduce the compensation time,but the far greater complications involved and the vast physical size of such a programme does not seem to justify this step.One possible step that could be taken to cut down the calculator time would be to replace the square-root function at the output of $D_c^*(z)$ (generated by a FORTRAN IV science library programme) by an analogue function generator on the input to the field coil amplifier;however,since a digital computer is used in the control system,utilisation of this to the full in order to minimise analogue components is necessary for economical operation.

Appendix II gives full details of the programmes used in the digital controller.

5.2.1 System Test on the Analogue Simulator

Fig.5.3 shows a complete block diagram of the hybrid control system.As indicated in 4.2.1 ,position control of the output is affected by changing the velocity command to the input when a desired position has been reached; this is effected by the dotted line shown in Fig.5.3.The required position and velocity commands are read into the computer and stored at the beginning of the control run.During the run,the various velocity commands are changed at the predetermined positions.These positions are measured from the output of the measurement system and are subject to the transient behaviour of the one-second time-constant output demodulator.It is possible to compensate for this transfer function in order to monitor position accurately,though this procedure tends to introduce more noise into the system.For the purposes of this investigation,however,such compensation methods have not been pursued.

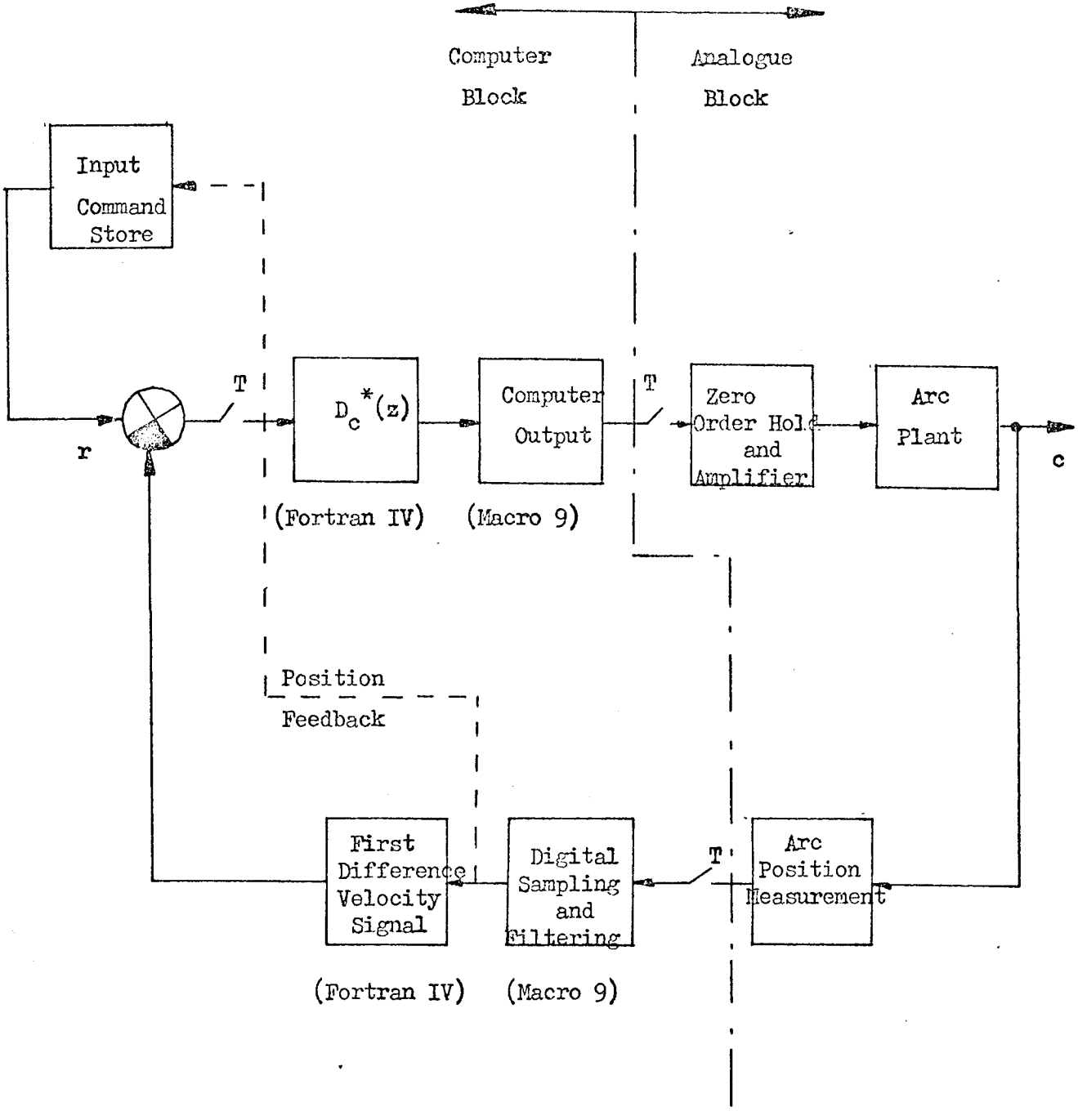

Fig.5.3 Complete control system

5.2.2 The Hybrid Test Circuits

Since the 'arc plant' has no time constants, its analogue model can be simply represented by an operational amplifier whose gain is the gain of the 'arc plant'. In order to approximately model the arc, the output of the amplifier should follow a square law with the input (see eqn.(3.13)); however, this is not necessary if the square-root function on the output of the discrete compensator is removed. Fig.5.4 gives the block diagram of the hybrid test circuit for the discrete compensator.

A further hybrid test circuit was used to check the analogue compensator discussed in 4.2.1, and is shown in Fig.5.5. The same computer programme was used for both tests, but in the case of the analogue-compensator test the discrete compensator section of the programme was by-passed. Full details of the programme are given in Appendix II.

5.2.3 Hybrid Test Circuit Performance

The outputs of both hybrid test circuits were recorded by photographing the traces on an oscilloscope. The input commands from the computer were set for unit steps, i.e. cycling between +1volt and -1volt.

Analogue Compensator

The value of τ used for this test was 11 seconds . Fig.5.6 a) shows the unit-step response of the system with G = 5 and H = 1 ; Fig.5.6 b) G = 10 and H = 1 ; Fig.5.6 c) G = 15 and H = 1.

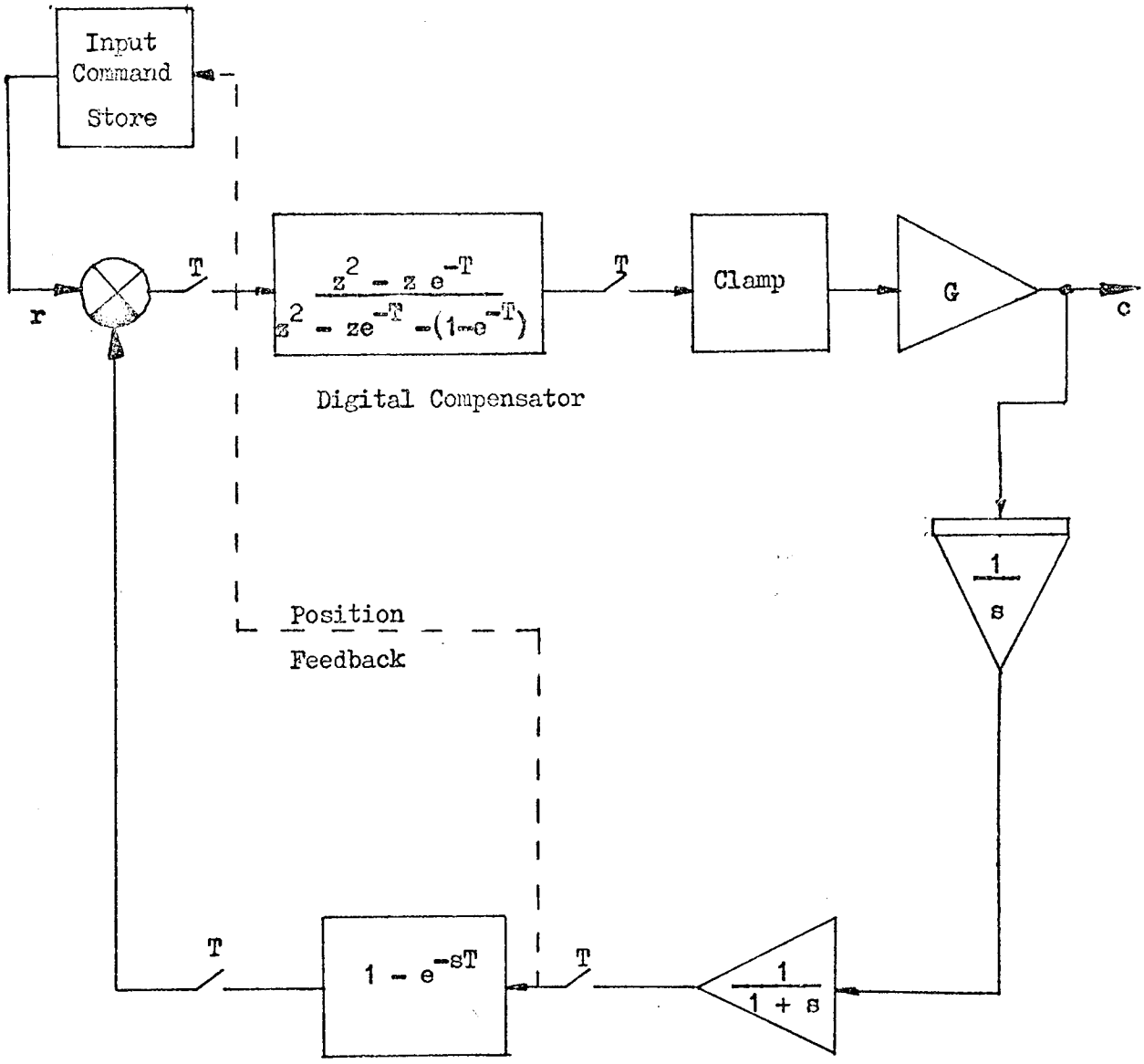

Fig.5.4 Block diagram of hybrid simulator using digital compensation

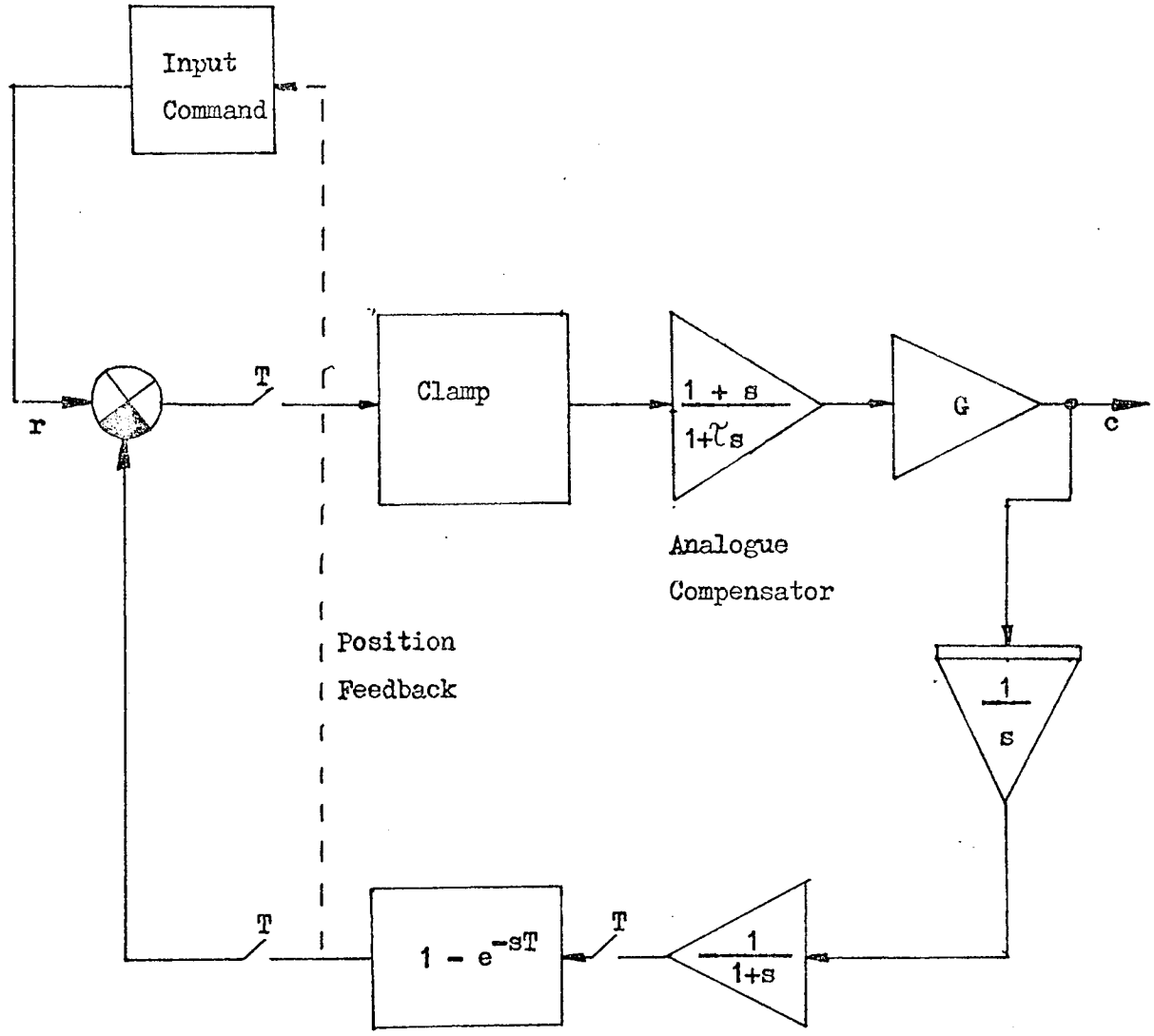

Fig.5.5 Block diagram of hybrid simulator using analogue compensation

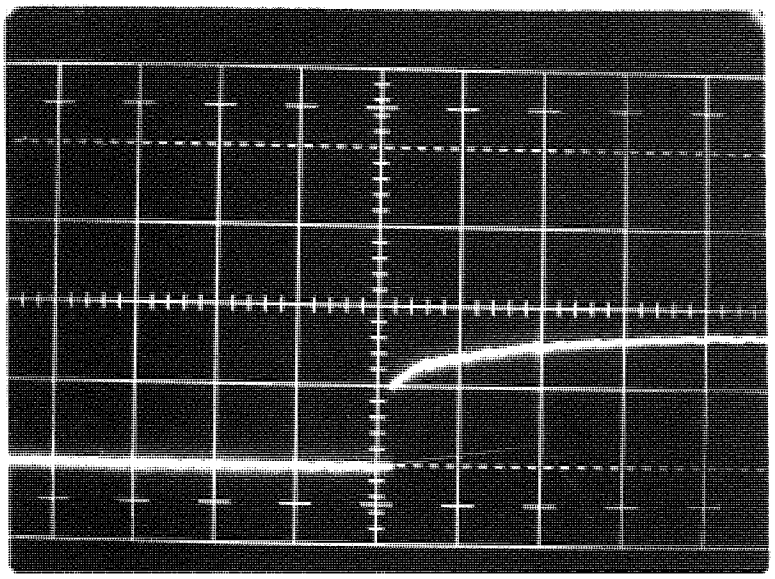

Scaling: X one division ≡ 1 second

Y one division ≡ 0.5 volts

a) H = 1.0 G = 5

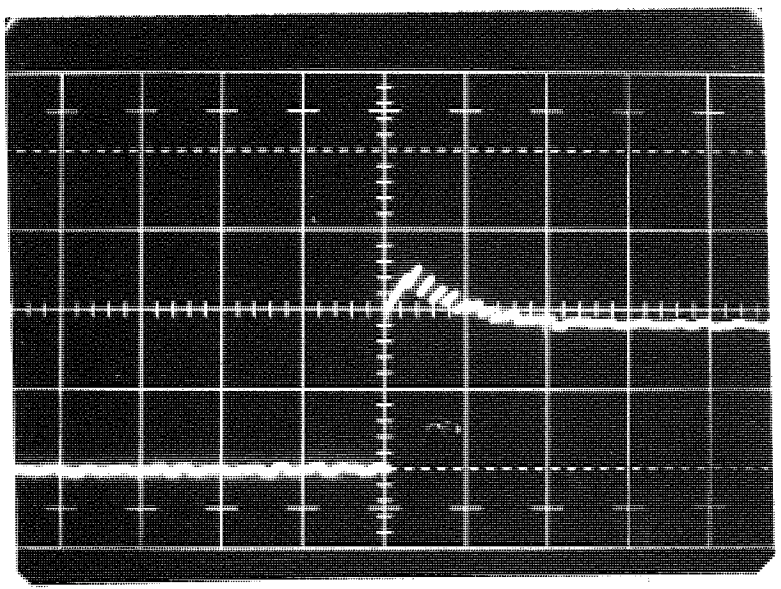

b) H = 1.0 G = 10

Fig.5.6 Output photographs of hybrid simulator using analogue compensation

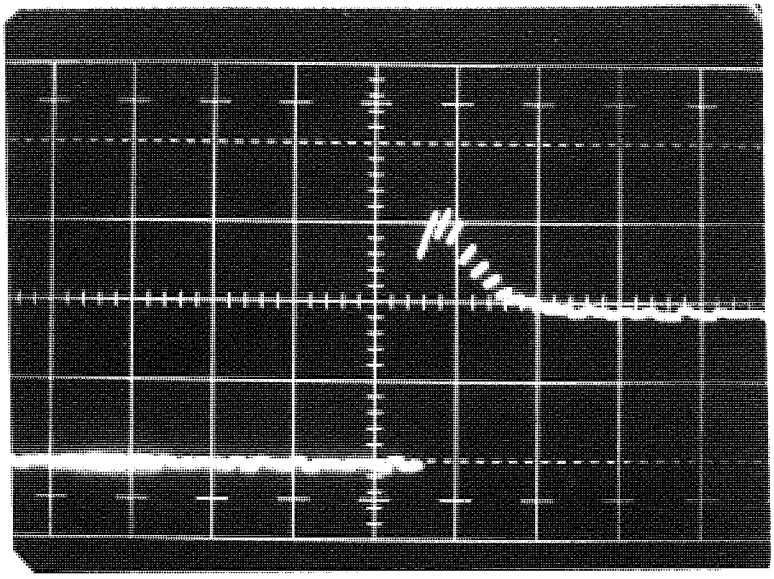

Scaling:

c) H = 1.0 G = 15 X one division ≡ 1 second

Y one division ≡ 0.5 volts

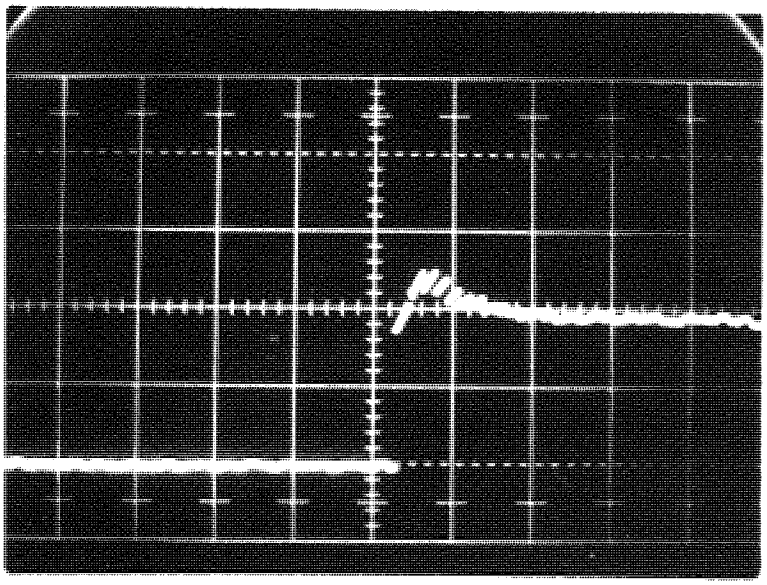

d) H = 1.0 G = 9

Fig.5.6 (continued)

The predicted outputs, as calculated by z-transform techniques, can be seen in Fig.4.8. Since modified z-transform methods were not used, Fig.4.8 represents the output of the system at the sample point, every T seconds, and as such compares favourably with the photographs of Fig.5.6 a) ,b) and c). Fig.5.6 a) ,however, shows that between sample times the output has an initial overshoot greater than the 10% predicted in 4.2.1 for a gain of 10. By decreasing the gain to G = 9 the unit-step response for this gain is far more acceptable; a typical response is shown in Fig.5.6 d).

Digital Compensator

Using the simulator of Fig.5.4 with a discrete-compensator gain of 1 ,output traces produced by the system for a step input were photographed. Fig.5.7 shows typical results for a) G = 0.5 and H = 1, b) G = 1 and H = 1, c) G = 1.5 and H = 1.

In this case, the predicted outputs of Fig.4.10 match the experimental results very well, since there are no time constants in the forward path of the simulated control system. This means that the output is held constant throughout the time between successive samples.

It is evident from the photographs that the steady state gain of the system, whilst being affected by the $\frac{G}{1 + G H}$ term in the analogue compensator (eqn.4.14), is completely independent of G in the discrete compensator, as predicted in 4.2.2.

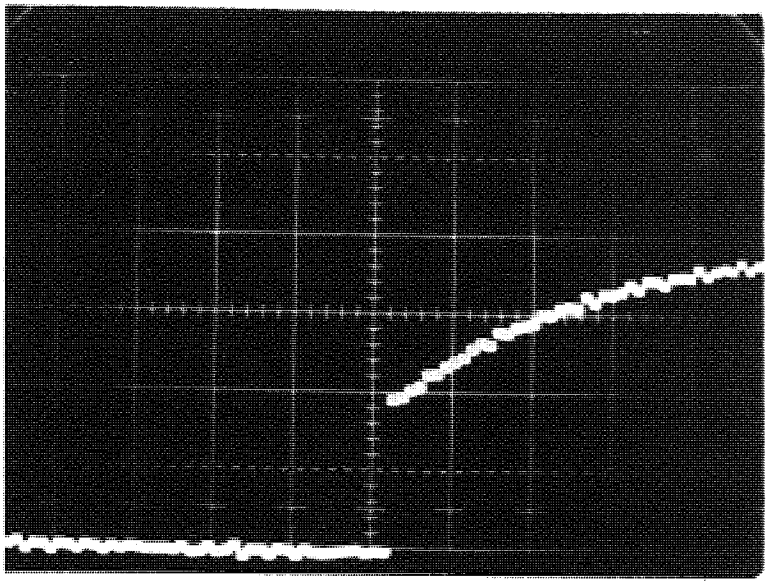

a) H = 1 G = 0.5

Scaling:

X one division ≡ 1 second

Y one division ≡ 0.25 volts

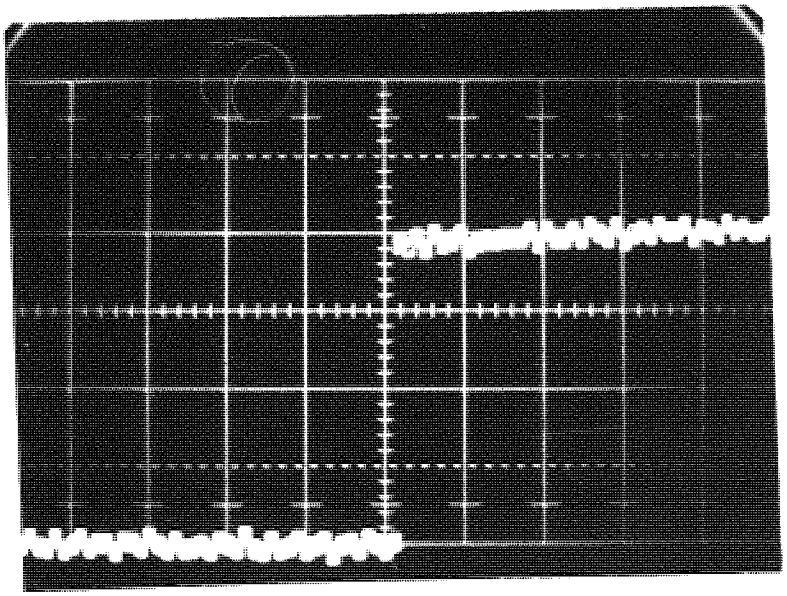

b) H = 1 G = 1

Fig.5.7 Output photographs of hybrid simulator using digital compensation

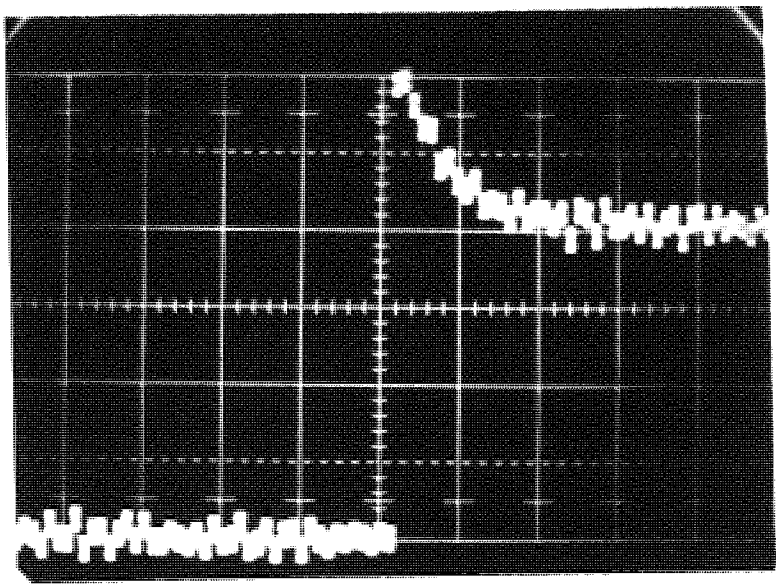

c) H = 1 G = 1.5

Scaling:

X one division ≡ 1 second

Y one division ≡ 0.25 volts

Fig.5.7 (continued)

5.3.1 Adaptive controller

Section 4.2.3 deals with the theoretical aspects of the adaptive controller. The gain of the plant, under steady-state conditions, is found from the division of the computer output by the input command, as given in eqn.(4.24).

As indicated in 4.2.3 , the prime purpose of the adaptive controller is to be able to produce an ideal system response regardless of its gain. The steady-state value of the system output, with the discrete compensator, is constant over a wide range of gains without the adaptive controller.

Section 4.2.3 outlines two methods of applying adaptive control to the discrete compensator:

1) Correct the compensator gain immediately before a change in input command
2) Continuously correct the compensator gain.

Theoretical results of gain change transients have been obtained for 1), see Fig.4.10 , but 2) requires more complex mathematical procedure and has not been analysed. The gain change transients can be observed by simulating the 'arc plant' on an analogue computer (see previous section). Using such a simulation, output photographs have been obtained from the system for sudden changes in gain.

Fig.5.8 a) shows the output of the simulator using type 1) adaptive control. The compensator is set for unity gain and has a unit-step input. The gain-change transient, produced by the change $G = 1 \longrightarrow 2$, is

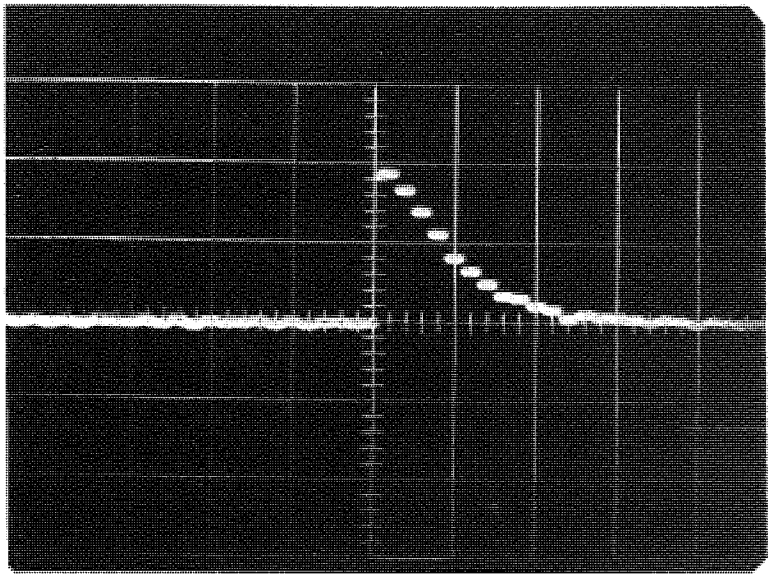

a) Type 1) adaptive control

Scaling:

X one division ≡ 0.5 secs.

Y one division ≡ 0.5 volts

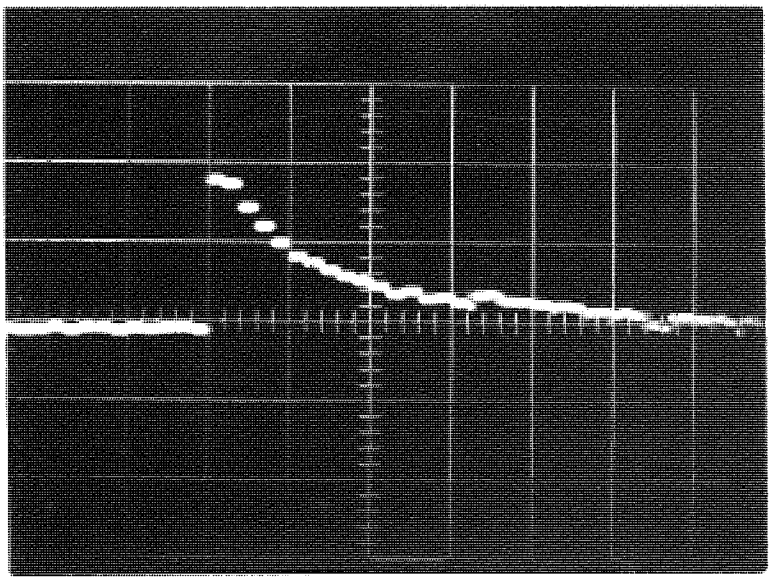

b) Type 2) adaptive control

Fig.5.8 Gain change reponses from the hybrid simulator

therefore the inverse of Fig.5.8 a). Using type 2) adaptive control the output of the simulator,for the same conditions,is shown in Fig.5.8 b). The theoretical gain change transient of Fig.4.10,for $G = 1 \longrightarrow 2$,is in very good agreement with the inverse of Fig.5.8 a).

From the output traces of Fig.5.8 a) and b) little difference is observed between the two methods of adaptive compensation;the adaptive compensation of type 1) is marginally better.

5.3.2 Performance of the Adaptive Compensator

Using the hybrid simulator with type 1) adaptive control,output photographs have been obtained for a wide range of simulated 'arc plant' gains.Fig.5.9 a) ,b) and c) show the output traces of the system with a complex input.The datum line for each photograph can be taken from the extreme right hand output value of -0.25 volts.The plant gain for a) is $G = 0.2$,and for b) $G = 2$ .The effectiveness of the adaptive controller is such that very little difference can be observed in the output response for a 1000% difference in gain.Fig.5.9 c) indicates the effect of sudden changes in gain on the output response.In this photograph,the first step change in gain is $G = 1 \longrightarrow 2$ and the second is $G = 2 \longrightarrow 1$ .Providing the gain-change transient has sufficient time to decay before a step change in command occurs, then the system will perfectly reproduce the command change;this is demonstrated in Fig.5.9 c) .Effects of changing the input command before a gain-change transient has had sufficient time to decay are demonstrated in Fig.5.10 a) and b).Both output traces indicate a step change in command of $+0.5 \longrightarrow -0.5$;in a) the gain is changed from $G = 1 \longrightarrow 2$ and b)

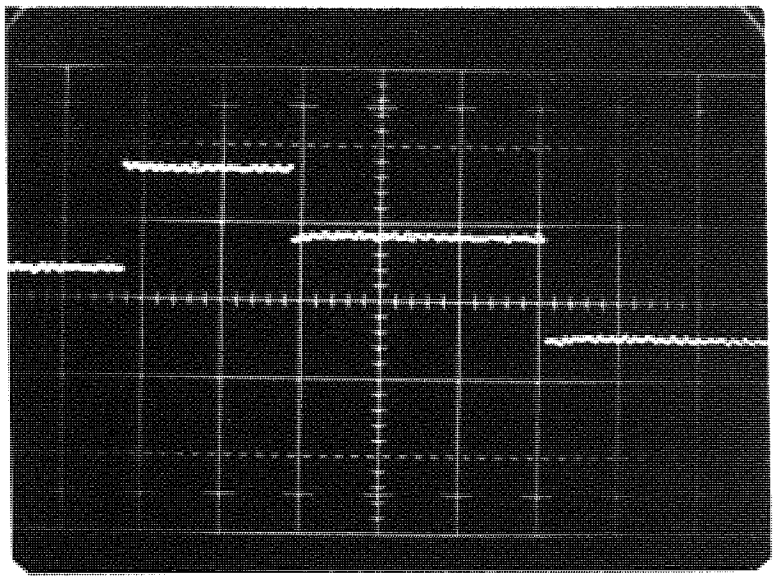

a) G = 0.2

Scaling:

X one division 2 seconds

Y one division 0.5 volts

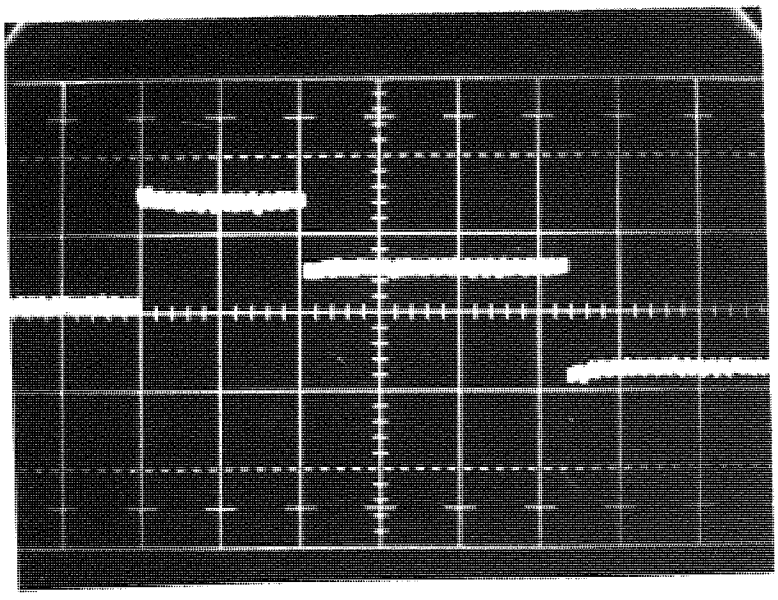

b) G = 2

Fig.5.9 Output from hybrid simulator using a complex input

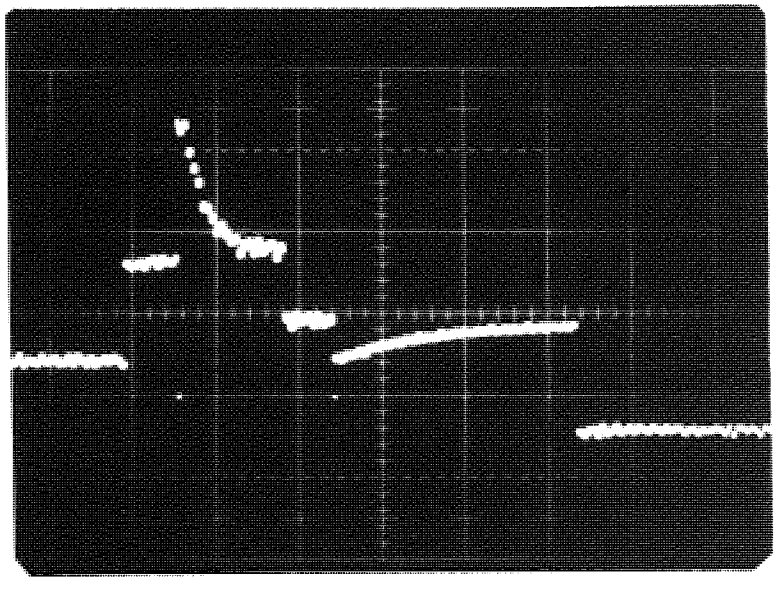

c) G = 1 ⟶ 2 and G = 2 ⟶ 1

Scaling:			
	X	one division	2 seconds
	Y	one division	0.5 volts

Fig.5.9 (continued)

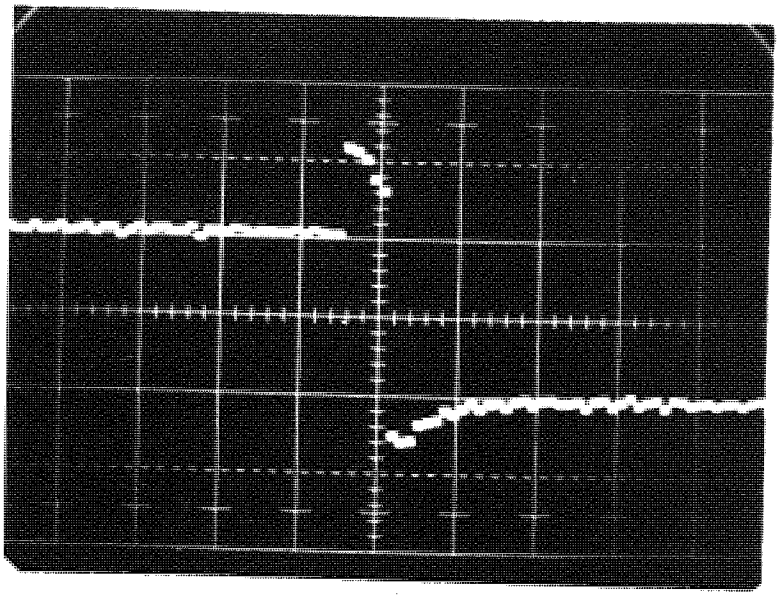

a) G = 1 2 Scaling: X one division 1 second

Y one division 0.5 volts

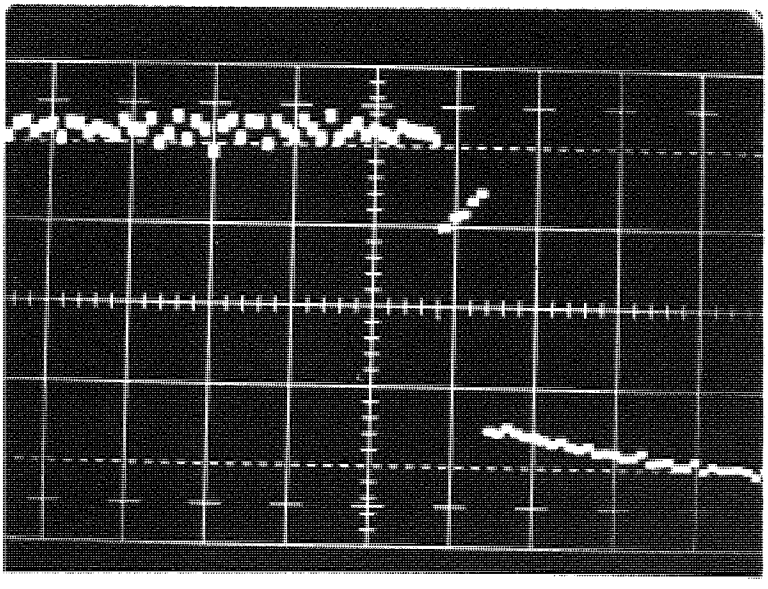

b) G = 2 1 Scaling: X one division 1 second

Y one division 0.25 volts

Fig.5.10 The effect of a step change in gain on the output of the hybrid simulator

$G = 2 \longleftrightarrow 1$;in both cases the gain change occurs a few tenths of a second before the command changes.

If the system exhibits rapid changes in gain (greater than one per second),then it is obvious that the controller will not be able to adapt to these changes.The controller will,however,respond to average values of the system gain (over several seconds of time) and will be able to adapt itself to average-gain changes.Thus,if the system exhibits rapid gain changes and also long-term gain changes (i.e. the steady build-up of oxidation on the electrodes of the 'arc plant'),perfect system response to step changes in input cannot be expected,but more consistent responses should be available with adaptive control than with a constant compensator gain.

5.4.1 Arc velocity control

The 'arc plant' discussed in sections 3.1.1 to 3.1.3 ,together with the measurement system of Chapter 2 were used to replace the simple model used in the analogue simulator of Fig.5.4. The complete block diagram of the final velocity-control system is shown in Fig.5.11 and a photograph of the laboratory set-up is shown in Fig.5.12.The measurement system and the arc-current controller are contained in the cabinets on the left of the picture;the 'arc plant' model can be seen on the right (the photographs of Fig.3.1 and Fig.3.2 show this in greater detail) and behind this part of the arc-current power supply is visible.The digital computer used in the control system was situated in another part of the building;input and output connections were made by the use of twin-core shielded microphone cable.

The block diagram of Fig.5.11 indicates two regions of noise occuring in the control loop.The first, ξ ,is associated with the gain of

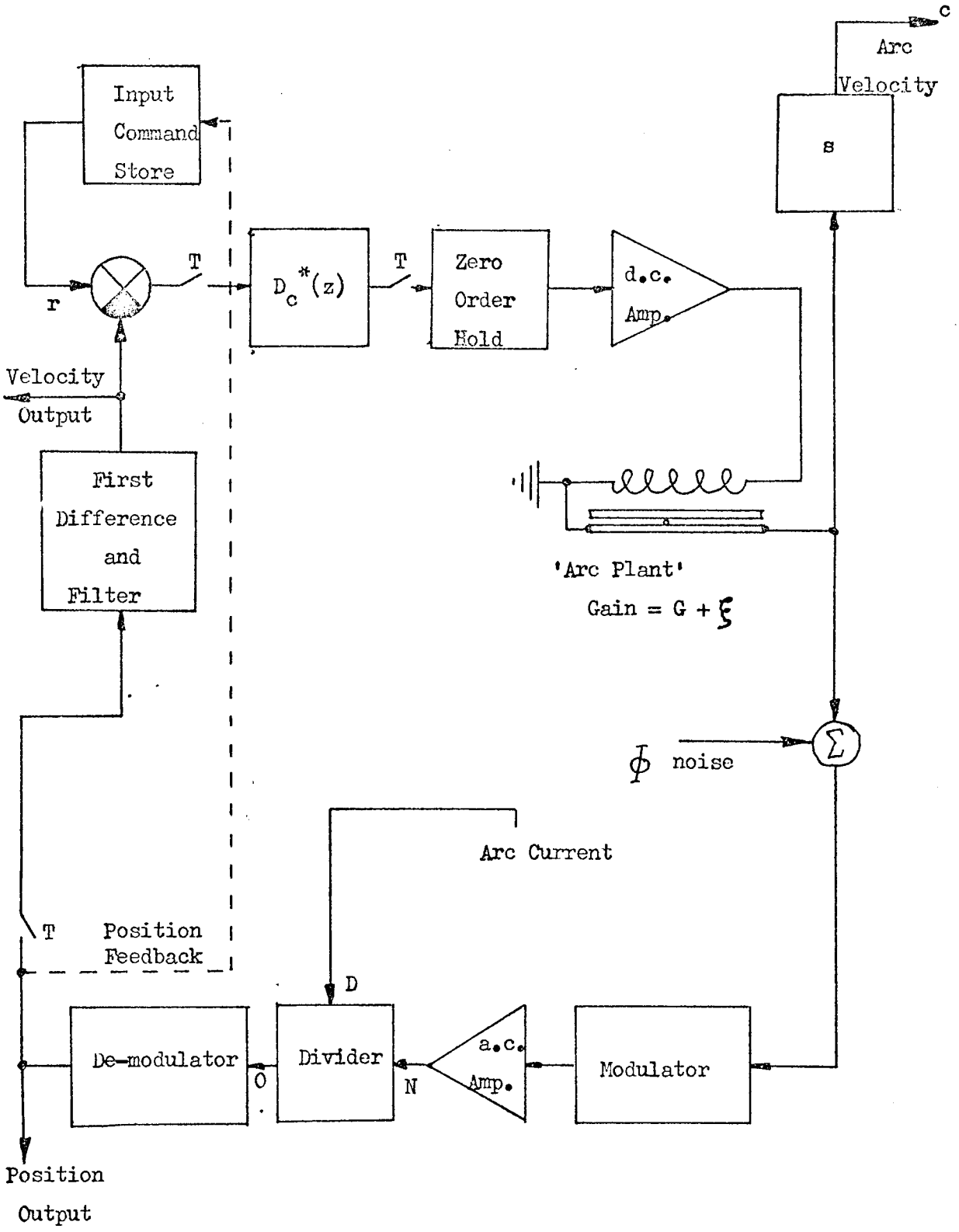

Fig.5.11 Final arc control system

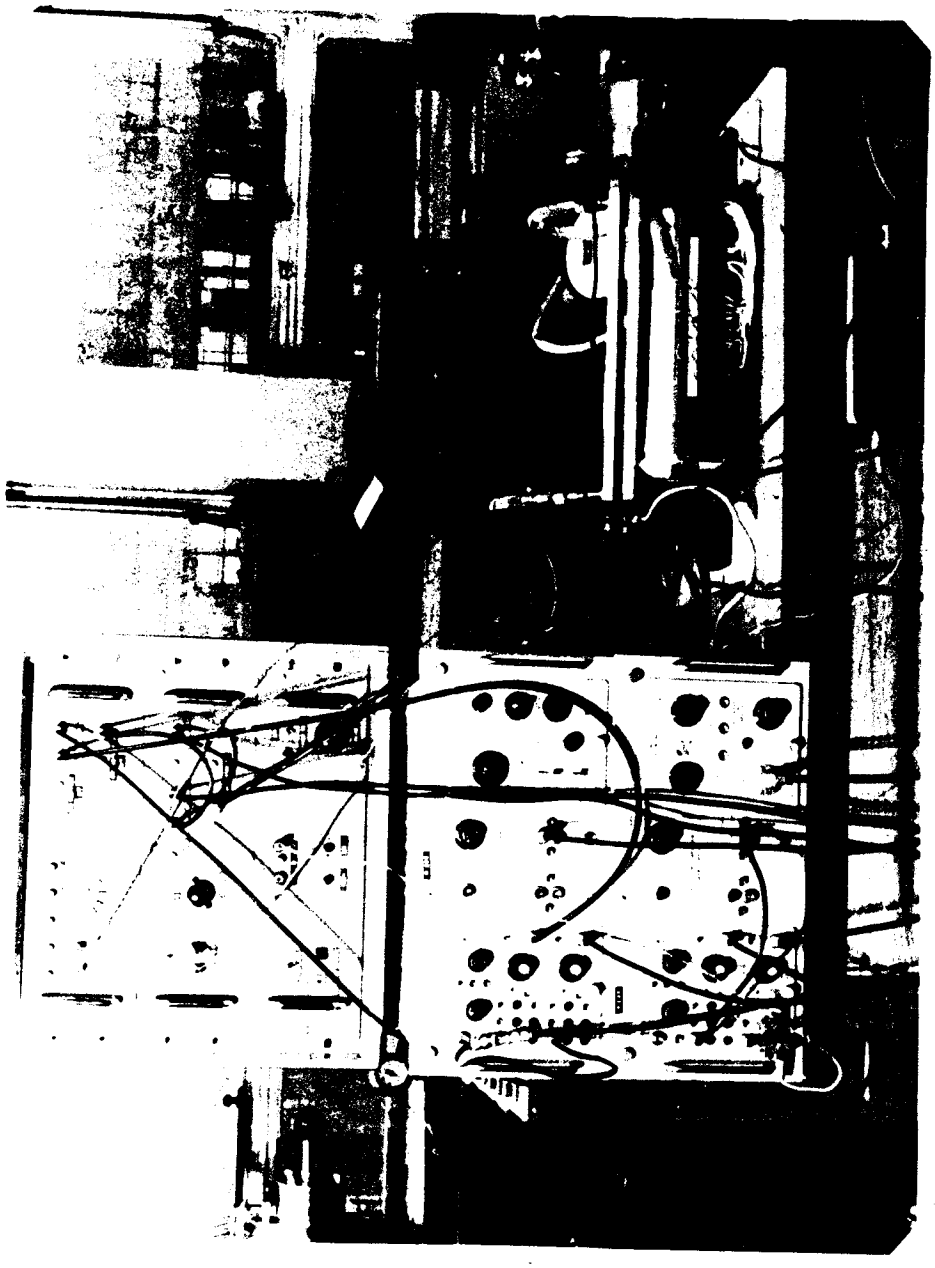

Fig.5.12 Laboratory set up for the final arc control system

the 'arc plant' and it is this rapid gain-changing function which gives rise to the discontinuous mode of arc motion observed.This gain noise is superimposed upon the average value of gain G ,and it is this gain, G , to which the adaptive controller will respond,as discussed in 5.3.2 . The second noise input, Φ ,occurs in the measurement of the arc position along the electrodes and it is caused by fluctuations in arc current and random arc movement.The input to the discrete compensator is the command minus the first difference velocity signal.Typical velocity signals are shown in Fig.2.12 a) and b) and from these it is evident that noise inputs from Φ and ξ are quite predominant.The output of the compensator will also have a noise content (a typical output is shown in Fig.5.13) and,since the adaptive controller calculates the system gain from the compensator output immediately preceeding a change in input command,it is evident that the calculated gain could be in error by a considerable amount during an arc run.There are two possible solutions to the problem:

1) The adaptive control element can be replaced by a fixed-gain compensator,the gain of which is determined by the conditions of the 'arc plant'.
2) Further filtering can be employed to reduce the noise content of the compensator output.

Method 2) is the more worthwhile,the filtering being accomplished by digital means within the compensator software.The digital filtering is performed by taking the average of the ten previous compensator output pulses immediately before the change in command input (the programme details are given in Appendix II).The square-root function on the output of the compensator,which was removed for analogue simulation tests,is included in the arc-velocity control system.

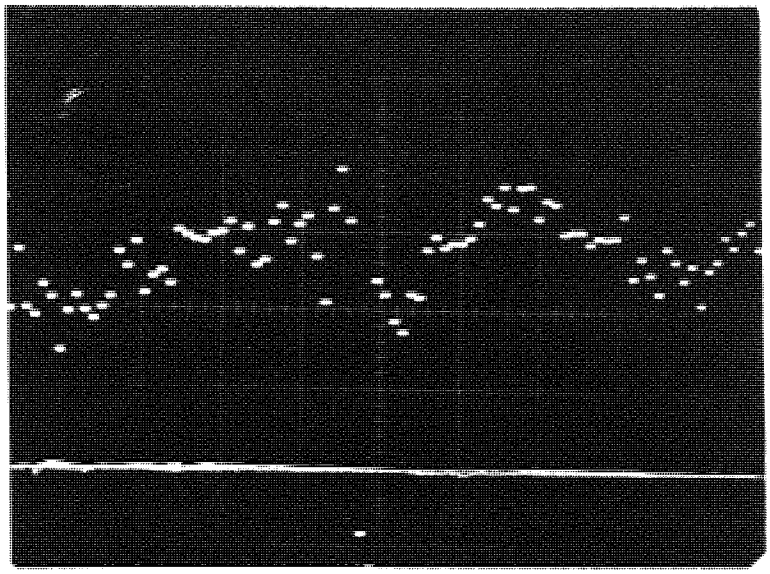

Scaling: X one division ≡ 1 second

Y one division ≡ 1 volt

Fig.5.13 Typical output from the discrete compensator $D_c^*(z)$

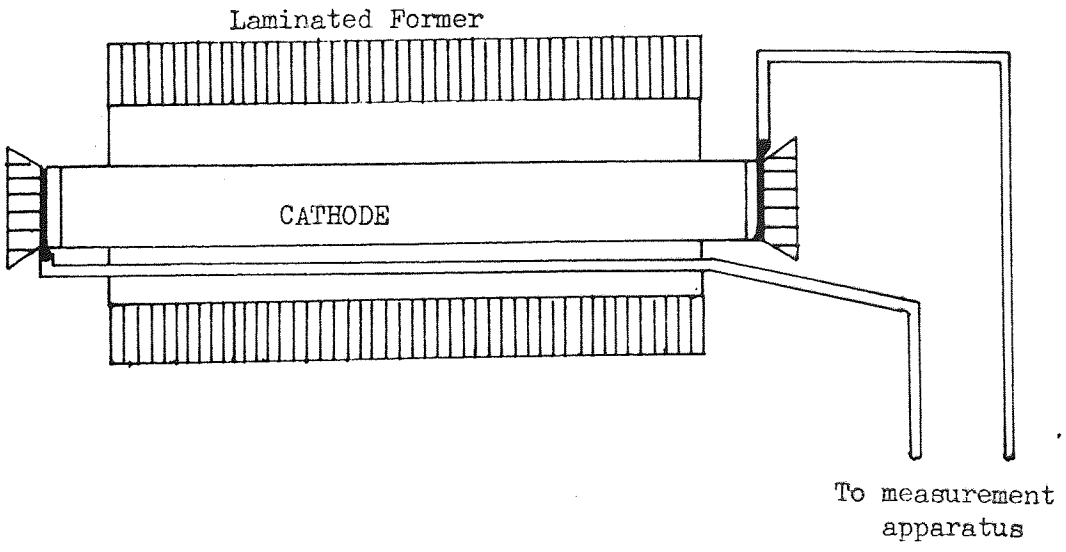

Fig.5.14 Modification to the arc position signal pick-up system

Since the position measurement electrode (cathode) is situated in the air gap of the laminated former, a step change in the field generated in the air gap will induce a voltage in the cathode electrode. This will give rise to an erroneous arc-position signal. In order to overcome this difficulty, one of the measurement leads from the cathode electrode is run parallel with the electrode; thus any induced voltage in the cathode will be cancelled by an equal and opposite voltage induced in the measurement lead. A diagrammatic representation is shown in Fig.5.14.

5.4.2 Control System Output Measurement

In order to assess the performance of the system two output points on the control loop are available and are indicated in Fig.5.11. Unlike the analogue simulator, it is not possible to monitor the arc velocity directly on the practical system, the signal being derived from the feedback loop of Fig.5.11, and so any velocity monitored will be subject to the transient behaviour of the one-second time constant associated with the measurement system. Although it would seem logical to observe the velocity signal available from the computer, in order to assess the performance of the system, the noise present on the velocity signal is such that a clear indication of the system performance is difficult to obtain. A more useful output is obtained at the output of the position-measuring system. Since this represents the integral of the computer velocity signal, most of the noise will be greatly attenuated. The degree of success of the control system in maintaining the arc velocity at a desired value can be examined by observing the slope of the position output trace. The output response of the recorder to a step change in input

command to the control system will be dependent on both the control system response and the response of the recorder.Unlike the demodulator stage of the measurement system,the recorder has effectively two filters;one is a passive capacitor/resistor filter on the input to the recorder and the other is the dynamic filter created by the drive apparatus in the control systems of the X andY axes.The combined dynamic filter has a characteristic which is flat up to 10 r/s and then falls off rapidly.At a typical pen speed of 5 seconds per inch,a step change of ramp input to the recorder produces a near perfect output response.It is therefore possible to examine the output response of the arc velocity control system to a step change of input command and to observe approximate degrees of overshoot and undershoot.

5.4.3 Arc Velocity Control System Performance

This section presents the results of various experiments carried out on the arc-velocity control apparatus.The results are in the form of arc position versus time and were recorded by a Hewlett-Packard chart plotter,as discussed in the previous section.

Initial tests were carried out on brass electrodes with an input command cycling between 0.0125 m/sec. and -0.0125 m/sec. over an electrode length of 0.22 metres. Fig.5.15 shows the position trace of a 10 Ampere arc moving on 'used' electrodes.The 'jitter' on the trace is due to the noise from the measurement system and the fact that the carrier frequency of this system 'beats' with the carrier frequency used in the chart plotter.

It is evident from this trace that velocity averaged over small sections of the electrodes (less than 0.005 metres) is beyond the control of

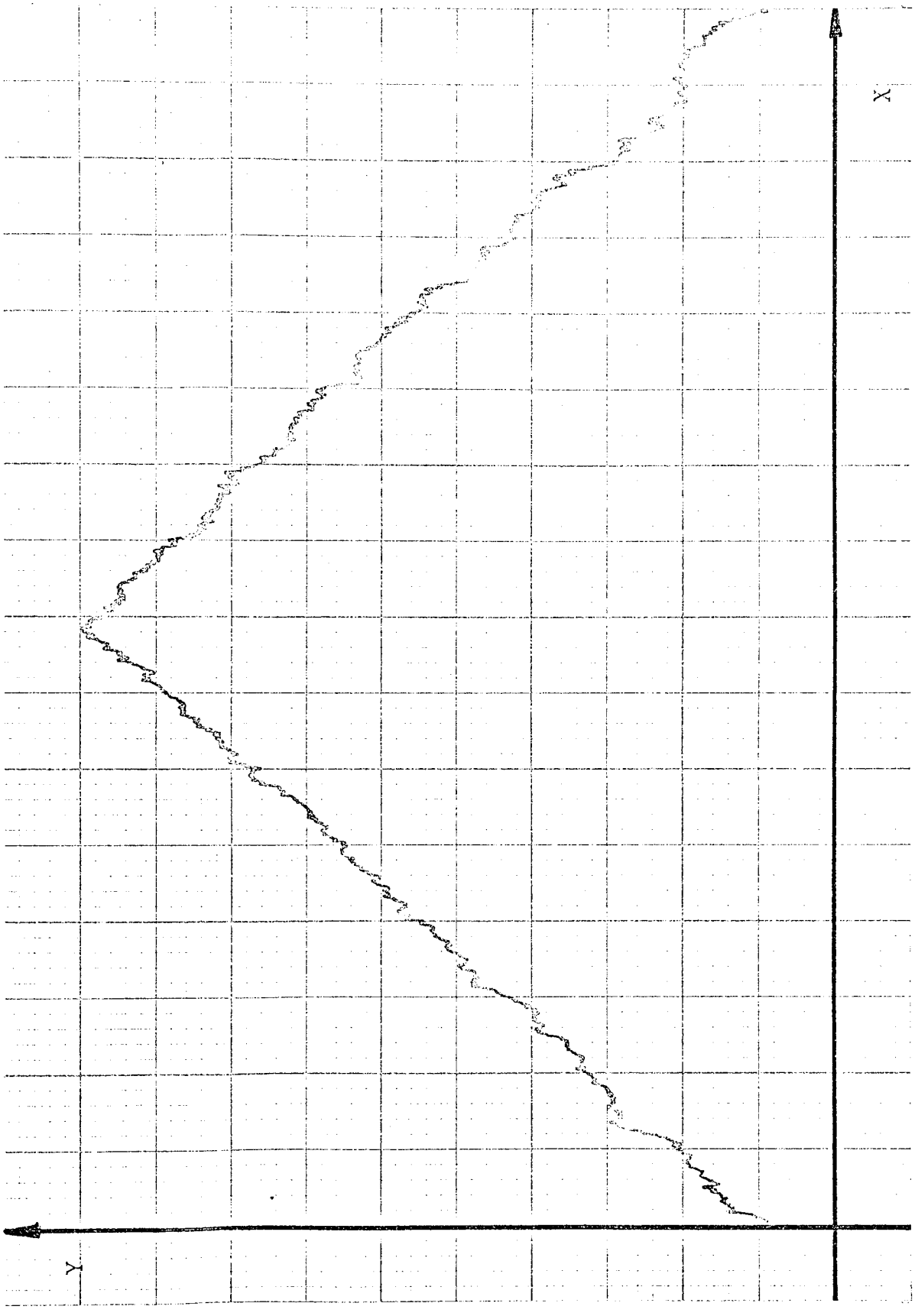

Scaling: X direction 2 division ≡ 5 seconds

Y direction 2 division ≡ 0.05 m of arc movement

Fig.5.15 Output from the chart plotter with the arc under closed loop control. Arc current = 10 Amperes

the system; this is particularly evident over the first few centimetres of arc travel (at the beginning and end of the trace) where velocity increases and decreases of well over 100% can be observed and at one point zero velocity persists for a short while. If the absolute velocity is now averaged over 0.05 metre sections of arc travel, this average value varies by less than 10% for the total arc travel and it is this average velocity over which the system extends its control. The average value of velocity measured for both directions of arc travel is $\pm$ 0.0115 metres/sec., which represents an error of 8% referred to the input command from the computer. This error is of little consequence in such a control system and can be accounted for by the fact that the value of sample time, T, is probably greater than the 100mS calculated†. Errors in this calculation will change the feedback coefficient from unity to, in this case, a slightly greater value and effectively reduce the gain of the system. The step response from positive to negative arc velocity is very good in this example and indicates an accurate electrode gain calculation, by the adaptive compensator, at the point of command change.

In order to assess the improvement in performance of the closed-loop control system over an open-loop system, an arc run was made using the system shown in Fig.5.16. The input command was chosen to produce a similar value of absolute velocity to that used in the closed-loop case. The open-loop

---

† The calculation of T involves a summation of the times taken to complete each computer programme instruction. With the MACRO 9 main programme this is a straightforward procedure, since each instruction time is known exactly. Because of the complexity of each FORTRAN IV instructions in the sub-routine, an approximation of the time taken to cycle this programme has been made by only considering instructions taking longer than 1 mS to perform (e.g. multiplication, division, square root).

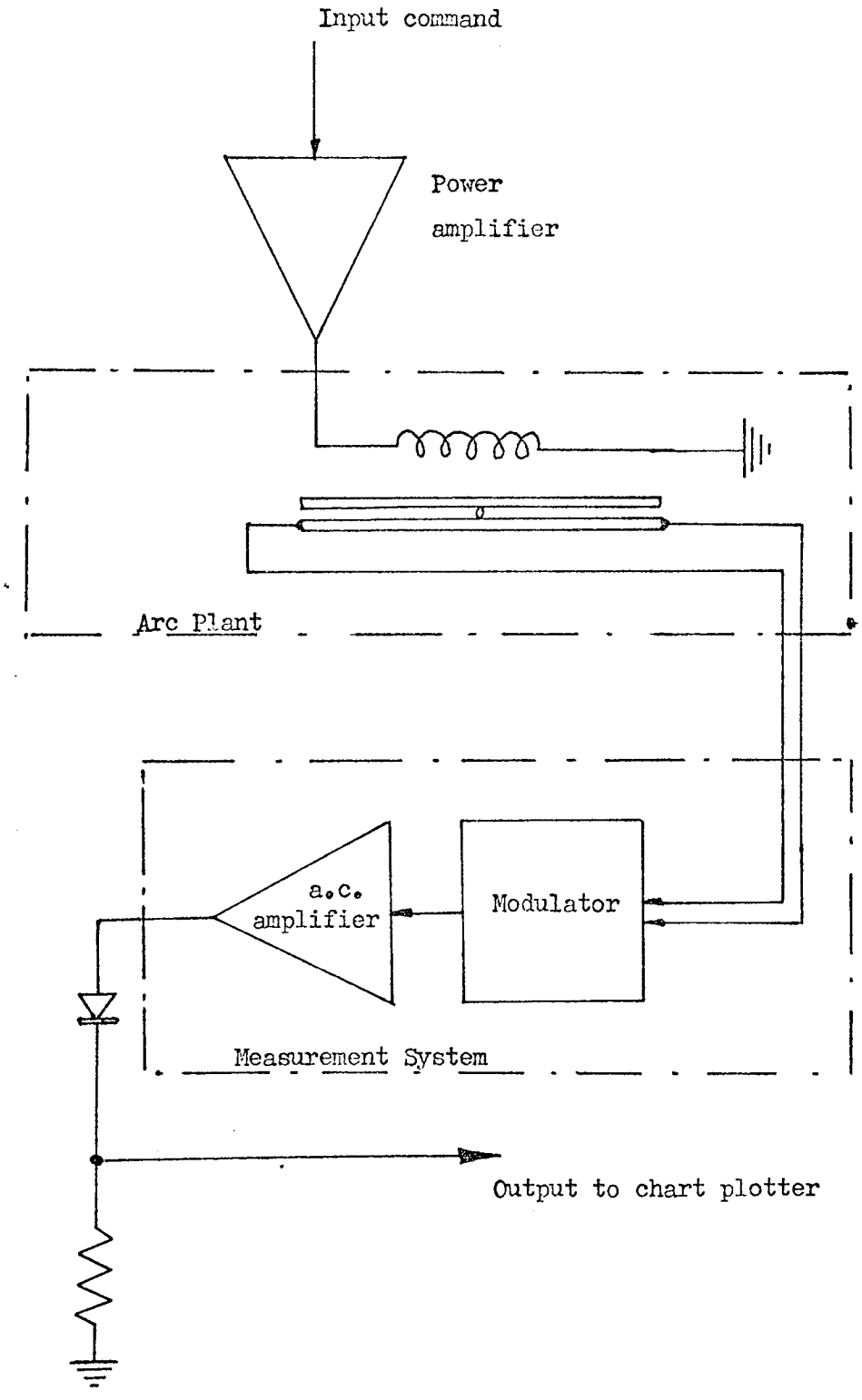

Fig.5.16 Open loop arc control system

run was made on the same electrodes and directly after the previous closed-loop run, thus almost identical surface conditions were obtained†. Fig.5.17 shows the output trace of the open-loop run with Fig.5.15 superimposed. The improvement afforded by closed-loop control over open-loop control is immediately obvious; measurements taken from the open-loop trace indicate that the velocity of the arc, averaged over 0.05 metre lengths, can vary by as much as 45% from the mean velocity.

Results were taken on a different set of brass electrodes for more complex input commands and these results are displayed in Fig.5.18 and Fig.5.19 . In both output traces the average velocity of the arc is within 10% of the input command. The responses of the arc to changes in input command are not so good as those indicated in the first trace of Fig.5.15. The cause of the imperfect responses is probably due to:

1) A sudden electrode gain change in the vicinity of the command change.
2) Inaccurate calculations of electrode gains by the adaptive compensator.
3) A non-linear forward path gain because of inaccuracies in the square-law model for the arc.

This latter suggestion will not affect the velocity change in Fig.5.15 since the command is only changed in sign, not in absolute value, and the response by the arc is immediate.

Fig.5.20 shows the output trace of an arc running between a brass cathode and copper anode on clean surface conditions. The input command is the

---

† This is justified by the fact that the electrodes had received five 10 Ampere arc runs (see 3.3.3).

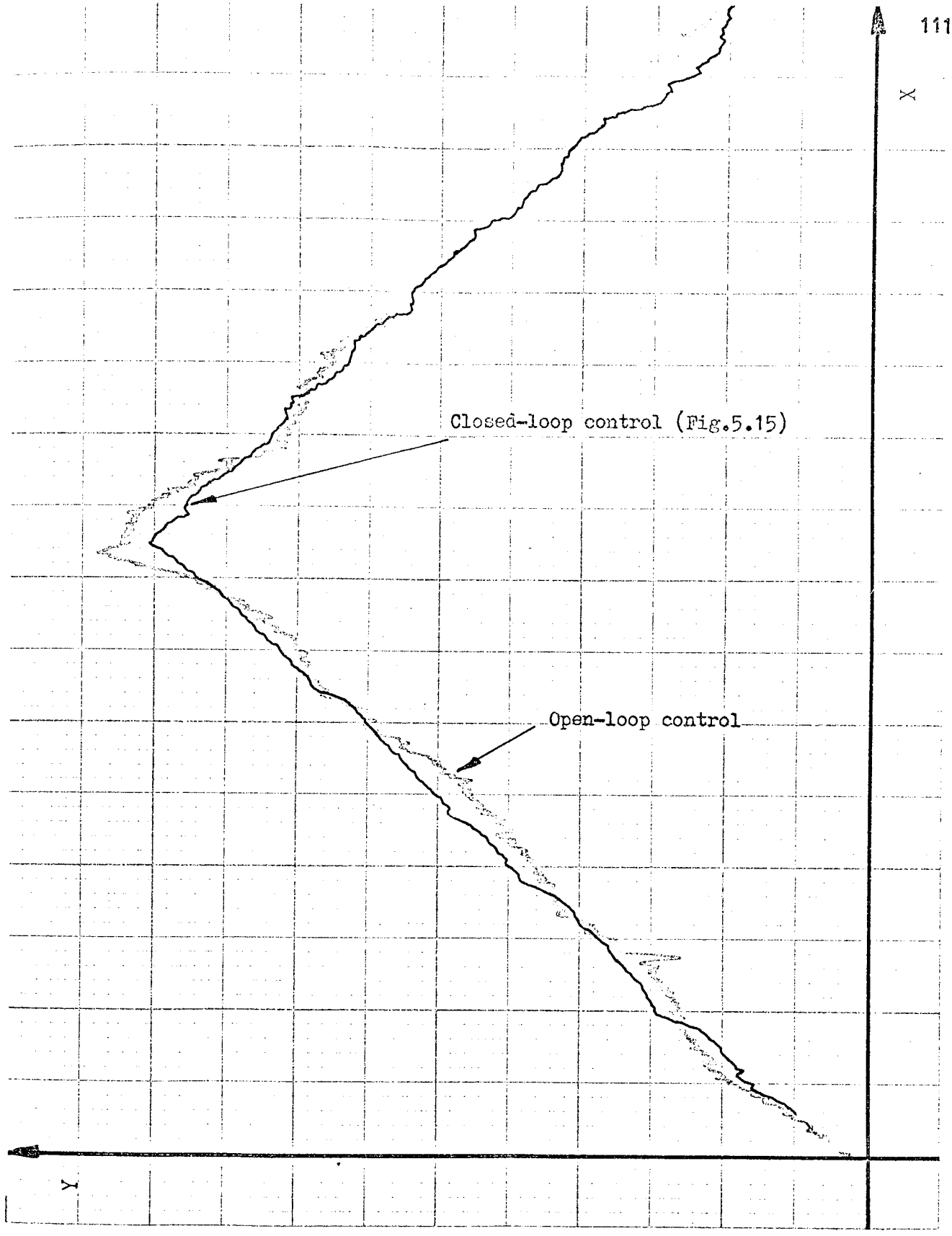

Scaling: X direction 2 division ≡ 5 seconds

Y direction 2 division ≡ 0.05 m of arc movement

Fig.5.17 Output from chart plotter with arc under open loop control (Fig.5.15 is superimposed for comparison) Arc current = 10 Amperes

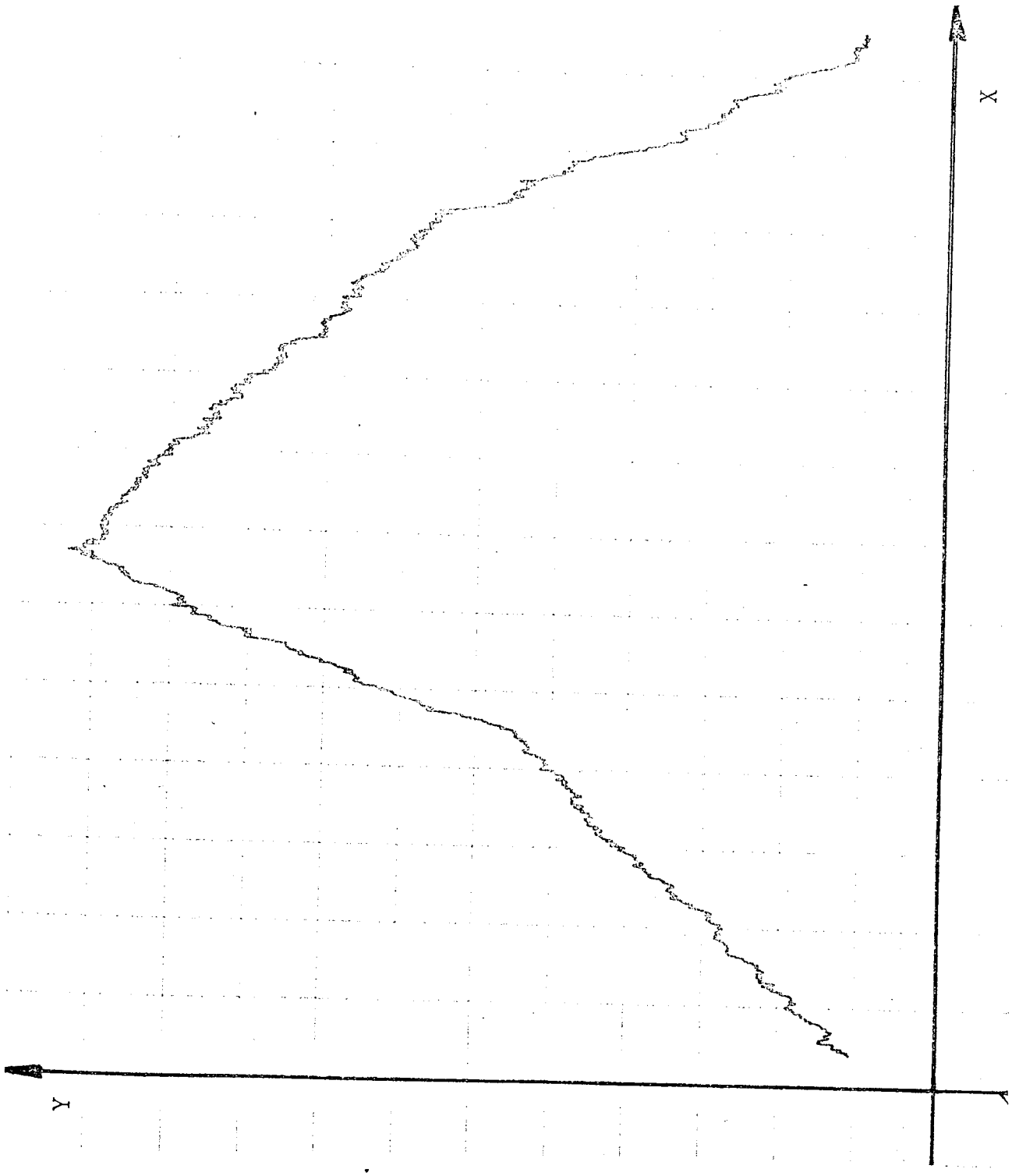

Scaling: X direction 2 division ≡ 5 seconds

Y direction 2 division ≡ 0.05 m of arc movement

Fig.5.18 Output from chart plotter with arc under closed loop control.
Input command +0.0125 m/s +0.025 m/s -0.0125 m/s -0.025 m/s

Arc current = 10 Amperes.

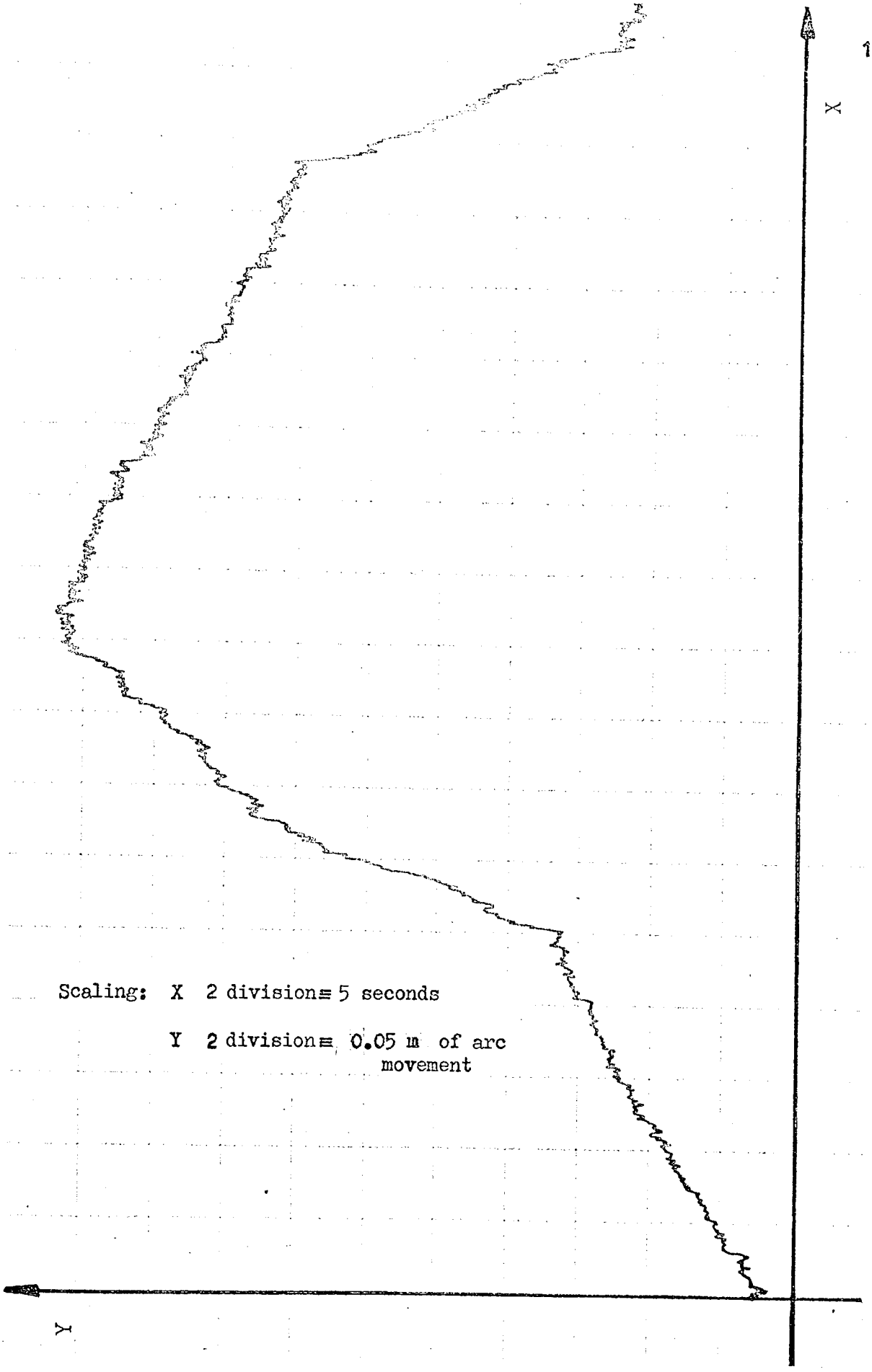

Fig.5.19 Output from chart plotter with arc under closed loop control. Input command +0.00625m/s +0.025m/s +0.0125m/s -0.00625m/s -0.025m/s -0.0125m/s . Arc current = 10 Amperes

same as that used for Fig.5.15 ; ± 0.0125 metres/sec. The configuration of copper anode and brass cathode is in the high gain range (see 3.2.4),as apart from the low-gain configuration of brass anode and cathode used in the previous tests.Apart from producing an arc model of higher gain,the copper electrode, enhanced by the clean surface conditions,introduces a certain element of instability into the arc motion and this can be observed in Fig.5.20. Near the change in command,the arc velocity falls to zero and then increases by well over 100% of its original value.The sudden drop in velocity was probably due to imperfections on the electrode surfaces† and the sudden increase in velocity was the result of the arc 'freeing' itself.The average absolute velocity of the arc trace in Fig.5.20 is about 0.011 metres/sec.,which is consistent with the results obtained previously with the all-brass configuration.

Further tests have been carried out on brass electrodes with arc currents up to 50 Amperes. Fig.5.21 shows the trace of a 30 Ampere arc moving on used surface conditions, and Fig.5.22 shows the trace of a 50 Ampere arc moving on the same electrodes. Both traces indicate a very stable arc motion, with an average velocity of 0.011 metres/sec.,but in both cases the step change of velocity undershoots. At arc currents in the order of 50 Amperes, instability occurs at velocities greater than 0.03 metres/second. This particular problem has also been encountered on open-loop tests (used in Chapter 3) where instability at these higher velocities has prevented arc runs at currents greater than 30 Amperes.

Throughout all the closed-loop tests the gain of the system has not been adjusted in any way ,the only adjustments required being those to

---

†Sudden drops in velocity have been observed by Cobine and Gallagher[36] where the cathode spot demonstrated reluctance at crossing even a small scratch on the cathode surface.

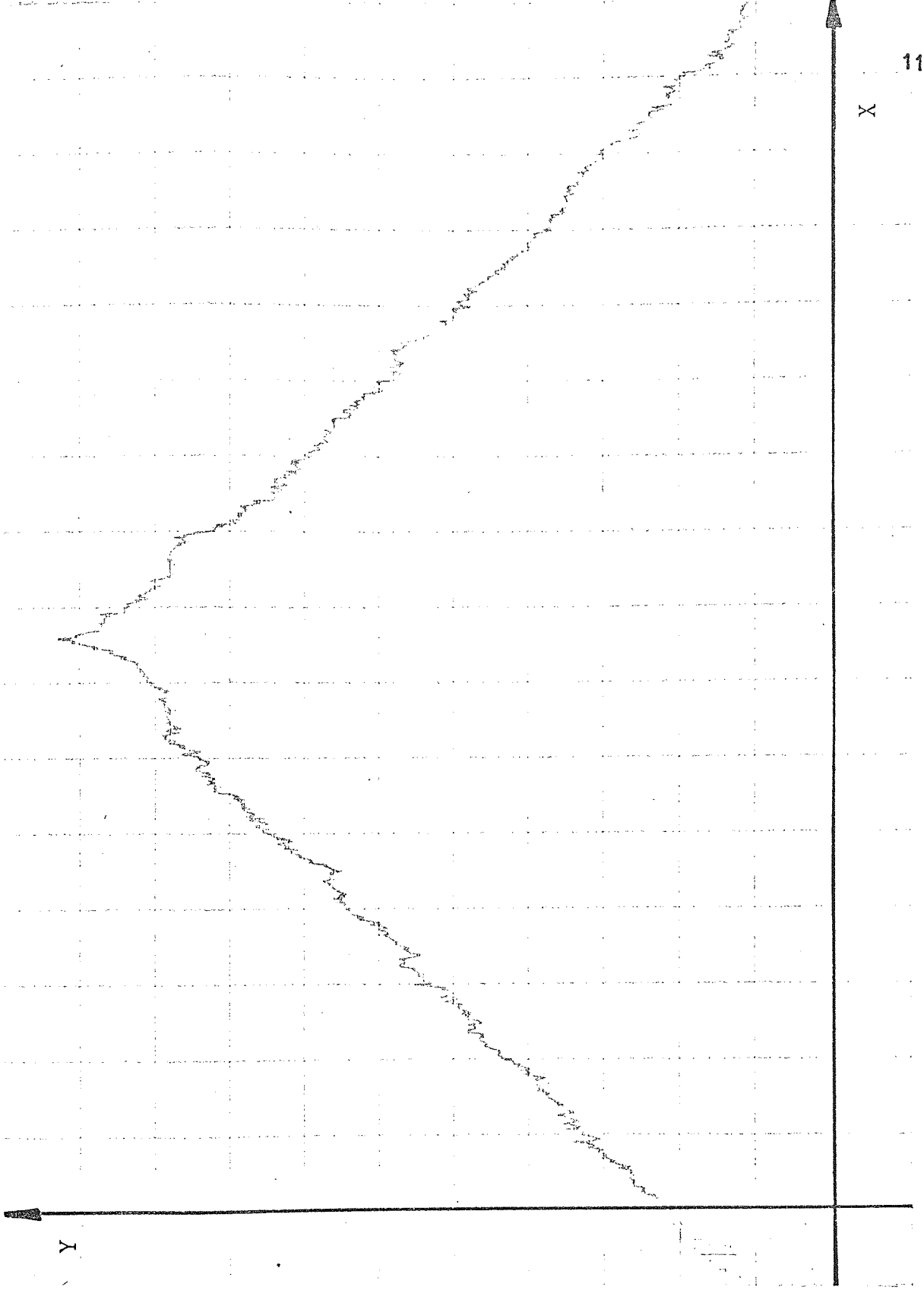

Scaling: X direction 2 division ≡ 5 seconds

Y direction 2 division ≡ 0.05 m of arc movement

Fig.5.20 Output from chart plotter with the anode material changed from brass to copper; input command as in Fig.5.15

Arc current = 10 Amperes

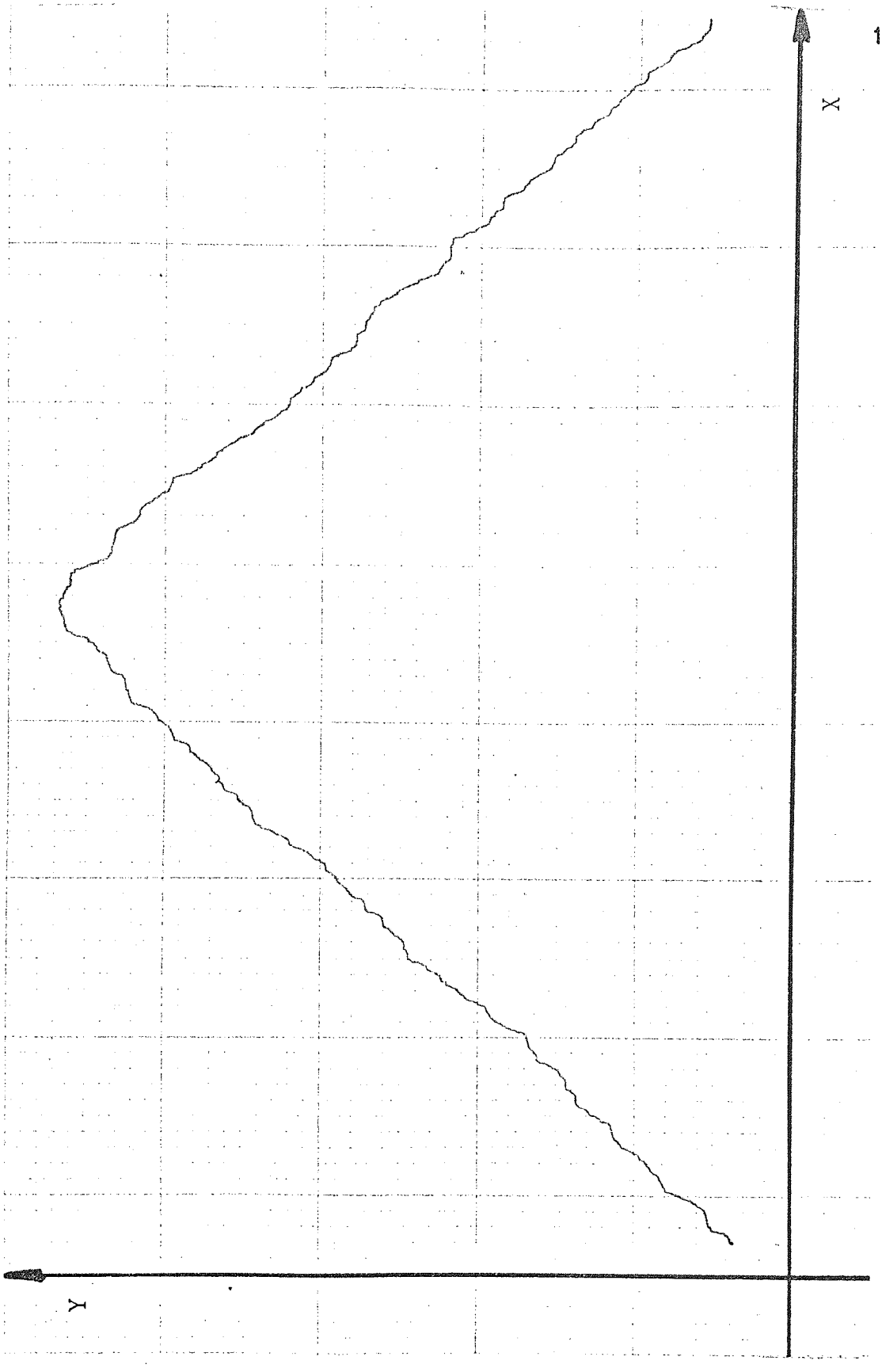

Scaling: X direction 1 division ≡ 5 seconds

Y direction 1 division ≡ 0.05 m of arc movement

Fig.5.21 Output from chart plotter for a 30 Ampere arc travelling on 'used' brass electrodes. Input command as for Fig.5.15.

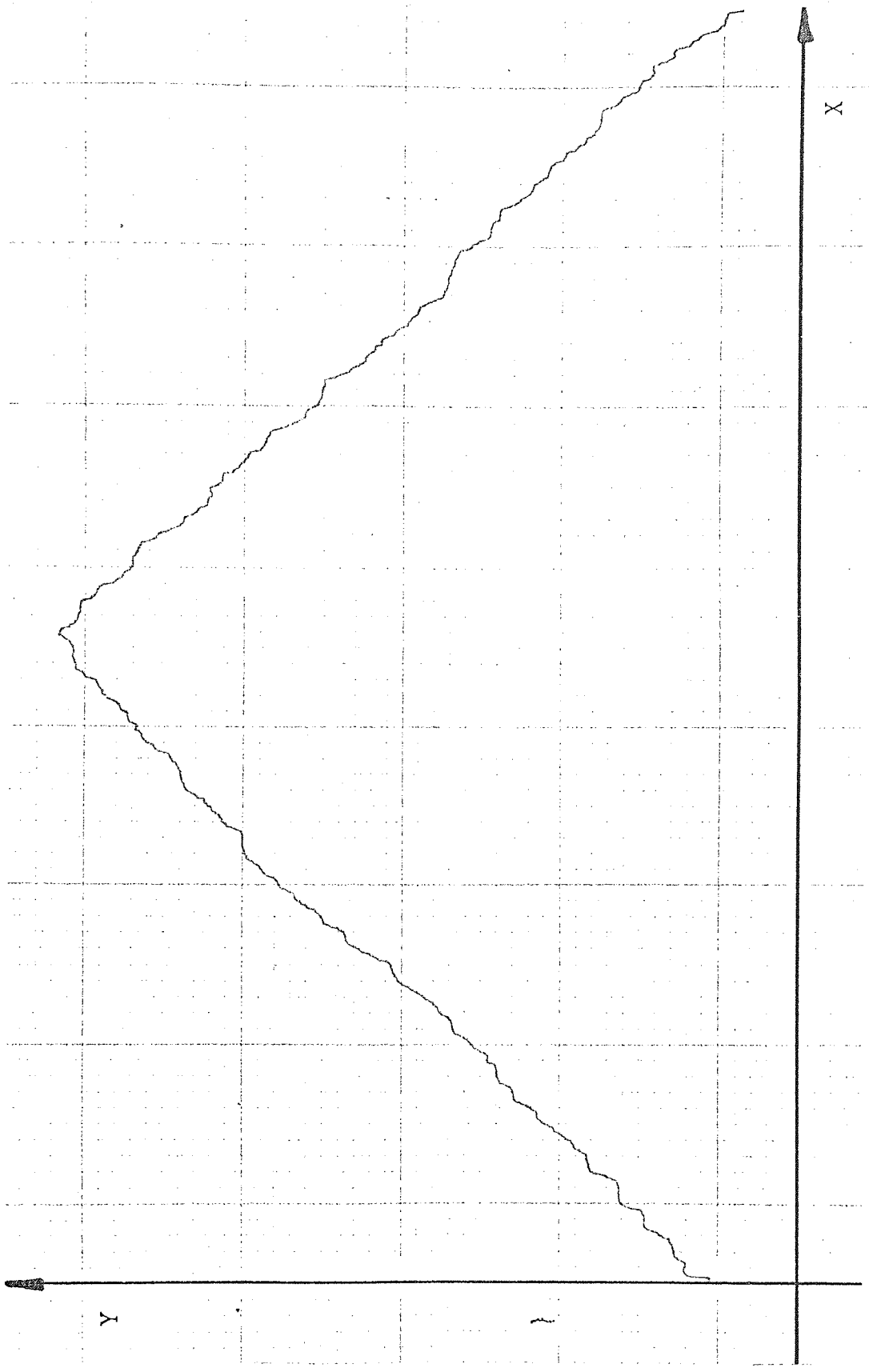

Scaling: X direction 1 division ≡ 5 seconds

Y direction 1 division ≡ 0.05 m of arc movement

Fig.5.22 Output from chart plotter for a 50 Ampere arc on brass electrodes. The arc run follows that of Fig.5.21 for the same input command.

re-calibrate the position-measurement apparatus for electrode changes.The consistently accurate responses of the arc to the input commands demonstrate the effectiveness of the controller in compensating for any change in the 'arc plant' conditions.

5.5 Summary

The theoretical control system analysis of Chapter 4 has been developed into practical software for an arc-velocity control system.Using a hybrid (digital/analogue) simulator,exhaustive tests have been carried out on the system which has behaved exactly as predicted in Chapter 4. An interesting result from the simulator is that,for a given complex input command,the output is identical over a total gain change of 1000%.

Finally,the control system has been applied to the 'arc plant' of Chapter 3,the results being displayed as arc position versus time.Although instantaneous values of arc velocity are beyond the control of the system, for constant input commands velocities averaged over 0.05 metre sections of the electrodes can be controlled,in the main,to within 10% of each other and the total average velocity to within 10% of the input command to the control system. Open-loop control of the arc velocity yields an average velocity (over 0.05 metre sections) of up to 45% and a visible deterioration in the output trace when compared with the arc under closed-loop control. Changes in electrode material (within the terms of reference of this investigation) ,electrode surface conditions and arc current reveal little changes in the average output velocity of the arc under closed-loop control.

CONCLUSIONS

A summary of the work carried out in this thesis is presented at the end of each of the four main chapters; this section critically surveys the work and discusses its importance in relevance to work produced by previous researchers and its practicability to industry.

1) An instrumentation system has been developed for measuring the position of a d.c. arc, along parallel electrodes, to a degree of accuracy well suited to industrial and experimental requirements. The principle embodies a simple but very effective original technique utilising the voltage developed across one of the electrodes and as such makes obsolete the method of using external optical or magnetic transducers as sensors†. The system has been developed, using components of modest performance, to a point where commercial manufacture is feasible.

Utilising a digital computer of the type commonly available in industry, an arc-velocity signal has been obtained with a signal of sufficient quality to be used successfully in the feedback path of an arc-velocity control system*.

---

† This remark is certainly true for industrial applications. In the author's opinion it is also true for many laboratory investigations where more delicate apparatus is permissible but not more efficient.

* By connecting a recording device (e.g. a chart plotter) to the output of the measurement system, a very useful tool is obtained in the recording of low velocity arc movement for future research in this field.

2) The research studies, over the past two decades, in the field of high velocity arc movement (greater than 1 metre/second) have now been extended to the low-velocity region. A mathematical model for the rapidly moving arc, developed by previous workers, and believed to be accurate to within $\pm$ 50% , has been shown to be totally inadequate when applied to the slowly moving arc.

Using existing mathematical results and correlating these with extensive experimental work on the slowly-moving arc, a new model has been developed which will predict arc velocities in the low region. This model is heavily dependent on the electrode surface conditions (a factor which does not seem to influence the higher-velocity arcs to the same extent) , and new experimental and mathematical methods of allowing for these surface conditions have been introduced. This model has been expressed in control engineering terms in order to assist in the design of arc-movement control systems. The electric arc is still a relatively unpredictable phenomenon and any mathematical model can only be representative of the average performance under a given set of conditions; but, nevertheless, this model represents a new advance in industrial arc control.

3) A system has been developed for controlling the velocity of a d.c. arc between parallel electrodes (of the prescribed materials). Although the arc model is not a detailed representation of a specific industrial process (such as seam welding, profile cutting and zone refining) it is a meaningful general representation of the industrial arc process and will be useful to future workers. Moreover, this model was eminently

suitable for the purpose of this research; i.e. the feasibility of closed loop controlling an arc, by a transverse magnetic field, for industrial purposes.

From initial open-loop tests it was found possible to control the low-velocity arc using a transverse magnetic field, but the introduction of a feedback control system considerably improved this control. Under near identical conditions, the velocity of an arc (averaged over an electrode length of 0.05 metres) can be closed-loop controlled to within 10% of a nominal value, whereas under open-loop control this factor increases to 45%.

For many everyday industrial uses of the arc, the accuracy obtainable by open-loop control could be sufficient. This research shows that increased accuracy can be obtained by closed-loop control incorporating the type of low-priced digital computer becoming increasingly available in industry. Furthermore, the closed-loop control system developed adapts itself to the surface conditions of the electrodes and so consecutive arc runs on the same workpiece, or changes of workpiece, can be made without adjusting the control system provided the measurement electrode is unchanged. If the measurement electrode is renewed (in the same material) a slight adjustment to the instrumentation system will be required. If the measurement electrode material is changed, a recalibration of the measurement system will be necessary before the first run.

This research was intended as a contribution towards the control of arcs in industrial processes. If it is found useful by future workers in this field then its purpose will have been achieved.

Some of the results have been published[23] and other papers are in preparation.

Areas for future research

This investigation has been concerned with the control of an arc under laboratory conditions. Future research should be concentrated on adapting the present control system to an industrial process by developing the existing 'arc plant'. Modification to the electrode configuration will be required since the lower electrode becomes the work-piece and the upper electrode becomes the measurement electrode. Modification to the measurement electrode cross-section may be necessary if instability of the arc proves to be a problem. A modification suggested by the author is to surround the wedge-shaped cross-section with a high-temperature ceramic material in order to prevent the arc from travelling up the sides of the wedge.

It is possible that the present low-velocity arc model will have to be modified for arcs used in industrial processes (previous research has indicated that on molten surfaces the electrode gain is far higher than on solid surfaces[37] and it may be that the square-law model is also inaccurate). Inaccuracies in the arc model, which is used for linearising the feedforward path in the control loop, will only affect processes requiring accurate command change responses (profile cutting); the use of the control system in maintaining a fixed arc velocity (seam welding and zone refining) will not be affected by such inaccuracies.

Improvements to the measurement apparatus could be made by decreasing the time constant of the demodulator stage without increasing the noise content of the signal. If such an improvement could be effected, the gain-change response time of the controller could be greatly reduced and a

far 'tighter' control exerted on the arc velocity.

REFERENCES AND BIBLIOGRAPHY

1 - Geach,G.A , Jones,F.O : 'An arc furnace for zone refining metals', Metallurgia, October 1958, 58 , 345 , 209 - 210 .

2 - Harry,J.E : 'High current arc discharge phenomena with particular reference to the plasma torch', Ph.D Thesis , May 1968 , University of Aston in Birmingham.

3 - Guile,A.E , Mehta,S.F : 'Arc movement due to the magnetic field of current flowing in the electrodes', Proc.I.E.E , December 1957 , 104 A , 533 - 540.

4 - Mechev,V.S , Dudko,D.A : 'Apparatus for welding with the arc rotating in a magnetic field', Autom. Weld. , 1966 , 19 , 10 , 41 - 45 .

5 - Mechev,V.S , Dudko,D.A : 'Welding with an arc rotated in a magnetic field', Autom. Weld. , 1967 , 20 , 1 , 64 - 68 .

6 - Somerville,J.M : 'The electric arc', Methuan , 1959 .

7 - Rimmer,G.M : 'A study of the mechanism of arc interruption in circuit breakers' , M.Sc. Thesis , August 1958 , University of London .

8 - Eather,R.H : 'The cold cathode arc' , Australian Journal of Physics , 1962 , 15 , 3 , 289 - 292 .

9 - Adams,V.W et al ,'Correlation of experimental data for electric arcs in transverse magnetic fields' , Proc. I.E.E , October 1967 , 114 , 10 , 1556 - 1558 .

10 - Guile,A.E : 'The movement of an arc between parallel horizontal rods fed from one end in still air and in a wind' , Elec. Res. Ass. , 1957 , Tech. Rep. O/T19.

11 - Eidinger,A , Rieder,W : 'Verhalten des lightbogens in transversalen magnetfeld' , Archiv fur Elektrotechnik , 1957 , 63 , p.94 .

12 - Blix,E.D , Guile,A.E : 'Column control in the magnetic deflection of a short arc' , Brit. J. Appl. Phys. , 1965 , 16 , 6 , 857 - 864 .

13 - Ecker,G , Muller,K.E : 'Theorie der "Retrograde Motion"' , Zeitschrift fur Physik, 1958 , 151 , p. 577.

14 - Guile,A.E et al : 'The motion of cold cathode arcs in magnetic fields' , Proc. I.E.E , 1961 , 108 C , 463 - 470 .

15 - Dautov,G.Yu , Zhukov,M.F : 'Some generalisations relating to the study of electric arcs', J. Appl. Mech. Tech. Phys. , 1965 , 2 , 89 - 97 .

16 - Yasko,O.I : 'Correlation of the characteristics of electric arcs moving in transverse magnetic fields' , Proc. I.E.E , 1963 , 116 , 3 , 453 - 456 .

17 - Guile,A.E , Naylor,K.A : 'Further correlation of experimental data for electric arcs in transverse magnetic fields' , Proc. I.E.E , September 1968 , 115 , 9 , 1349 - 1354.

18 - Brichkin,A.V et al : 'Dynamics of electrode spots in an electric arc' , Soviet Physics - Tech. Physics , 1967 , 11 , 7 , 929 - 934 .

19 - Bron,O : 'The electric arc in control apparatus' , Gosenergoizdat , 1954 .

20 - Windsor,L.P , Lee,T.H : 'Properties of a d.c arc in a magnetic field' , Trans. A.I.E.E , May 1956 , 75 , 1 , 143 - 148 .

21 - Burkhard,G : 'On the influence of oxide layers on arc movement in a magnetic field' , R.A.E Libr. Trans. , October 1966 , No. 1181 .

22 - Lewis,T.J , Secker,P.E : 'Influence of the cathode surface on arc velocity' , J. Appl. Phys. , 1961 , 32 , 1 , 54 - 64 .

23 - Roots,W.K , Jullien,G.A : 'Industrial arc instrumentation' , I.E.E.E Trans. Instrumentation and Measurement , June 1969 , IM - 18 , 2 .

24 - Jackson,A.S : 'Analogue computation' , McGraw - Hill , 1960

25 - Todd,C.D : 'Silicon epitaxial F.E.T's - Part 6 F.E.T as a chopper switch' , Electronic Components , July 1966 , p.663.

26 - Brichkin,A.V et al : 'Dynamics of electrode spots in an electric arc' , Sov. Phys. - Tech. Phys. , 1967 , 11 , 7 , 929 - 934 .

27 - Hull,A.W : 'Cathode spot' , Phys. Rev. , 1962 , 126 , 5 , 1603 - 1610 .

28 - Secker,P.E et al : 'Skin effect as a factor in the movement of cold cathode arcs' , Brit. J. Appl. Phys. , 1962 , 13 , 6 , 282 - 287 .

29 - Guile,A.E et al : 'Arc motion with magnetised electrodes' , Brit. J. Appl. Phys. , 1957 , 8 , 444 - 448 .

30 - Guile,A.E , Secker,P.E : 'Arc cathode movement in a magnetic field' , J. Appl. Phys. , 1958 , 29 , 12 , 1662 - 1667 .

31 - Secker,P.E , Guile,A.E : 'Arc movement in a transverse magnetic field at atmospheric pressure' , Proc. I.E.E , 1959 , 106 A , 311 - 320 .

32 - Gvozdetskii,V.S , Mechev,V.S : 'Research into welding arcs (plane and tapering) rotating in magnetic fields' , Autom. Weld. , 1963 , 16 , 12 , 1 - 5 .

33 - Jury,E.I : 'Sampled-data control systems' , John Wiley and Sons Ltd. , 1958 .

34 - McCracken,D.D : 'A guide to FORTRAN IV programming', John Wiley and Sons Ltd. , 1965.

35 - Cleary,J.F : 'General Electric Co. Transistor Manual' , Syracuse (N.Y) , 1964 .

36 - Cobine,J.D , Gallagher,C.J : 'Current density of the arc cathode spot', Physical Review ,1948 , 74 , 10 ,1524 - 1530 .

37 - Bachelis,I.A , Varlamov,I.V : 'Movement of the electric arc in a magnetic field', Autom. Weld. , 1966 , 19 , 4 , 43 - 49 .

APPENDIX I

POWER SUPPLY ANALYSIS AND CIRCUITRY

This section presents an analysis and circuit details of the arc-current closed-loop system.

Fig.AI.1 shows a block diagram of the open-loop arc-current power supply system.The variable element is a saturable-core transductor,which has the property of having an inductance whose value depends upon the current flowing through a bias winding around the inductor core.By varying voltage v_i (driving the bias winding amplifier) the current in the primary loop ,supplying the isolation transformer, may be varied considerably.The output of the transformer is rectified using a bridge circuit and smoothed by a bank of heavy duty capacitors.The 'arc plant' is driven from the power supply via a 2.7 Ω stabilising resistor,the arc current being monitored by the voltage,v_o, developed across a 0.15Ω resistor.

The linearity of the open-loop system is demonstrated by the graph in Fig.AI.2.For this plot,the input power amplifier gain was set to $G = 1$ and an arc was struck between the electrodes.The dynamic gain of the system is constant up to $v_o = 5.5$ volts and begins to reduce after this value,this is because,at high values of v_i ,the impedance of the transductor is low and approaches the value of impedance of the rest of the circuit.At $v_i = 0$ the transductor is at maximum impedance but,since this is not infinite,a small output signal is present ($v_o = 0.9$ volts).The dynamic gain of the system over the linear region is 1.5 ;therefore with an amplifier gain of G the overall system gain is $1.5\,G$.

Two time constants are present in the system: 0.5 seconds and 0.015 seconds.These are the result of the transductor bias-winding circuit and the power-supply filter respectively.Thus,the open-loop system can be

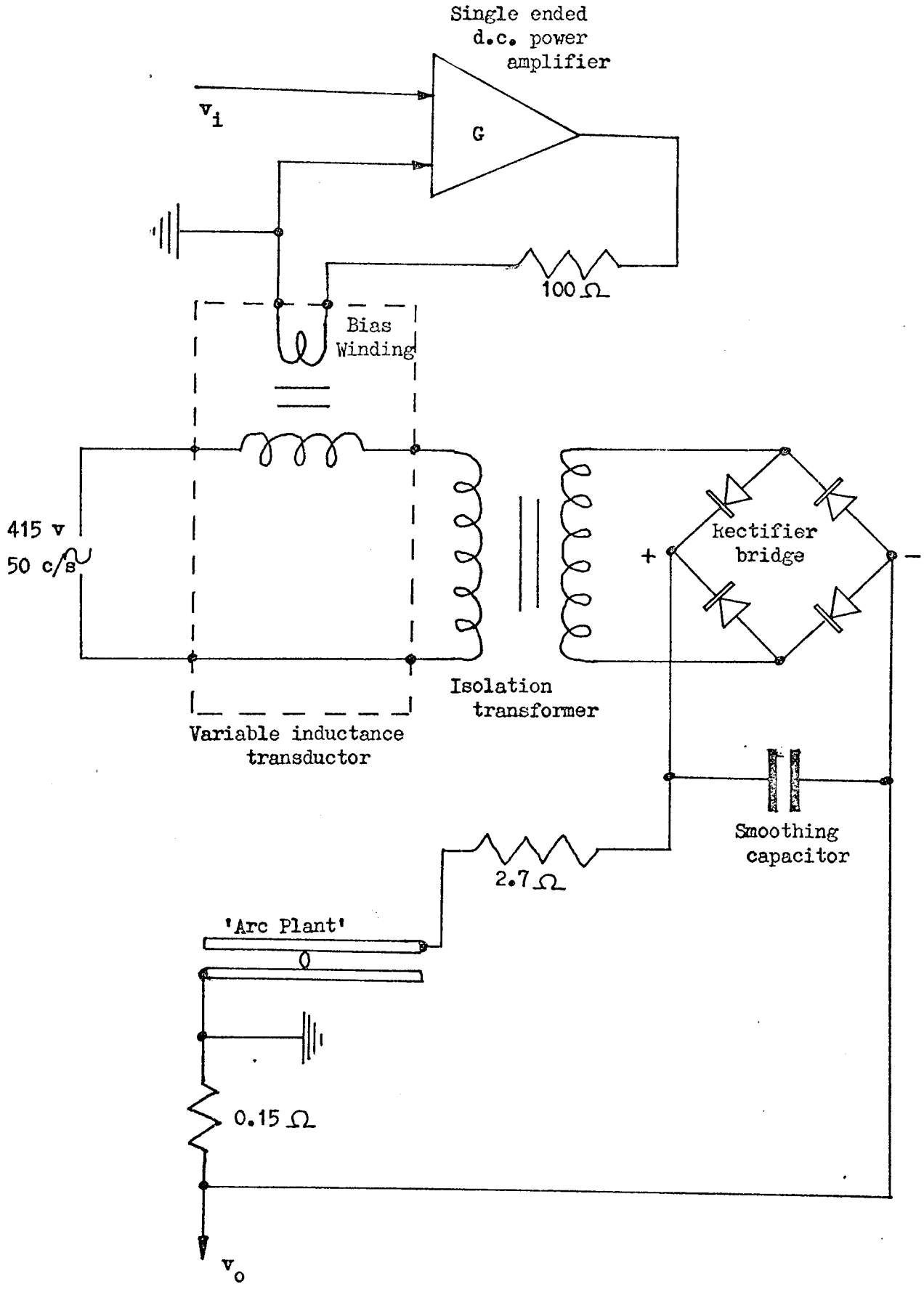

Fig.AI.1 Block diagram of open-loop arc current supply

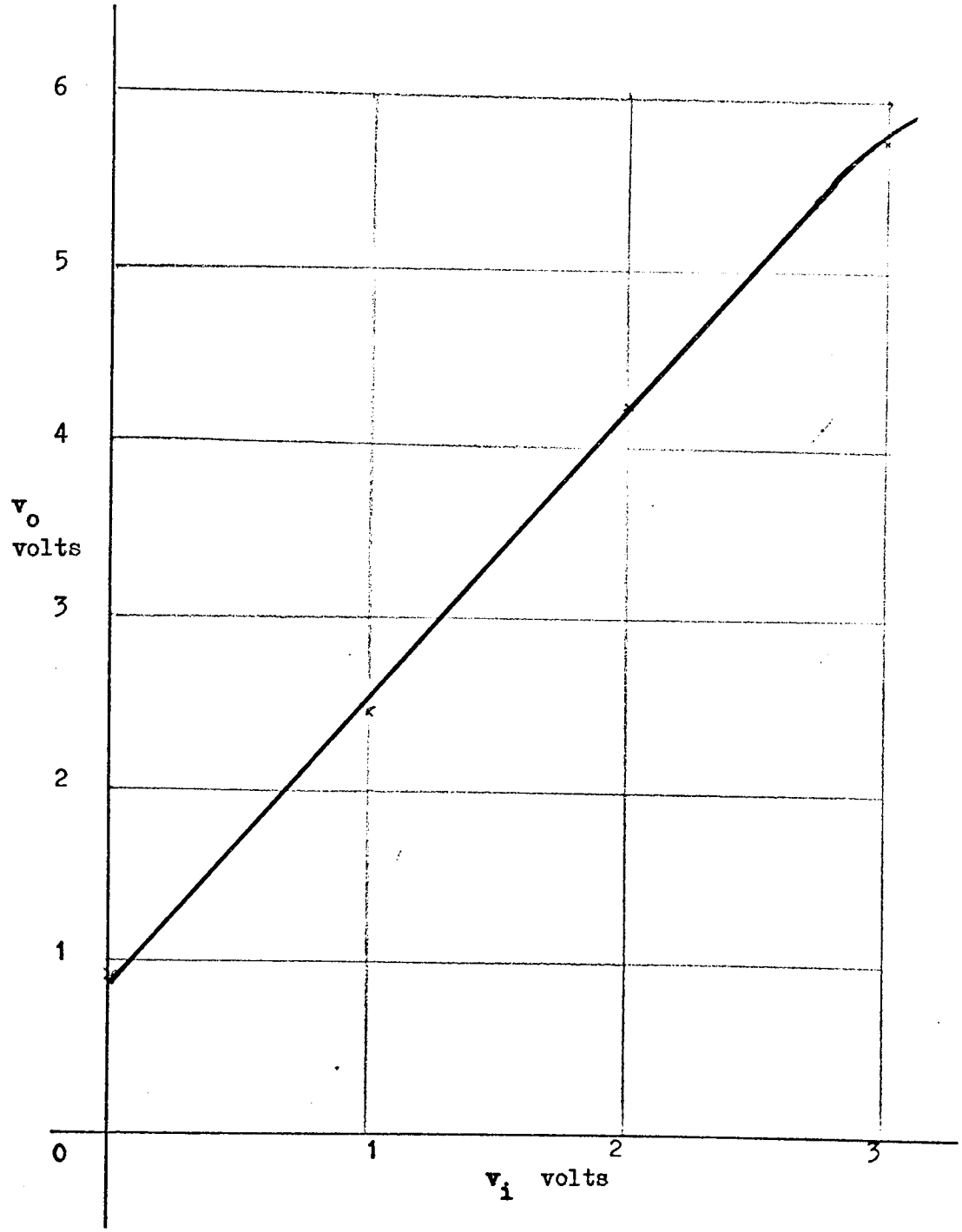

Fig.AI.2 Open-loop system characteristic curve

represented mathematically as:

$$\frac{1.5\ G}{(1 + 0.5s)(1 + 0.015s)} \qquad \text{.....(AI.1)}$$

The introduction of a closed-loop controller improves the regulation of the power supply and helps to minimise fluctuations in arc current as the arc moves over varying electrode surfaces.

Applying unity feedback, the closed-loop transfer function is:

$$\frac{v_o}{v_i} = \frac{1.5\ G}{0.0075s^2 + 0.515s + (1 + 1.5\ G)} \qquad \text{.....(AI.2)}$$

From the characteristic equation of this controller (equating the denominator to zero) we can identify the damped frequency of oscillation ω_n and the damping factor ζ from the general characteristic equation:

$$s^2 + 2\zeta\omega_n s + \omega_n^2 = 0$$

$$\text{therefore } \omega_n = \frac{1 + 1.5\ G}{0.0075} \qquad \text{and} \qquad \zeta = \frac{0.515}{0.0075 \times 2\,\frac{1 + 1.5\ G}{0.0075}}$$

If we choose a critically-damped system, then $\zeta = 1$ and:

$$G = \frac{\left\{\left[\frac{0.515}{0.015}\right]^2 \times 0.0075\right\} - 1.0}{1.5} = 5.25$$

Hence, the steady state gain of the system for critical damping is:

$$\text{Open-loop gain} = 5.25 \times 1.5 = 7.9$$

$$\text{Closed-loop gain} = \frac{7.9}{8.9} = 0.88$$

The final closed-loop current control system is shown in Fig.AI.3. The input-command circuitry is driven from the main power supply (see Appendix III) and consists of 6 discrete switching positions (0 to 50 Amperes) with a variable control on each position. A safety circuit has been built into the controller to prevent large current surges when re-igniting an extinguished arc. If an arc is extinguished, the feedback signal falls to zero and the input command is multiplied by the gain of the bias winding amplifier (5.75). This means that when the arc is re-struck there is a large current surge before the system settles. This is particularly undesirable when operating at low currents. In order to prevent this, a comparator circuit is used to detect for zero feedback signal and, under such a condition, a large feedback signal is instantly switched into the controller. The comparator and switching circuit is shown in Fig.AI.4. The comparator consists of a long-tailed pair (T1 and T2) with one input held at ground and the other input connected to the feedback signal. When this signal drops to zero, T2 and T3 switch on, connecting a +15 volt feedback signal to the controller. Diode D1 prevents this signal from feeding back to the arc current monitor resistor (0.15Ω).

Tests have been carried out on the system for a nominal arc

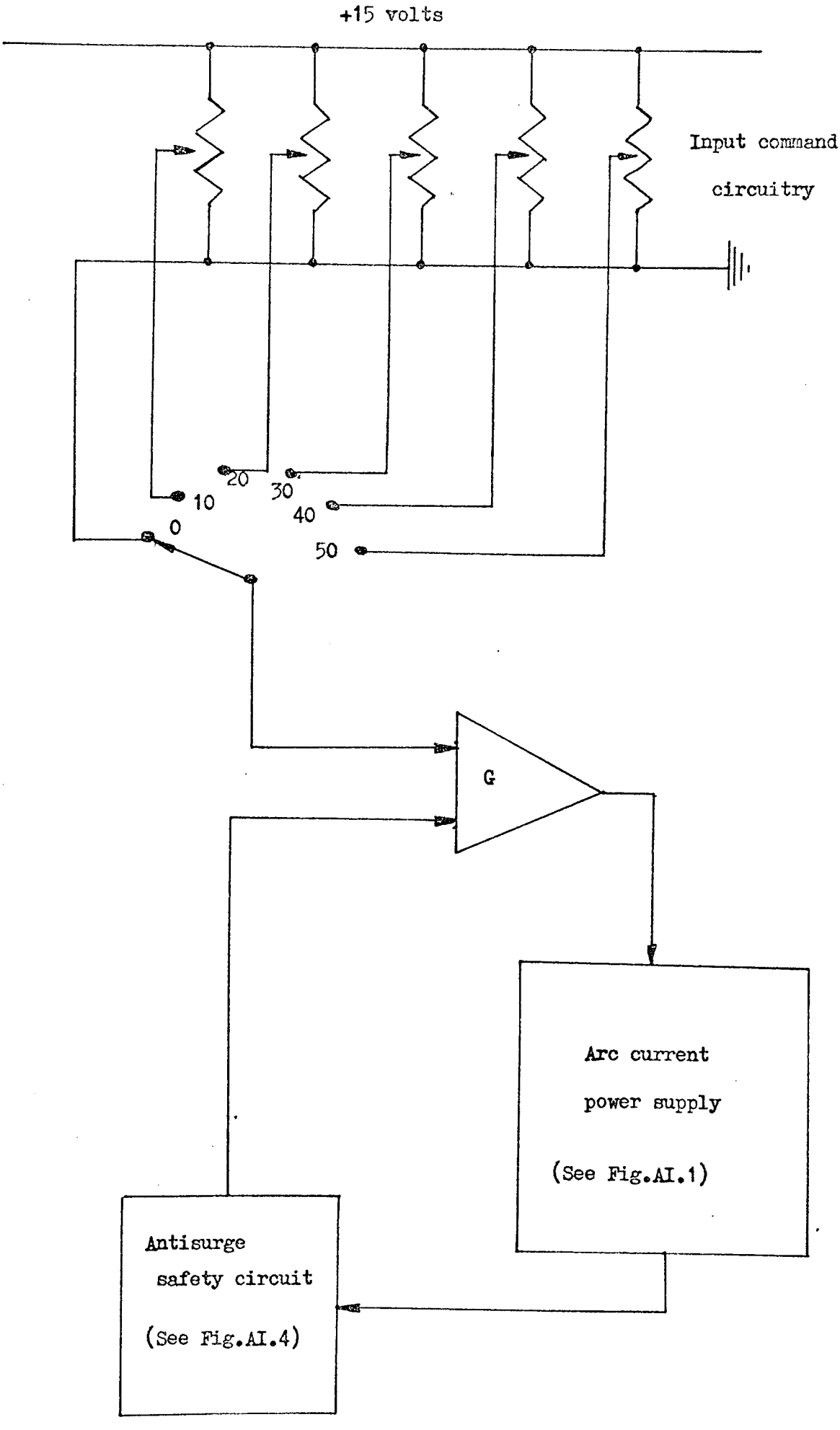

Fig.AI.3 Closed-loop system

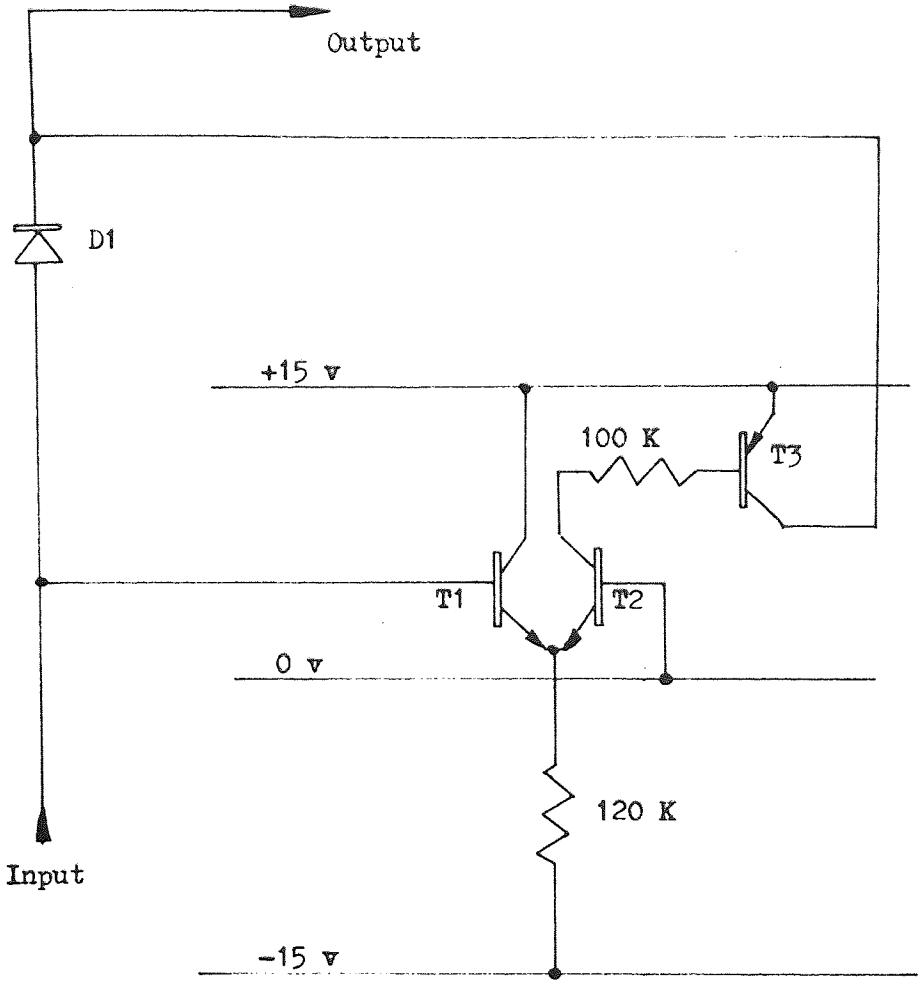

Fig.AI.4 Antisurge safety circuit

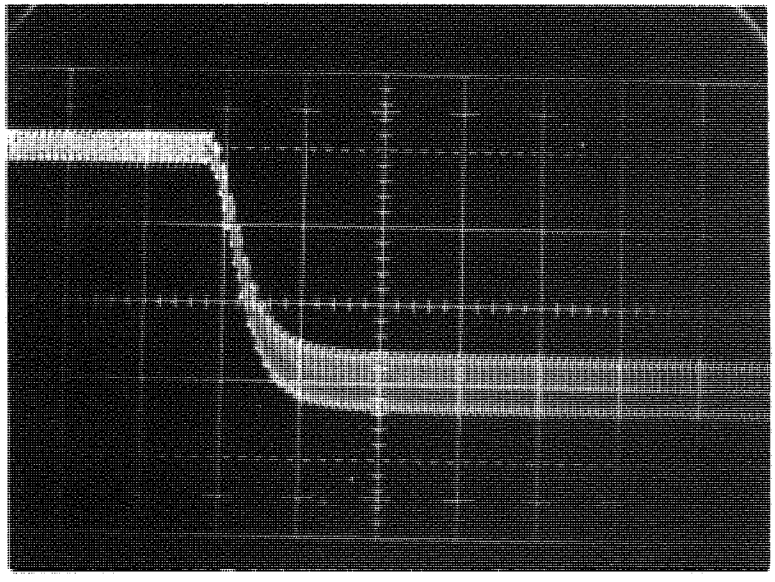

Scaling:

X 1 div. ≡ 0.1 s.

Y 1 div. ≡ 1.25 A

Fig.AI.5 Output from closed-loop system for a current change 5 Amperes to 10 Amperes

current of 20 Amperes.A drop of 50% in the supply voltage resulted in a 7% drop of arc current,as compared with a 95% drop using the open-loop system of Fig.AI.1. The drop in arc current,in the closed-loop system,from by-passing the 'arc plant' to running an arc between the electrodes was 0.5% as compared with 10% in the open-loop system.Better figures could be obtained by increasing the open-loop gain,though compensation to the control system would be necessary to prevent excessive transient overshoot;the figures, however,seem adequate for the purpose of controlling the arc current.A typical step response is shown in Fig.AI.5 for a current change of 5Amperes to 10 amperes (in this,negative voltage indicates positive arc current).The rise time is just under 100 mS and demonstrates the ability of a closed-loop controller to substantially reduce the values of the open-loop time constants.

APPENDIX II

COMPUTER PROGRAMMES ANALYSIS

This Appendix gives details of the computer programmes mentioned in the main body of the thesis.

Output response calculations

A total of four programmes have been used to calculate output responses of various systems.These responses are shown in detail in Chapter 4,together with a summary of the mathematics used in the calculations.

All four programmes are developed on a similar principle and this is discussed in detail by McCracken[34].The programme written to calculate and plot outputs of the uncompensated control system is taken as an example. Fig.AII.1 presents the computer programme (written in FORTRAN IV) and Fig.AII.2 shows a block diagram representation of the programme.The main variables in the system, T , G and H are read into the computer at the beginning of the programme run.This allows for programme flexibility,in that the variables may be changed at the end of each response plot.The variables are used to calculate the system output at increasing values of nT $(n = 0 \longrightarrow 30)$ and this output is scaled so that the steady-state output appears in the centre of the trace.The graph axes and curves are plotted using characters typed in from the computer teleprinter at the start of the plot.A safety factor is built in to check whether or not complex roots occur with the variables chosen.

On-line programmes used in the arc velocity control system

As indicated in 5.2.1,the on-line programme is written in two languages,

```
      REAL T,G,H,LINE,EX,ALPHA,BETA,AL,BE,ALBE,MID,SQ,OUT
      INTEGER J,N
      DIMENSION LINE(61)
1     READ(1,2) T,G,H,BLANK,DOT,X,O
2     FORMAT (3F4.2,4A1)
      EX=1.0/EXP(T)
      SQ=EX**2/4.0-G*H*(1.0-EX)
      IF (SQ.LE.0.0) GOTO 6
      ALPHA=EX/2.0+SQRT(SQ)
      BETA=EX/2.0-SQRT(SQ)
      AL=1.0-ALPHA
      BE=1.0-BETA
      ALBE=ALPHA-BETA
      MID=G*(1.0-EX)/(AL*BE)
      WRITE (2,11) MID
11    FORMAT (1H1,41HUNIT STEP RESPONSE    CLOSED LOOP GAIN = ,F5.3)
      DO 3 J=1,61
3     LINE(J)=DOT
      DO 10 N=1,30
      OUT=MID+G*ALPHA**N*(EX-ALPHA)/(AL*ALBE)
      OUT=OUT+G*BETA**N*(BETA-EX)/(BE*ALBE)
      J=30.0*OUT/MID+1.5
      IF (J.LE.61) GOTO 8
      LINE(61)=O
      GOTO 13
6     WRITE (2,7)
7     FORMAT (14H COMPLEX ROOTS)
      GOTO 1
8     IF(J.GE.0) GOTO 12
      LINE (1)=O
      GOTO 13
12    LINE(J)=X
13    WRITE(2,9) LINE
9     FORMAT (1H ,61A1)
      DO 4 J=1,61
4     LINE(J)=BLANK
10    LINE(31)=DOT
      GOTO 1
      END
```

Fig.AII.1 Programme used to determine the output response of the uncompensated control system

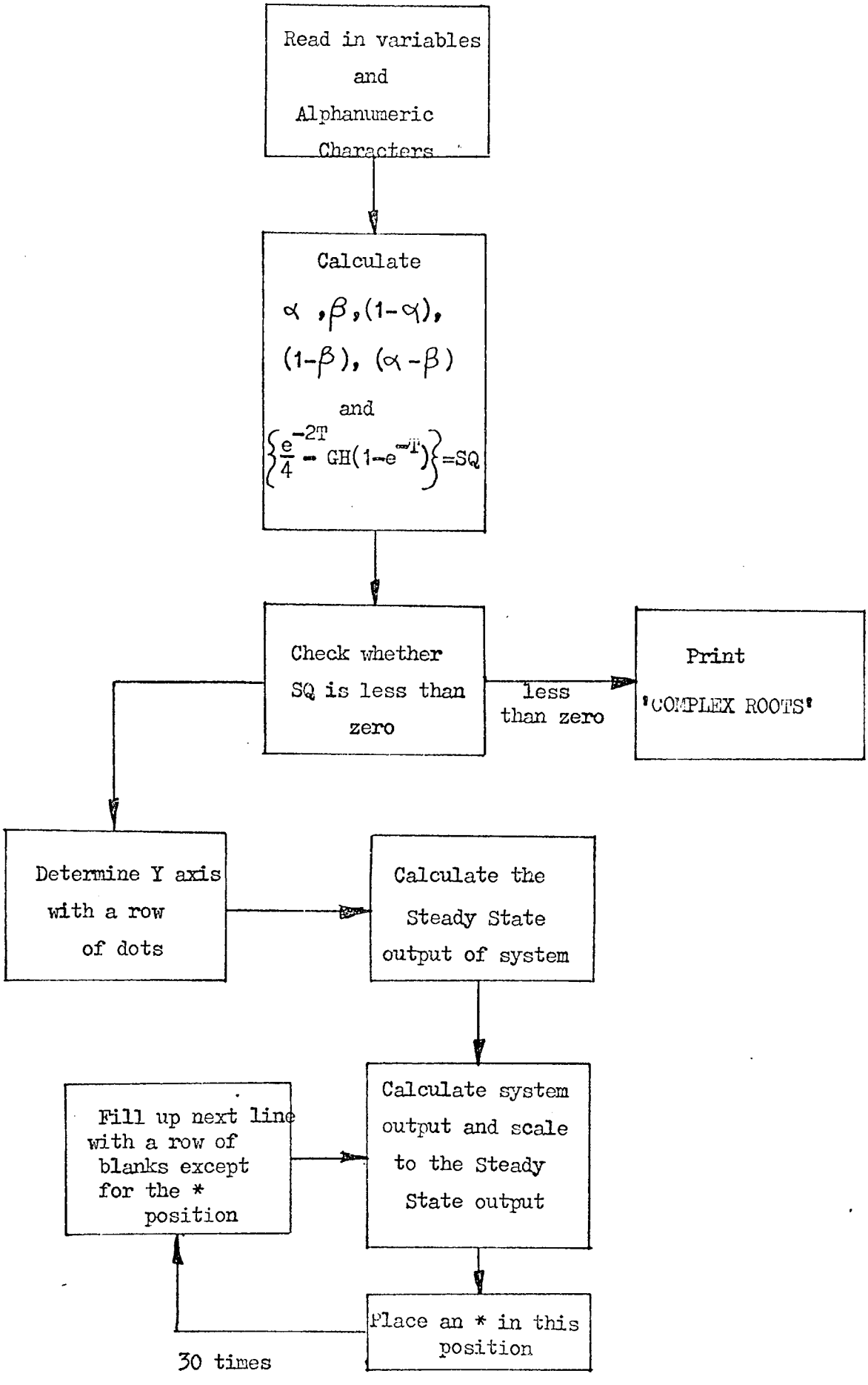

Fig.AII.2 Block diagram of uncompensated control system response programme

FORTRAN IV and MACRO 9 .The main programme COMP is concerned with the sampling and digital filtering operations. Fig.AII.3 presents the computer programme and Fig.AII.4 the block diagram representation of this programme. After the programme stores have been set at their initial conditions, samples are taken from the analogue-to-digital converter and filtered as indicated in section 2.3.3. The sub-routine DIG performs the first difference and compensation operations, the outputs from DIG being transferred to the digital-to-analogue output unit. Because the ADC requires 35 μS to convert a signal to a 12 bit sample, this time is utilised by scaling the previous sample. In this way, it is possible to perform 1024 samples in a time of 85 mS. The 6-place scaling to the right in the main programme (COMP), (rather than the 5-place scaling indicated in 2.3.3) is necessary because the most-significant digit gives the sign of the sampled value and erroneous results can occur, when changing from negative to positive sampled values, if this extra scaling place is not included.

The FORTRAN IV sub-routine is given in Fig.AII.5, with the block diagram representation in Fig.A.II.6. The first part of the programme operates in conjunction with COMP and is a start and stop facility. The control run is started by both switching on an accumulator switch on the computer console and reducing the voltage from the measurement system to below 75 mV. This allows for starting the control run in the laboratory, without immediate access to the computer. The run is stopped by either switching off the accumulator switch or by a predetermined input command. The data required for the control run is read into the allotted stores and the programme returns to COMP. During the control run, the filtered position signal is transferred from COMP to DIG. A first-difference calculation is performed with this and the previous signal and an error signal obtained using the

```
            .GLOBL DIG
            .IODEV 2
ADSM=701103
ADSC=701304
ADRB=701312
DAL1=705101
DAL2=705102
/INITIAL CONDITIONS
START       IOF
            LAC (1
            ADSM
/INITIALISE BEFORE EACH 100MS SAMPLE
LOOP1       LAS
            DAC COM
            IOF
            LAC (-40
            DAC TAG2#
            DZM ST3#
            LAC (400000
            DAC ST2#
/100MS SAMPLE AND DIGITAL FILTER
LOOP3       LAC (-40
            DAC TAG1#
            DZM ST1#
LOOP2       ADSC
            LAC (-2
            DAC SHFT2#
            LAC (-5
            DAC SHFT#
            LAC (-6
            DAC SHFT1#
            LAC ST2
            SPA!CLL
            STL
            SMA
            NOP
            RAR
            NOP
            ISZ SHFT1
            JMP .-7
            TAD (4000
            TAD ST1
            DAC ST1
```

Fig.AII.3 Main programme COMP used in the on-line control system. Programme language MACRO 9.

```
            ADRB
            DAC ST2
            ISZ TAG1
            JMP LOOP2
            LAC ST1
            SPA!CLL
            STL
            SMA
            NOP
            RAR
            ISZ SHFT
            JMP .-6
            TAD ST3
            DAC ST3
            ISZ TAG2
            JMP LOOP3
            LAC ST3
/DIGITAL COMPENSATOR AND VELOCITY MEASUREMENT
            DAC IN
            ION
            JMS* DIG
            JMP .+5
            .DSA IN
            .DSA OUT
            .DSA COM
            .DSA BIAS
            LAS
            SNA
            JMP START
/VELOCITY OUTPUT
            LAC BIAS
            DAL1
            LAC OUT
/COMPENSATED ERROR OUTPUT
            DAL2
/RETURN FOR NEXT SAMPLE
            JMP LOOP1
IN          0
OUT         0
COM         0
BIAS        0
            .END
```

Fig.AII.3 (continued)

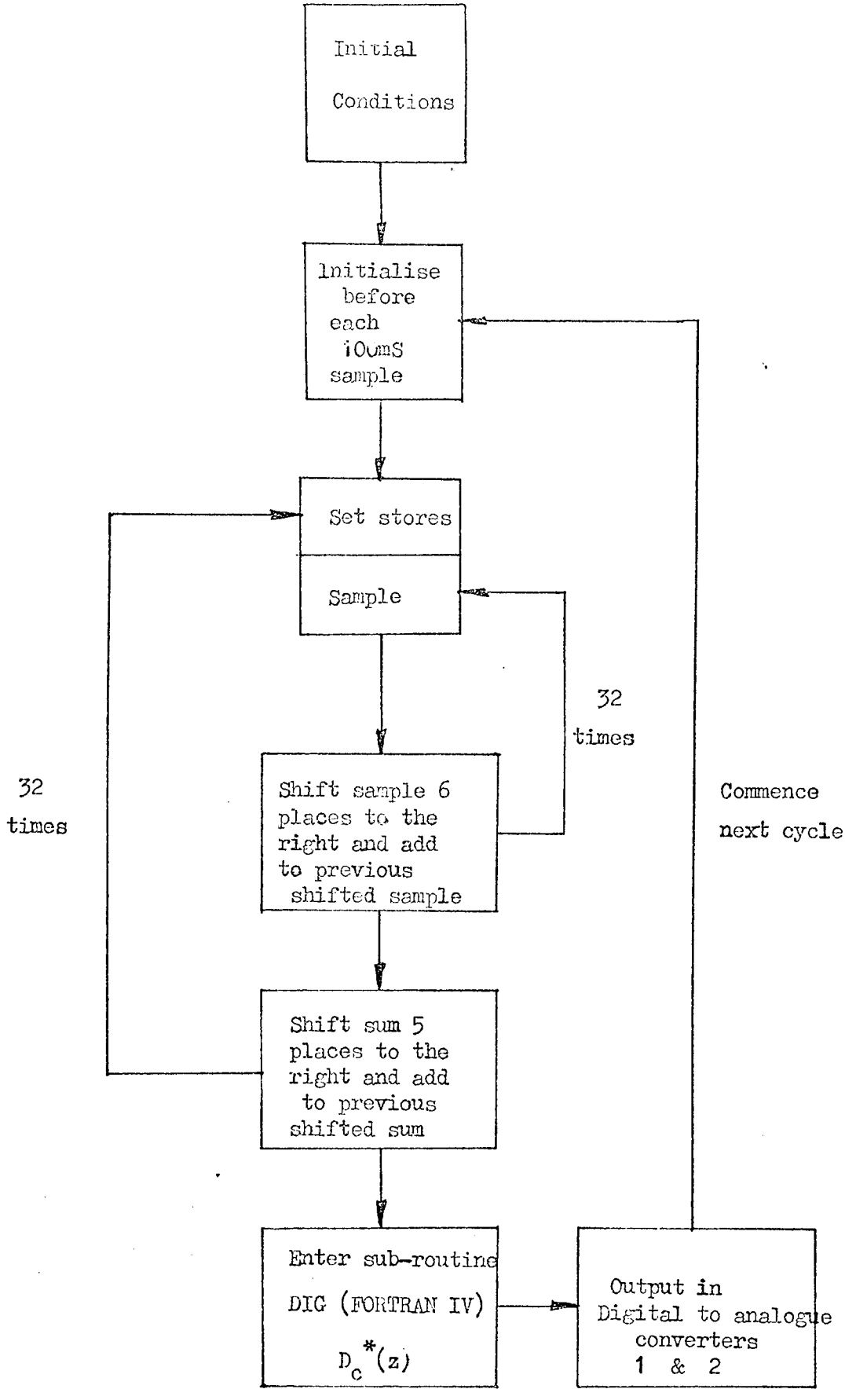

Fig.AII.4 Block diagram of main programme COMP.

```
      SUBROUTINE DIG (IN,OUT,COM,BIAS)
      INTEGER OUT,COM,BIAS
      DIMENSION A(100),B(100),GAIN(11)
      IF (COM.EQ.0) GOTO 3
      IF((COMAND.EQ.0.0).AND.(POS.EQ.0.0)) GOTO 6
7     J=1
      IF (COMAND.LT.0.0) GOTO4
      IF (PRES.GE.POS) GOTO 15
      GOTO 5
4     IF (PRES.LE.POS) GOTO 15
5     DEL=PRES
      PRES=IN
      R1=R
      V=(PRES-DEL)/0.50
      R=(V-COMAND)/GAV
      C2=C1
      C1=C
      C=R+(C1-R1)/1.10517+C2/10.50833
      IF(C.LE.(-13107.0)) C=-13107.0
      IF (C.GE.13107.0) C=13107.0
      G=ABS(COMAND/C)
      IF(G.LE.0.1) G=0.1
      AVGAIN=0.0
      GAIN(11)=G
      DO 17 K=2,11
      AVGAIN=AVGAIN+GAIN(K)
17    GAIN(K-1)=GAIN(K)
      IF(C) 10,11,11
10    OUT=-IFIX((SQRT(ABS(C/13107.)))*131070.)
      GOTO 12
11    OUT=(SQRT(C/13107.))*131070.
12    BIAS=V/0.1
      RETURN
1     READ(3,2) I
2     FORMAT (I3)
      DO 14 L=1,I
      READ (3,14) A(L),B(L)
14    FORMAT (2F5.3)
```

Fig.AII.5 Sub-routine DIG used in the on-line control system.

Programme language FORTRAN IV.

```
      L=0
15    L=L+1
      COMAND=A(L)
      POS=B(L)
      COMAND=COMAND*2621.44
      POS=POS*13107.2
      GAV=AVGAIN/10.0
      J=1
      GOTO 5
3     C=0.0
      J=0
      C1=0.0
      PRES=0.0
      COMAND=0.0
      POS=0.0
      OUT=0
      R=0.0
      AVGAIN=50.0
      DO 16 K=2,10
16    GAIN(K)=5.0
      RETURN
6     IF(J.EQ.1) GOTO 13
      IF(IN.GT.1000) RETURN
      GOTO 1
13    OUT=0
      RETURN
      END
```

Fig.AII.5 (continued)

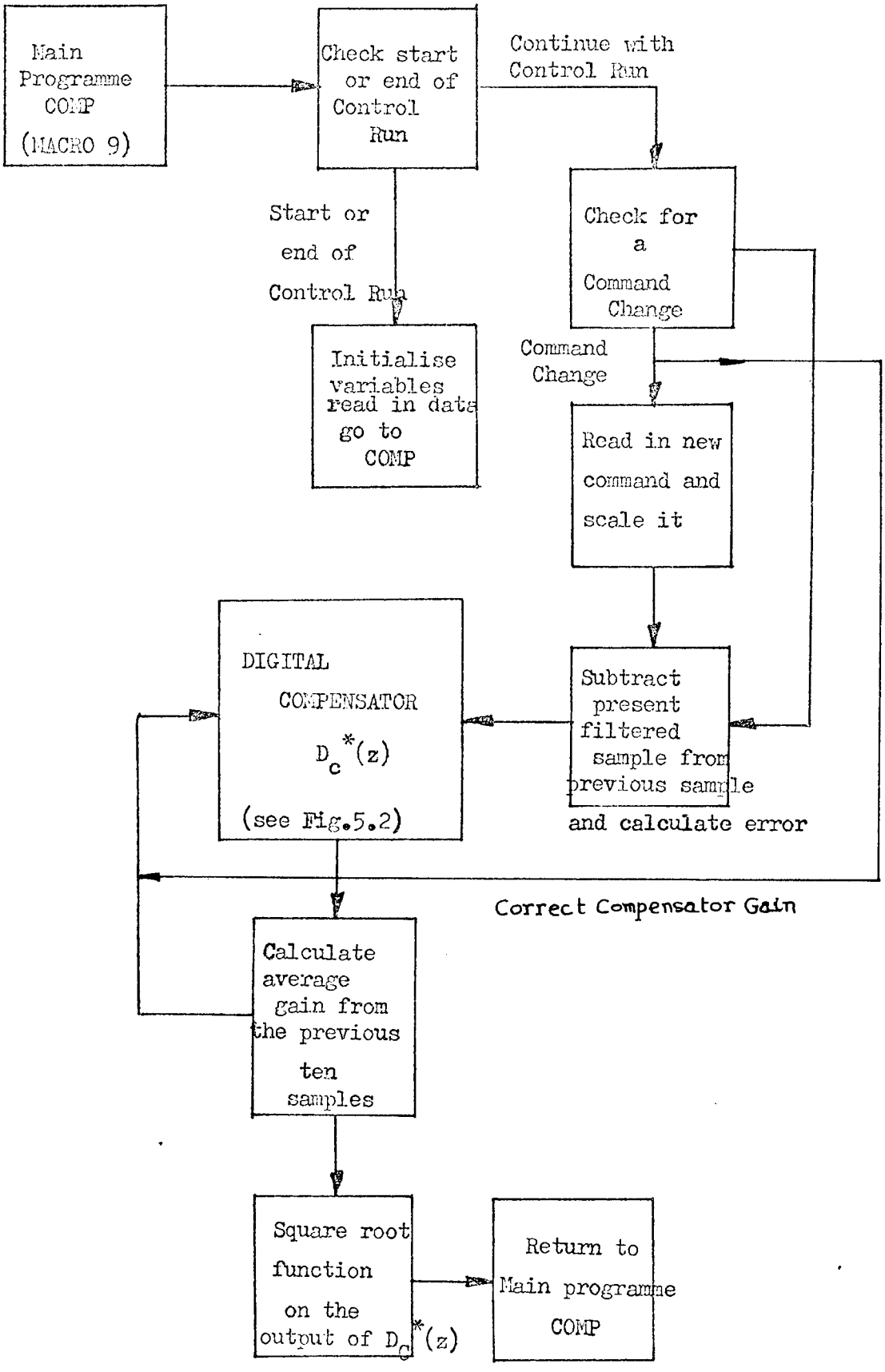

Fig.AII.6 Block diagram of sub-routine DIG.

command input. This error signal is fed into the compensator, the output being transferred back to COMP. During each 100 mS cycle, DIG checks the position of the arc and determines the point at which to change the input command from the data read in at the start of the control run.

The digitally-compensated output appears at the terminals of DAC 1 and this is the output used for the arc-control system. The output available at DAC 2 is a direct, uncompensated, velocity signal for use in the analogue compensation system discussed in Chapter 5.

APPENDIX III

ELECTRONIC CIRCUITRY

This appendix gives details of some of the electronic circuitry used in the arc-velocity and current control systems.

Position Signal Modulator

This circuit uses the d.c. voltage developed across the 'arc plant' measurement electrode to modulate a 500 Hz. square wave.The modulation is performed by 'chopping' the measurement voltage,using two FET s as shown in Fig.AIII.1,and feeding this signal into an a.c. differential amplifier.The FET s are switched by 180° out-of-phase square waves which perform the following cycle of operation:

1) Open-circuit the measurement voltage lead and short-circuit the two inputs of the a.c. differential amplifier.(This is the OFF position).

2) Connect the measurement voltage lead to the a.c. amplifier input and separate the two inputs.(This is the ON position).

The switching waveforms are generated by a multivibrator circuit driving two cascaded switching transistors via an amplification stage.

A safety circuit has been built into the modulator to protect the FET s from high voltages arising from an incorrect connection of the measurement leads to the 'arc plant'.The circuit allows a maximum of 11 volts across the series connection of the FET s,and ensures that each input to the a.c. differential amplifier is no more than 5.6 volts from earth

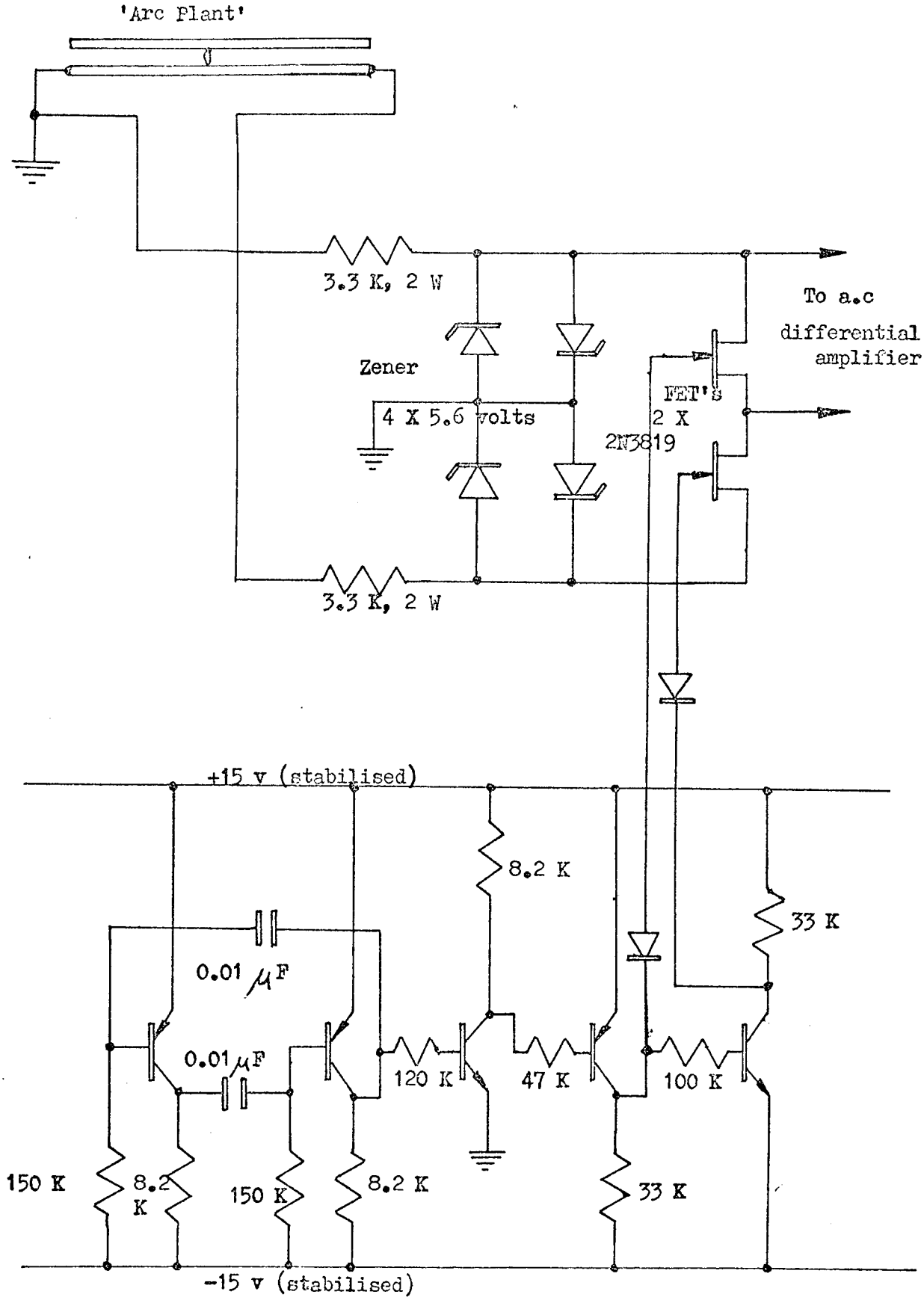

Fig.AIII.1 Position signal modulator

potential.

External Field-Coil Amplifier

This amplifier is used to drive the field coil producing the 'arc plant' transverse magnetic field.The power amplifier uses a commercial low-power d.c. amplifier in the input stage,and this drives a push-pull power output stage capable of driving $\pm$ 1 Ampere into the field coil;the circuit diagram is shown in Fig.AIII.2.The variable feedback allows the amplifier gain to be adjusted.Two inputs are provided;one is for the output from the computer output amplifier and the other is connected to a variable voltage supply;this is used for biassing off the magnetic field produced by the current in the 'arc plant' electrodes.

Single-Ended Power Amplifier

This amplifier is used in the feedforward path of the closed-loop arc - current supply;the circuit diagram is shown in Fig.AIII.3. Since the amplifier is only required to operate at one polarity,the circuit is not so complex as the amplifier of Fig.AIII.2.The input stage uses the same commercial amplifier as used previously and this drives a medium-power output stage.Variable feedback is again used and the amplifier has a facility for two inputs (input command and feedback signal).The final emitter-follower power-output stage is built into the transductor cabinet and is provided with its own unstabilised power supply.

Two other power supplies have been built to power the electronic circuitry;

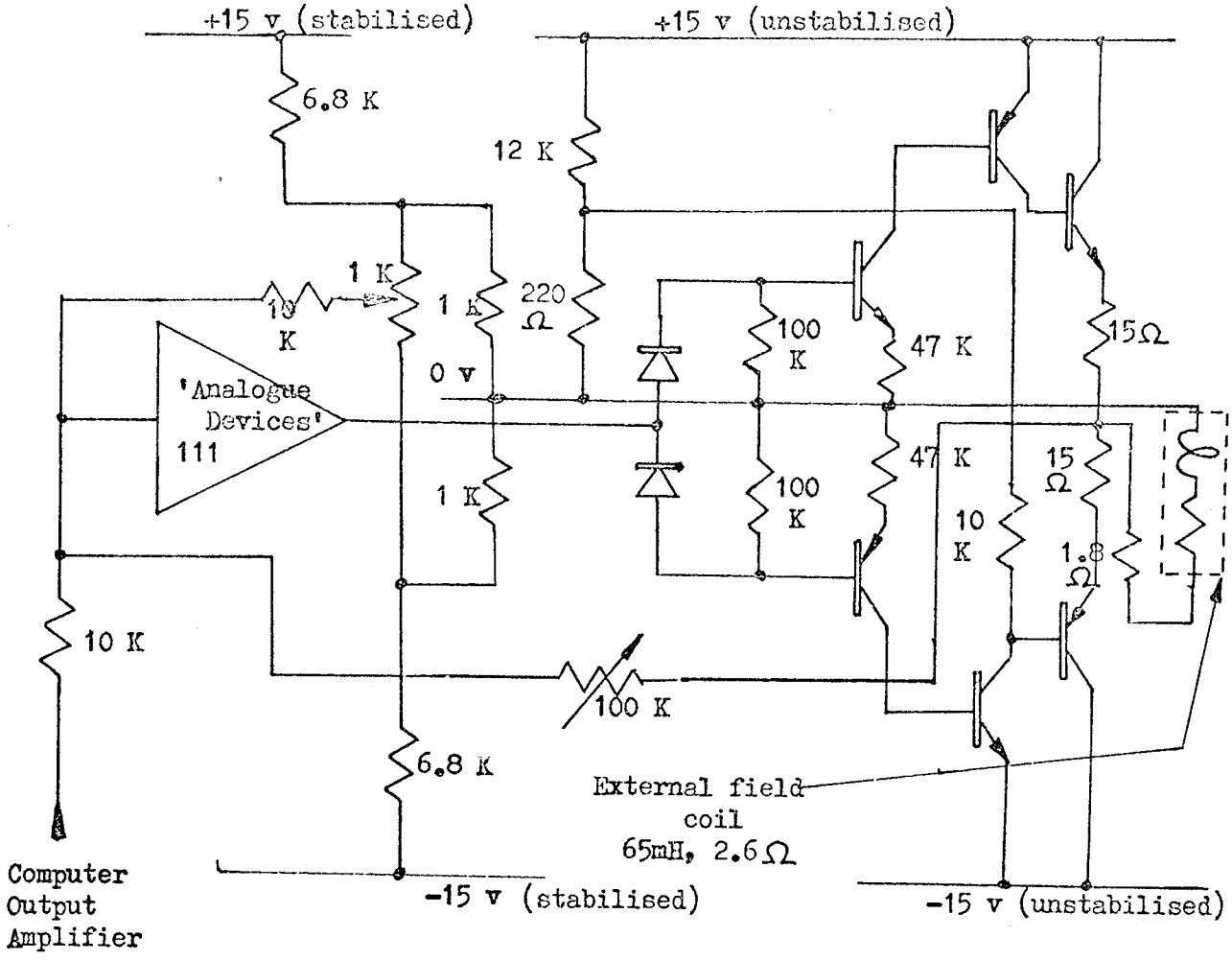

Fig.AIII.2 External field coil amplifier

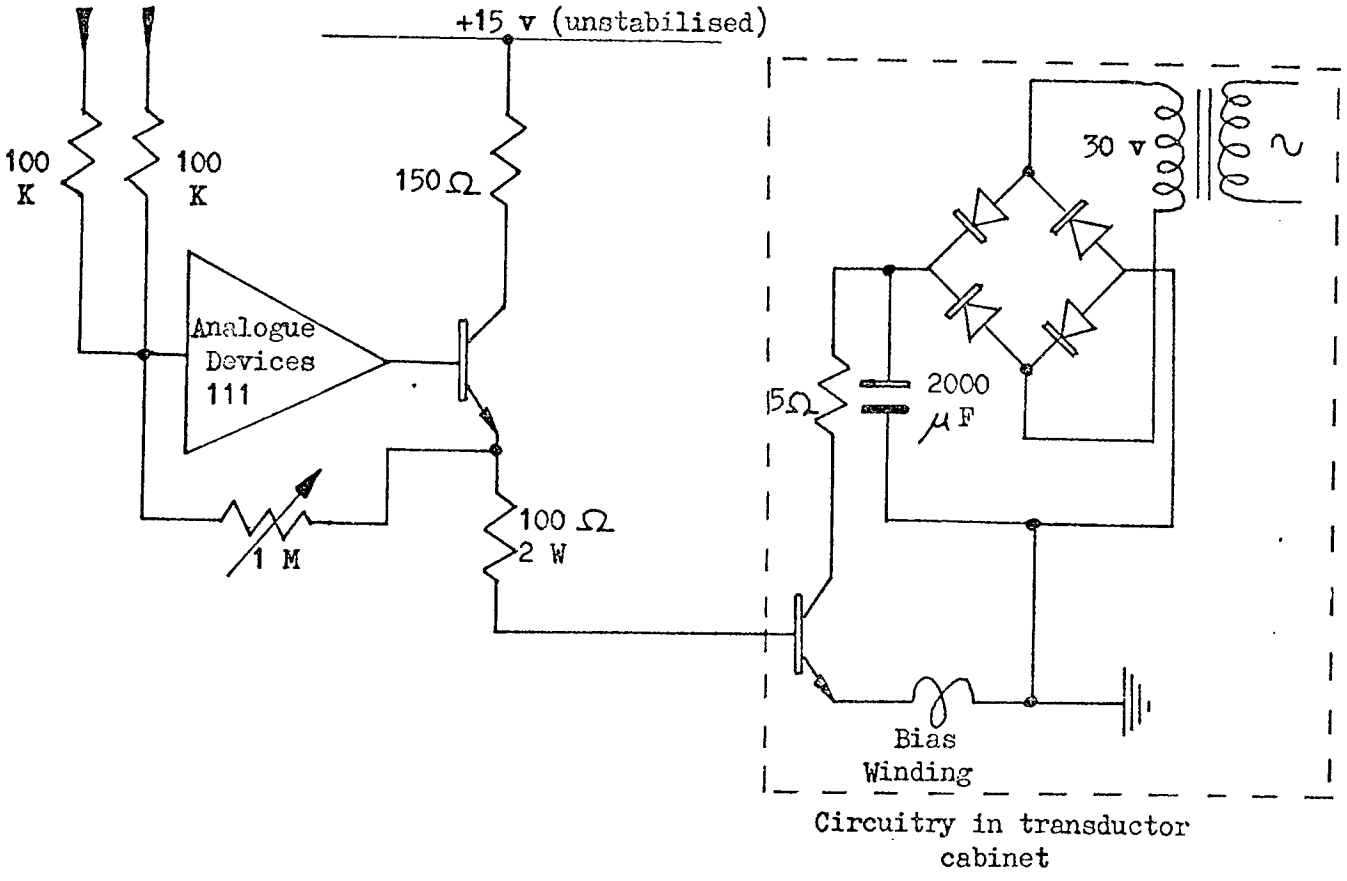

Fig.AIII.3 Single ended power amplifier

the circuit diagrams are not included here, since the circuits are of a well-established design and can be found quite readily in the literature[35]. The first supply is stabilised and provides ±15 v (± 100mA) ; this is used to power the commercial d.c. amplifiers, and the other low-power circuitry as indicated on the circuit diagrams. The second supply is unstabilised and has a capacity of ± 4 Amperes at a voltage of ± 15v. This supply is used for the power-output stages, as indicated in the circuit diagrams.